ON THE CAPACITY ANALYSIS OF A DS/FH CDMA SYSTEM FOR THE PCS

By

ALLEN NAN HE, B.S. (Peking University, Beijing, China)
M.S. (Peking University, Beijing, China)
M.S. (McMaster University, Hamilton, Ontario, Canada)

A Thesis
Submitted to the School of Graduate Studies
in Partial Fulfilment of the Requirements
for the Degree
Ph. D

McMaster University
March 17, 1995
©Copyright 1995

ON THE CAPACITY ANALYSIS OF A DS/FH CDMA SYSTEM FOR THE PCS

PH. D (1995) MCMASTER UNIVERSITY
(Electrical and Computer Engineering) Hamilton, Ontario

TITLE: **On the Capacity Analysis of A DS/FH CDMA System for the PCS**

AUTHOR: Allen Nan He
B.S. (Peking University, Beijing, China)
M.S. (Peking University, Beijing, China)
M.S. (McMaster University, Hamilton, Ontario, Canada)

SUPERVISOR(S): Dr. M. K. Wong
Professor, Department of Electrical and Computer Engineering
McMaster University, Hamilton, Ontario, Canada
Fellow, I.E.E.
Co-Supervisor:
Dr. Q. Wu
Research Engineer, Department of Electrical and Computer Engineering
McMaster University, Hamilton, Ontario, Canada

NUMBER OF PAGES: vi,162

ABSTRACT

The main objective of this thesis is to design a PCS system with high capacity. We find that the hybrid DS/FH CDMA method is a promising technology to achieve this goal. Designing such a system and analyzing its capacity are the major contributions of this thesis.

CDMA technology potentially offers higher capacity than the other multiple access methods. However, there are serious problems in implementing DS-CDMA to PCS. These are the long acquisition and "near-far" problem. Both these two problems reduce the system performance, and require complicated hardware solutions.

The idea of applying hybrid DS/FH CDMA technique to PCS system is initiated for trying to solve the long acquisition problem. We also find that by taking advantage of FH, we can solve the "near-far" problem without increasing system complexity.

The capacity of CDMA systems is limited by mutual interference of users, and the interference level is determined by two major factors: the precision of synchronization and the code property. The most important property of the codes is the cross-correlation. The lower the cross correlation among the codes, the higher the capacity will be. Based on this criterion we explore the performance of different codes. In addition, we proposed to use codes generated from the same maximum-length sequence with a unique phase, which offer the lowest cross correlation in the family of non-orthogonal codes.

Another detriment to the performance of the system is the imperfection of synchronization due to random access and propagation delays. We propose to implement

time slots and deterministic coordinated hopping patterns. Such a measure not only helps to save acquisition time and power control, but also increases the capacity dramatically, by way of establishing synchronous access and avoiding frequency collisions. We show that quasi-synchronous access can be achieved for uplink and completely synchronous access can be achieved for downlink. Our theoretical analysis as well as simulations showed that, by ignoring the adjacent cell interference, system capacity in a single cell can approach its hard limit defined as the ratio of total bandwidth to the message bandwidth for a reasonable bit error rate.

A major concern in applying CDMA to PCS is the interference from adjacent cells, since the whole spectrum is reused in all the adjacent cells. Mathematical models for calculating such interference power have been developed, in terms of propagation characteristics, code properties, etc. The results reveal significant impairment on the capacity due to this interference. Voice activity cycle plays an important role now and can triple the capacity in one cell to approach the hard limit N. Without it, the capacity can only be about $\frac{N}{3}$ in one cell, for an acceptable BER (10^{-3}) and reasonable E_b/N_0. The capacity of this hybrid system has the potential of being much larger than that of TDMA system.

Acknowledgement

I want to thank my supervisor, Dr. Max K. Wong, for his constant encouragement, generous financial support, and unfailing help. I am indebted to my co-supervisor, Dr. Q. Wu, for his guidance and stimulating discussion with me. To my Ph.D committee members, Drs. Jim Reilly, Patrick Yip, I am grateful for their time in reading this thesis. I also want to thank all my former supervisors, Drs. Z. Y. Yue, S. Haykin, and especially to Dr. Ralph E. Pudritz, who's encouragement and help have so much impact on my academic path. Finally, I would like express my deep gratitude to my family, particularly to my mother and my wife, for their many year support and understanding, which enables me to pursue a Ph.D persistently.

Contents

List of Figures

List of Tables

Chapter 1

Introduction

The major concern of this thesis is the application of code-division-multiple-access (CDMA) to the personal communication service (PCS) systems. CDMA originated from spread spectrum techniques. In this chapter we provide a short review of spread spectrum to illustrate the fundamental principles. Following this we will introduce the evolution path to PCS systems. Finally the outline of this thesis is described.

1.1 Review of Spread Spectrum

1.1.1 Spread Spectrum Concept

Spread spectrum(SS) has a long and interesting history. Systems based on the SS technique have been developed as early as the mid-1950's. The initial applications have been to military anti-jamming tactical communications, guidance systems, and experimental anti-multipath systems, etc. Scholtz [83] gave a comprehensive review on the state-of-art devices using SS techniques up to the mid-60's. The most recent achievements are summarized in many books and journal papers, see [37], [38], [39], [40], [41],[42],[87], [106]. For the tutorial papers, see [65], [84].

A definition of spread spectrum that adequately reflects the characteristics of this technique is given by Pickholt[65], et al. as follows:

> "Spread spectrum is a means of transmission in which the signal occupies a bandwidth in excess of the minimum necessary to send the information; the band spread is accomplished by means of a code which is independent of the data, and a synchronized reception with the code at the receiver is used for despreading and subsequent data recovery"

Under this definition, standard modulation schemes such as FM and PCM which also spread the spectrum of an information signal do not qualify as spread spectrum.

There are many reasons for spreading the spectrum. Spread spectrum affords an opportunity to give a desired signal a power advantage over many types of interference (e.g., jamming). The underlying principle is that of distributing a relatively low dimensional data signal in a high dimensional environment so that a jammer with a fixed amount of total power (intent on maximum disruption of communications) is obliged to either spread that fixed power over all the coordinates, thereby inducing just a little interference in each coordinate, or else place all of the power into a small subspace, leaving the remainder of the space interference free. Consider, for example, a military communication system which might be jammed by a continuous wave (CW) tone near the modem's center frequency or by a distorted retransmission of the modem's own signal. The interference cannot be modeled as stationary additive white Gaussian noise (AWGN) in either of these cases. The severe degradation in system performance caused by the pulse-noise jammer can be largely eliminated by using a combination of SS techniques and forward error correction coding with appropriate interleaving. Assuming a jammer transmits pulses of band-limited white Gaussian noise having total average power J referred to the receiver front end. Let $N_J = J/W$ be the one-sided average jammer power spectral density and W be the transmission bandwidth. The effect of the spectrum spreading will be able to enhance the E_b/N_0 to KE_b/N_0 where $K = W/R$, is called *Processing Gain*, and R is the data rate of the SS-system. E_b is the energy per data bit. N_0 is the power spectrum density of gaussian noise.

Besides the applications for SS in military communications, there is growing interest in the use of this technique for mobile radio networks (radio telephony, packet radio, and amateur radio), timing and positioning systems, some specialized applications in satellites, etc[6], [15],[50],[64],[68], [81],[82],[94]. While the use of SS naturally means that each transmission utilizes a large amount of spectrum, this may be compensated for by the interference reduction capability inherent in the use of SS techniques, so that a considerable number of users might share the same spectral band. Therefore the SS techniques offer an alternative for multiple users accessing the network simultaneously, in contrast to the conventional methods such as the *frequency division multiple access* (FDMA) and the *time division multiple access* (TDMA). Since the users are "isolated" from each other by different access codes, such a method is often called *code division multiple access* (CDMA). In the earlier literatures it is also referred as *spread spectrum multiple access* (SSMA), which substantially focused on the situation of a very small number of simultaneous users. There is no easy answer to the question of whether spread spectrum is better or worse than conventional methods. Performance analysis must be carefully carried out by the system designers for the particular environment in which the system is employed.

The major system questions associated with the design of a SS system are: How is the performance measured? What kind of coded sequences are used and what are their properties? How much jamming/interference protection is achievable? What is the performance of any user pair in an environment where there are many spread spectrum users? How is the relative timing of the transmitter-receiver codes established (acquisition) and retained (tracking)? Some performance criterions are inter related. For example, to offer a better interference protection, one may wish to spread the signal spectrum as wide as possible. This means the employment of long period codes. On the other hand, such a measure will increase the difficulty of acquisition. An actual SS system is a compromise of all the desired performance factors.

1.1.2 Type of Spread Spectrum

The means by which the spectrum is spread is crucial. The typical techniques are *direct sequence* (DS) modulation, *frequency hopping* (FH), and *time hopping* (TH). Hybrid combinations of these techniques are frequently used.

In the DS modulation, the data modulated signal is modulated again using a very wide-band spreading signal. This second modulation is usually some form of digital phase modulation. The spreading signal is chosen to have properties which facilitate demodulation of the transmitted signal by the intended receiver, and which make demodulation by an unintended receiver as difficult as possible. If the bandwidth of the spreading signal is large relative to the data bandwidth, the spread spectrum transmission bandwidth is dominated by the spreading signal and is nearly independent of the data signal. Consider, for example, the case when both data and code use the rectangular pulse, while the data bits have the duration of T_b and the code bits have the duration of T_c. We call the code bits *chips* throughout this thesis. Typically T_b is much larger than T_c. The spectrum of data bits is illustrated in 1.1a, together with the spectrum of chips. The result of the final modulation is the convolution of these two spectra if multiplicative modulation is adopted in the time domain. The spectrum of the data bits is like a "pencil-beam" compared with that of chips, so the final spectrum is virtually the same as the spectrum of the chips, as shown in 1.1b.

The attributes of DS in comparison with FH or TH can be listed as follows:

- Advantages
  - Good noise and anti-jam performance
  - Difficult to detect
  - Good discrimination against multipath
- Disadvantages
  - Requires wideband channel with little phase distortion

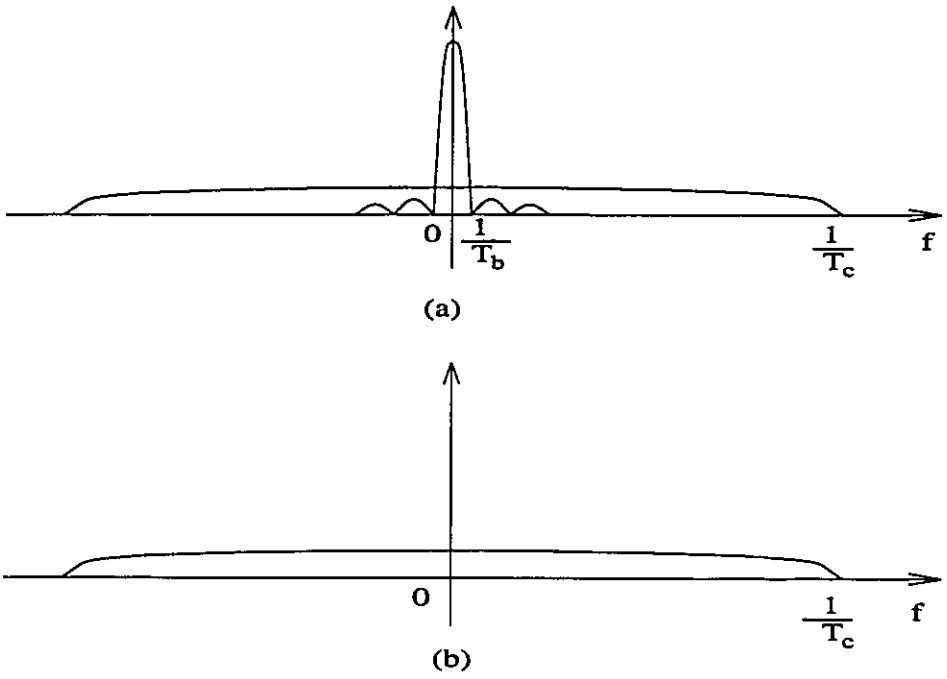

Figure 1.1: Spectrum of DS-CDMA systems

- Long acquisition time
- Fast code generator needed
- Near-Far problem. Strong power signals overwhelm weak signals.

A second method for widening the spectrum of a data-modulated carrier is to change the frequency of the carrier periodically. Typically each carrier frequency is chosen from a set of frequencies which are spaced approximately the width of the data modulation spectrum apart, although it is not absolutely necessary. The spreading code in this case does not directly modulate the data-modulated carrier but instead is used to control the sequence of carrier frequencies. Because the transmitted signal appears as a data-modulated carrier which is hopping from one frequency to the next, this type of spread spectrum is called frequency-hop (FH) spread spectrum. In the receiver, the frequency hopping is removed by mixing with a local oscillator signal which is hopping synchronously with the received signal.

There are two ways for doing FH. One is fast FH, which makes two or more hops

for each data bit. The other is slow FH which takes two or more data bits per hop. Due to the limitation of today's technology, the slow hopping is used in Mega-Hertz or higher bands[92].

The way to spread the spectrum of data signals for FH is different from that of DS. It is complicated to analyse the spectrum of the result. However, intuitively, for the slow FH, we may view the final spectrum in a plausible way: At each hopping interval, it still takes on a narrow band spectrum; as the carrier hops around, this narrow band spectrum appears on the different parts of the whole bandwidth. Finally, in a longer time base, it "seems" like a wide band spread spectrum since the narrow band spectrum fills every part of the total bandwidth.

A summary of the attributes of FH systems relative to DS or TH systems is as follows:

- Advantage
  - Great amount of spreading
  - Can be programmed to avoid portions of the spectrum
  - Relatively short acquisition time
  - Less affected by near-far problem
- Disadvantages
  - Complex frequency synthesizer
  - Not useful for range measurement
  - Error correction needed due to frequency collisions.

The third way for spreading the spectrum is time hopping (TH). During the time slot T_s the data is sent in bursts dictated by a hopping pattern. The time interval between bursts also can be varied. Those random bursts can assume very wide bandwidth, and therefore spread the spectrum.

A time hopping system has the following attributes, compared with DS or FH methods:

- Advantage
  - Implementation simpler than FH
  - Useful when transmitter is limited in average power but not limited in peak power
  - Near-far problem can be avoided for users with different power sending bursts at different time
- Disadvantages
  - Long acquisition time
  - Error correction needed

When two of the above techniques combined together in one system, it is called a *hybrid* system. A hybrid system can have the advantages of both techniques, with increased complexity of implementation. Hybrid techniques are currently the only practical way of achieving extremely wide spectrum spreading.

1.1.3 A Highlight of FDMA, TDMA and CDMA

The multiple access schemes are used to serve simultaneous users with no or little mutual interference. Partition to the user's signals must be provided in certain way. From the signal space point of view, each user's signal should be independent of the others. Since the number of independent coordinates is invariant to the basis, the capacity which is defined as the maximum number of orthogonal signals is the same regardless of the access methods.

If such a partition is in the frequency domain, it is called FDMA. The whole bandwidth is divided into many subbands and each user gets a dedicated frequency

interval. Roughly speaking, the hard limit of the total number of simultaneous users for FDMA is the ratio of the whole bandwidth to the message bandwidth (assuming all the users have the same message bandwidth). However, due to the imperfection of narrow band filters, guard bands are usually provided to reduce the excessive sidelobe interference. Also the system needs a large number of frequency synthesizers.

If the partition is in the time domain, it is called TDMA. A typical TDMA system provides a time frame, and transmits the information in a frame by frame way. A frame is further divided into many time slots, and each user occupies a dedicated time slot. The hard limit of the total number of simultaneous users for TDMA is the ratio of frame length to the duration of time slots. The synchronization between the transmitters and the receivers is crucial in a TDMA system. To guard against the slip of system clocks and the delays caused by various reasons, guard slots are usually provided at both ends of the frame. Comparing with FDMA, TDMA provides better frequency efficiency. The high speed semiconductor switches used for time gates are also easier to obtain than the high quality narrow band filters. TDMA is naturally compatible to digital communications, and is a more popular method in telephone and satellite communication systems. But in a time delay spread environment, equalizers are needed to combat the inter symbol interference.

CDMA systems isolate users by their unique codes. If non-orthogonal codes are used, there is no hard limit to the number of simultaneous users. However, CDMA system is interference limited. Each existing user contributes some interference to all the others. Unless some special measures have been taken, CDMA system is inferior to TDMA or FDMA, in terms of capacity and spectrum efficiency, e.g. Viterbi[97],[98].

1.2 Introduction to Wireless Communications and PCS

1.2.1 A brief review of wireless communications

Over the past few years, the provision of voice and data communications to users away from their wireline terminals has become a major communications frontier. Current popular approaches to portable communications, such as cordless telephones, mobile radio telephones, radio modems, and radio paging, can be viewed as evolutionary steps along the way to more universal digital portable radio communications systems, which are collectively called Personal Communication Systems(PCS).

Cordless telephone sets consist of two separate units, the base unit and the handset, each containing a radio receiver and a low power transmitter. The base unit connects to a telephone line and appears to the telephone network like a conventional telephone. The low transmitter power is compatible with long periods of battery operation, light weight, and offers relative safety from electromagnetic radiation hazard for use close to a person. The duplex radio link is provided by continuously transmitting on separate frequencies from the handset and the base unit. The frequencies available for cordless telephones are very limited in number(up to 10 duplex channels), and no mechanism exists for specifying a particular channel for each customer. This results in severe limitations on cordless radio telephones: (1) either a very limited user density or excessive co-channel interference because of chaotic, limited, undisciplined and uncoordinated radio channel assignment, (2) a very limited service area of a few hundred feet radius, and (3) continuous need for house wiring from the telephone network.

Radio paging fulfills the function of alerting the pagee that someone wishes to communicate with him or her. In more advanced paging systems, a simple message may also be sent to the pagee. These systems provide one-way alerting or paging function over a large service region by multiple paging from all base stations dis-

tributed throughout the region. The obvious severe communication limitations are that they provide only one way limited communication.

Cellular mobile radio telephone system was developed in the United States in the 1940s at the Bell Laboratories. However, the service did not become public until 1970, when the Federal Communications Commission (FCC) allocated 40 MHz of the spectrum 800/900 MHz to cellular radio telephone (CRT). Later, an additional 10 MHz was allocated again. In 1981, FCC decided to split up the 40 MHz of spectrum into two equal blocks to be allocated to telephone companies in each metropolitan area. Cellular systems has enjoyed an exponential growth in demand.

Cellular systems provide communications to wide ranging mobile users[52],[53]. The fixed ends of these radio systems are connected to conventional telephone networks. Each mobile radio telephone set used in the system contains a receiver and a transmitter capable of operating on any duplex radio channel available to the system. Hand-held portable radio sets can be used in these radio telephone systems.

Handoff is provided for cellular system for users moving from cell to cell. When the signal strength for a channel falls below an acceptable threshold, the mobile switching office coordinates additional signal strength measurements from base stations surrounding the one serving the call. It attempts to switch the call to another duplex channel if another base station is receiving a stronger signal.

1.2.2 The structure and evolution of cellular systems

Ideally, the cellular systems have the structure shown in figure 1.2. Each cell is a hexagon. The base station is located at the center of the cell. The key concept in cellular system is the *frequency reuse*, that is, the same spectrum will be used in different cells. The first generation of cellular system in north America is the analog FDMA system. Each channel is 30 KHz in width, and uses frequency modulation scheme. To reduce the cochannel interference, neither the same spectrum nor the adjacent spectra will be used in the adjacent cells. *Frequency reuse pattern* is the

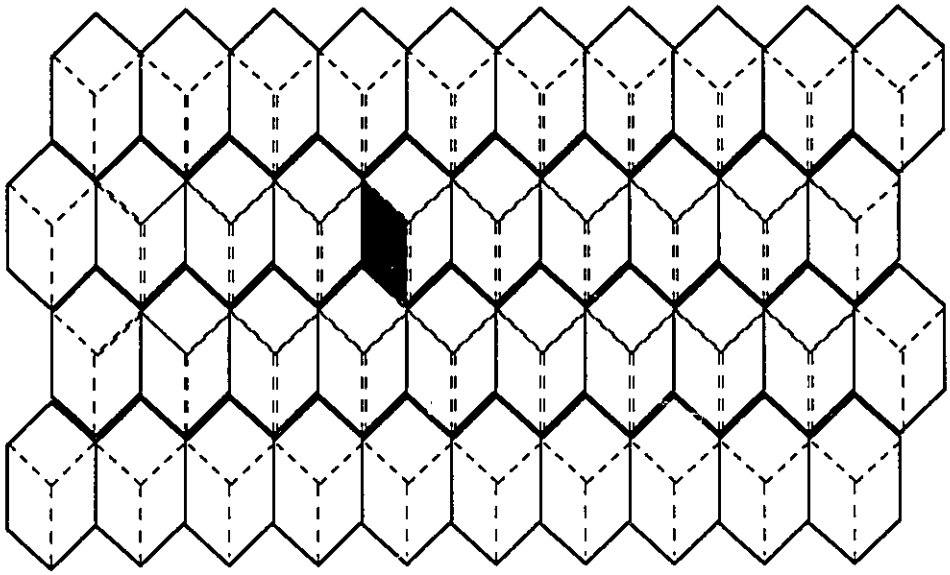

Figure 1.2: Cell structure of cellular systems

minimum number of adjacent cells which uses different spectra[49], [51]. For the analog FM cellular system, the frequency reuse pattern is 7, as shown in figure 1.3a.

The second generation of cellular systems was introduced around 1991 due to the saturation of capacity for the analog FM systems. The American Digital Cellular (ADC) and the pan-European Group Speciale Mobile (GSM) system are the major standards. These new standards use the TDMA technique, and the frequency reuse pattern can be 4 or even 3 (shown in figure 1.3b), since they are less sensitive to the interference of adjacent spectrum. Also digital speech compression techniques were adopted. As a result, the capacity of digital cellular system is 4-10 times of it analog counterpart[14], [74], [30].

Slightly later than those TDMA standards, some companies, represented by QUALCOMM Inc., proposed the CDMA standard for cellular. In this scheme, the 12.5 MHz one way spectrum (not a continuous spectrum) was segmented into ten 1.25 MHz subbands. DS-SS technique was used in each subband. Many publications addressing the performance of the CDMA technique in cellular environment, focused on the DS technique. As pointed out by Lee, Gilhousen, etc[24], [25], CDMA technique offers

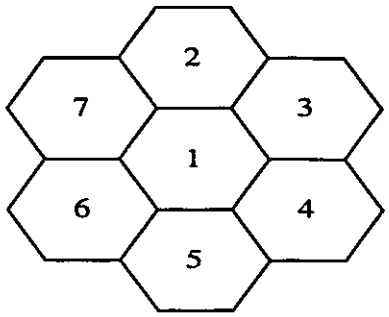

(a) Frequency reuse pattern of analog FM cellular systems

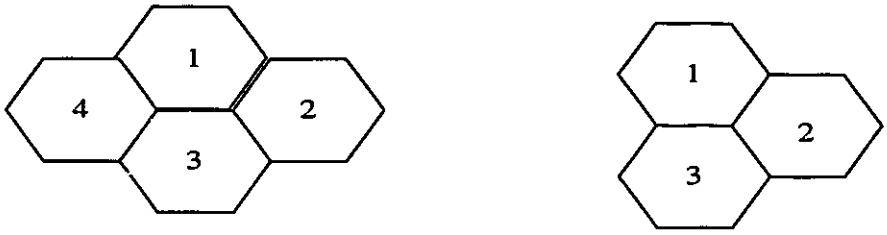

(b) Frequency reuse pattern of digital TDMA cellular systems

Figure 1.3: frequency reuse patterns of cellular systems

the following advantages:

- Voice activity cycles: The human voice activity cycle is 35%. The rest of the time we are listening. When users assigned to the channel are not talking, all others on the channel benefit with less interference in a CDMA radio channel. This increases the channel capacity by three times.

- No equalizer needed: only a correlator is needed instead of an equalizer at the receiver. The correlator is simpler than the equalizer.

- One tranceiver per site.

- No guard time in CDMA.

- Sectorization for capacity: In CDMA, the sectorization is used to increase capacity by introducing three radios in three sectors within a cell and three times

the capacity is obtained as compared with one radio in a cell in theory. (See figure 1.2).

- Less fading: CDMA offers the frequency diversity which reduces the fading problem.
- Easy transition from analog systems to digital systems.
- No frequency management or assignment needed. The same frequency band can be reused in the immediate adjacent cells.
- Soft capacity: each additional user will slightly degrade the voice quality for all the others.
- Coexistence: easy to share the frequency band with analog system and other microwave services.

As a result, it can be shown that the capacity of a CDMA cellular system can be 4 times as much as a TDMA system and 20 times as much as the FM analog system by some plausible calculation.

A rudimentary indication of adequate signal quality in the presence of co-channel interference is provided by continuously monitoring a specific baseband frequency (tone) that is looped round-trip from the base station through the mobile unit. Calls are terminated if excessive interference causes this tone to drop out. Thus cellular mobile radio systems are configured and controlled to help maintain the quality of telephone service to vehicles over a large region while making relatively efficient use of scarce radio channels. However, the coverage area and frequency reuse design constraints for mobile systems do not include an excess attenuation factor for radio propagation into buildings. Therefore the service areas within buildings are further limited.

Mobile systems are designed to work primarily with vehicular mounted radio equipment. Since a power source and substantial mounting surfaces are available,

the vehicular equipment typically transmits power levels in the range of several watts to several tens of watts. This results in minimum coverage radius of about 10 km around fixed base stations. Thus hand-held portable sets that operate in mobile systems must transmit approximately a watt in order to have reasonable but still quite limited service areas. Even these power levels raise questions of radiation safety and place severe restrictions on portable set and the duration of time the set can be used free of a battery charger. The need for high transmitter power also translates into large, complex high-power base stations. Tall base station antennas are usually erected to further increase the radio coverage radius from each base station. Because of the expense of these complex base stations, every effort is made to minimize the number of stations required to cover a service region. The analog mobile radio duplex channels are single FM channels, a lack of communications privacy also exists in these systems.

1.2.3 Objectives of PCS

The success and limitation of mobile cellular systems created the demand for a new generation of personal communication networks. As early as 1987, Cox [7] already gave a detailed description of the emerging systems. At that time, FCC has not decided on the spectrum for PCS yet. Specifications on the technologies for PCS can be found in the later papers[8],[37],[75].

The aim of PCS is to make communications truly personal, and to resolve the capacity saturation problem in current cellular systems. The inherent limitations in the approaches discussed previously suggest some objectives for PCS. These objectives include the following:

- Quality, Cost, Reliability Equivalent to Wireline Telephone:
  - two way duplex
  - low noise and crosstalk

  - high circuit availability
  - cost comparable to wire line service.

- Ubiquitous Integrated Services for all Portable Telephones and Data Terminals:
  - compatible systems in residences and offices
  - integrated voice and data transmission
  - one user identification applicable anywhere
  - large service regions.

- Privacy and Security Equivalent to Wireline Telephone Networks
  - encrypted radio links.

- Small Lightweight Easy to Use Portable Telephones and Data Terminals:
  - low power consumption

- Automatic Coordinated Frequency Reuse
  - efficient use of radio spectrum.

- Small Unobtrusive Fixed Radio Ports Connected to Telephone Networks:
  - low power
  - short antenna poles in residential areas
  - connected to and controlled by wireline telephone networks.

- Safety of Users from Strong Electromagnetic Fields
  - low transmitted power.

Some features of CRT system will be retained in PCS, such as the cell structure, hand off scheme, duplex channels for uplink and downlink, two licenses for separate

companies in each service area, etc. However, PCS is not a simple extension of CRT. The key difference is the frequency band and the cell size. The frequency band allocated by FCC for PCS will be in the 1.8 $\sim$ 2GHz, and potentially other higher bands will be assigned. The cell size of PCS will be just a few hundred meters, accompanied with the low transmission power(around 10mW). The same spectrum can be reused more frequently in different geographical area compared with that of cellular systems, therefore a much higher capacity is expected.

Digital techniques will be adopted to boost the capacity, in the way of speech compression, channel coding, and the implementation of system optimization algorithms. TDMA and CDMA are the two major candidate methods. Their relative advantages and disadvantages discussed in CRT be largely preserved for the PCS.

1.2.4 Review of work on CDMA and its implementation to CRT and PCS

Using spread spectrum techniques as a multiple access method started as early as 60's. The major performance measurement is the bit-error-rate (BER). The early analysis work focused on the synchronous access, that is, all the users start a new period of their codes simultaneously, e.g. Anderson and Wintz[2]. In the late 70's, attention was focused on the performance evaluation for the asynchronous access, as represented by Pursley[70], etc. Pursley, Geraniotis, and their colleagues have done extensive foundation work on the variety of modulation scheme, the channels, and methods of spread spectrum [4], [16], [17], [18], [19], [20], [21], [22], [23]. [54], [55], [69], [70], [71]. Those models are not specifically set up for CRT or PCS environment, and all the users are assumed to have the same power. Other performance evaluation on these general models can be found in the works of Agusti[1], Dou and Milstein[11], Hegde and Stark[33], Holtzman[35], Huth[36], Turin[93], Verhulst, Mouly and Szpirglas[96], Wang and Moeneclaey[99], Weber, Huth and Batson[100].

Works on the performance evaluation of cellular CDMA system appeared much

later. Important work includes Dornstetter and Verhulst[9], Eklundh[12], Grob, etc[31], Kavehrad and Ramamurthi[43], Lam and Steel[48], Mandell[58], Milstein, Rappaport, and Barghouti[59], Stuber and Kchao[91], Turin[94]. CDMA systems can also be implemented in cellular network for data transmission, in which the throughput is also a major concern as well as BER. Analysis on this can be found in Gluck and Geraniotis[26], Morrow and Lehnert[61], Raychaudhuri[76], Sousa[90], Yang and Stuber[105].

There are also works on the improvement of detection for CDMA signals, such as Balaban[3], Elhakeem, etc[13], Kohno, etc[46], Kuehls and Geraniotis[47], Sampaio-Neto and Scholtz[80], Simon and Divsalar[87], Varanasi and Aazhang[95], and Xie, Short and Rushforth[103].

1.3 Thesis major contributions and outline

In this thesis, the feasibility of CDMA-PCS is studied. The major contributions are the following:

1. A hybrid DS/FH CDMA system for PCS is designed. By taking the advantages of the PCS configurations, this new system can prevent the conventional CDMA system from suffering two major difficulties, namely long acquisition and power control. Time slots have been introduced to further boost the system capacity.

2. The capacity of the system in which only home cell is considered is analysed. The capacity is defined as the number of users the system can accommodate when certain bit error rates are given. Code properties are the major concern here.

3. The models to analyse the system capacity including all the interference from the first layer adjacent cells are developed. Path loss and cell structures are considered, in addition to code properties.

4. Finally, the situations in which voice activity is considered are simulated.

The structure of this thesis is as follows: In chapter 2, the system design concepts are introduced. In chapter 3, the various codes available to CDMA and their properties relevant to the system capacity are discussed. In chapter 4, the bit error rate performance in the home cell is examined, and in chapter 5, the bit error rate performance with the inclusion of the interference from the adjacent cells is analyzed. In chapter 6, the conclusion for this thesis is presented.

Chapter 2

An Efficient Hybrid CDMA System for Personal Wireless Communication

Typically, the baud-rate in a CDMA system is much higher than that in a TDMA system. In digital communications, this will increase the difficulty for setting up the synchronization. A major motivation of this thesis is trying to make this process easier. In this chapter, we will first introduce the acquisition problem in digital communication systems, especially in CDMA systems. Then we will discuss the important concepts in designing a hybrid CDMA system for PCS.

2.1 The Philosophy of Acquisition and Detection

The two basic problems associated with any communications system are "How does it start?" and having started, "How does it operate?" The problem of locating and connecting up with the proper communication target is called the *acquistion problem*, while the subsequent attempt to convey information in some commendable manner is the *efficient operation problem.* Typically, the acquistion problem will involve

acquisition in several different dimensions. In the case of analog RF communications, the acquistion process may simply need receiving antenna first to be pointed at the transmitter, then the receiver to be tuned to the proper frequency.

For coherent reception, a phase acquistion is also required. Synchronization should be set up in the phase of acquisition and be maintained in the phase of operation. Three general methods are used for synchronization in digital modulation schemes[86]. These methods are:

1. Use of a primary or secondary time standard.
2. Utilization of a separate synchronization signal
3. Extraction of clock information from the modulated waveform itself, referred to as self-synchronization.

In the first method, the transmitter and receiver are slaved to a precise master timing source. This method is often used in large data communication networks. Separate synchronization signals in the form of pilot tones are widely used in data communication systems. In this method, a special synchronization signal or a sinusoidal signal of known frequency is transmitted along with the information carrying modulation waveform. This can be implemented as a special pilot tone coinciding with a null of spectrum of the signaling waveform for FDMA, or a short period of time during which the synchronizing signal is transmitted for TDMA.

The self-synchronization method extracts a local carrier reference as well as timing information from the received waveforms. A typical implementation is shown in figure 2.1 by making use of a phase lock loop (PLL). The local generated carrier is compared with the received carrier, the difference in phase and frequency is fed back in voltage form to the voltage-control-oscillator(VCO) to make the error small. Then gradually the local generated carrier will be synchronized to the received signal carrier.

Acquisition for digital communications system requires more than just tuning the receiver to proper frequency. Conceptually, data stream composed by a sequence

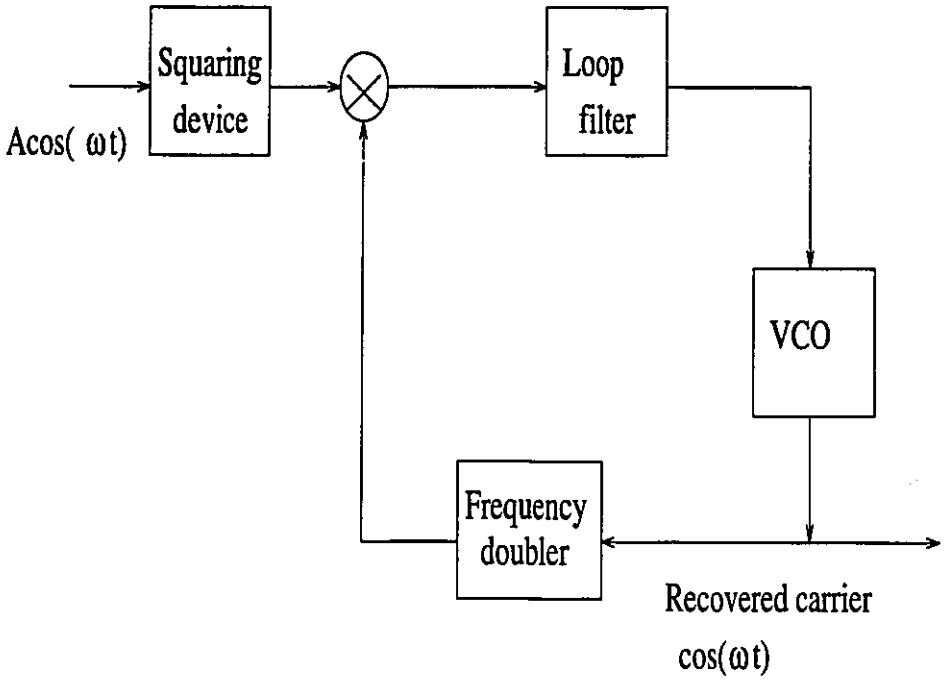

Figure 2.1: Extraction of local carrier for coherent demodulation of PSK signals

of ONE's and ZERO's or of ONE's and MINUS ONE's is transmitted as digital signals. In practice, the forms of digital signals include Amplitude Shift Key (ASK), Frequency Shift Key (FSK) and Phase Shift Key (PSK), depending on how the data bit is encoded into the analog signal wave form. For optimum demodulation of ASK, FSK and PSK waveforms, timing information is needed at the receiver. Orthogonality plays an important role in digital signal detection. Signals belonging to different users are made as orthogonal as possible to minimize the mutual interference. This is achieved by multiple access scheme, such as FDMA, TDMA or CDMA. For optimum detection, the wave form of data bits for ONE's and ZERO's are also made orthogonal in the sense:

$$\int_0^T g_i(t)g_j(t)dt = \begin{cases} 1 & \text{if} \quad i = j \\ 0 & \text{otherwise} \end{cases} \tag{2.1}$$

here $g_1(t)$ stands for the waveform of symbol ONE and $g_0(t)$ stands for the waveform of symbol ZEROs. T is the duration of symbol waveforms. The optimum receiver can be a bank of correlators, as shown in figure 2.2. The received signal $s(t)$ is correlated

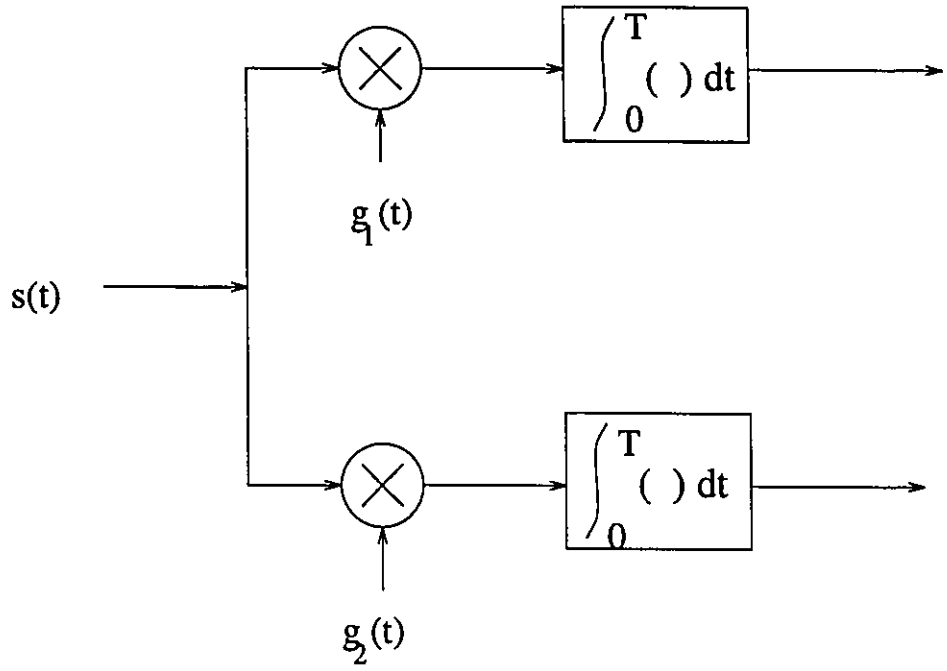

Figure 2.2: Correlator detection for digital signals

with both symbol waveforms. In a noisy environment, the branch with the larger output is assumed as the one with signal and a decision of ONE or ZERO is made correspondingly. Clearly the integration interval $(0, T)$ is crucial to the orthogonal relationship in equation (2.1). Any offset on this will move the correlators away from their optimum working status and excessive decision error will be induced. The main purpose of acquisition in digital communication is to set up synchronization to ensure the orthogonality conditions for digital signals. In practice, certain measurements must be taken to guard against possible slip in time reference. This is called *tracking*.

2.2 Operation of Acquisition and Tracking in Conventional CDMA Systems

The acquisition and synchronization of the spreading waveforms is a significant problem in spread spectrum system design. Phase/frequency synchronization is difficult

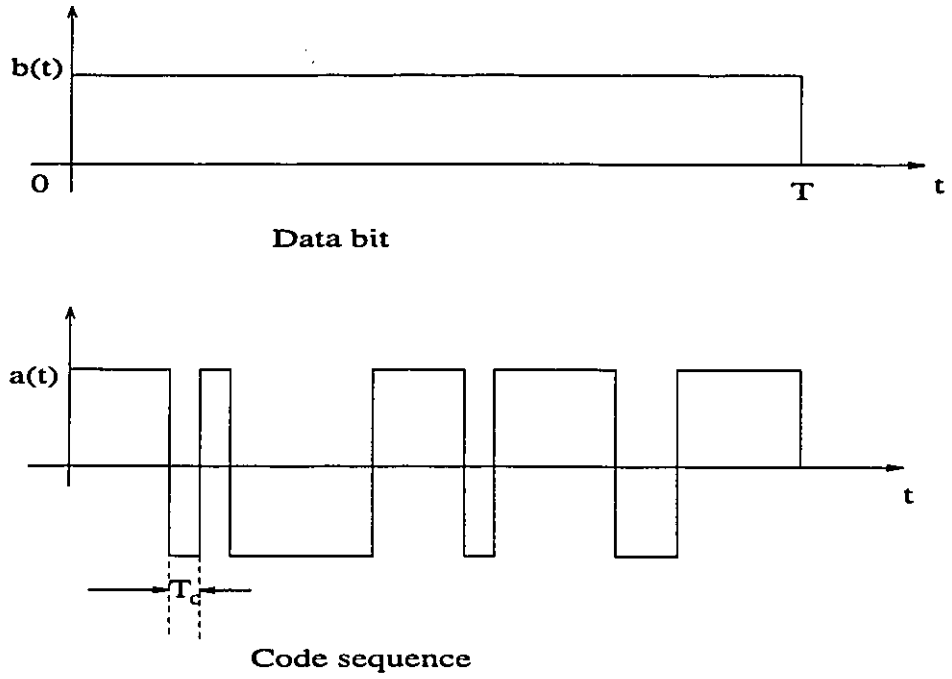

Figure 2.3: Date bit and code chip waveforms

because typical spreading waveform periods are long and bandwidths are large. Thus uncertainty in the estimated propagation delay τ translates into a large number of symbols of code phase uncertainty. The correct code phase/frequency must be found quickly using the minimum amount of hardware possible. In many cases this process must be accomplished at very low signal-to-noise ratios.

We first consider the case of DS-CDMA system. Let $a_i(t)$ denotes the code for the ith user, $b(t)$ denotes the data bits, T is the data bit duration and T_c is the chip duration. Usually $T \gg T_c$, and T_c is chosen such that the ratio T/T_c is an integer number and equals to the period of the code sequence, as shown in figure 2.3 To detect a signal from a multi-user environment, we need to maintain the orthogonality among user's codes in the sense:

$$R(k,i) = \int_0^T a_k(t)a_i(t)dt = \delta_{ik} \tag{2.2}$$

That is, the user's code sequences are orthogonal within one data bit duration. In practice, the locally generated code sequences for the ith user is correlated with

the incoming signals to detect the presence of ith user. However, because of the propagation delay, a time delay τ_i exists at the receiver end, and the ith code is actually $a_i(t-\tau_i)$, a delayed version of the code sequence at the receiver. Typically the code sequences have the property that for a shift of one or more chip duration, $\int_0^T a_i(t-\tau_k)a_i(t)dt \cong 0$. To demodulate the ith user's spread spectrum signal, the receiver needs to accurately estimate the delay of code sequence from the transmitter and give the same delay τ_i in the locally generated sequence to match with the ith incoming signal. This process is the major concern of acquisition for DS-CDMA systems. Such estimation should be precise enough to control the phase error to less than $\pm\frac{T_c}{2}$ where T_c is the PN sequence chip duration, so it can pass both the received code and locally generated code to the tracking loop.

The same principles holds for FH-CDMA systems. During the acquisition phase, the receiver needs to estimate the delay of code which control the frequency hopping pattern such that it can be tuned to the proper frequency at the right time. If the timing error is less than one hopping interval, the acquisition part has finished it work and the tracking loop can be started.

It is possible, in principle, for spread-spectrum receivers to use matched filter or correlator structures to synchronize to the incoming waveform. Consider, for example, a direct-sequence amplitude modulation synchronization system as shown in figure 2.4. In this figure, the locally generated code $a(t)$ is available with delays spaced one-half of a chip($T_c/2$) apart to ensure correlation. If the region of uncertainty of the code phase is M chips, $2M$ correlators are employed. If no information is available regarding the chip uncertainty and the PN sequence repeat every N chips, then $2N$ correlators are employed. Each correlator is seen to examine λ chips, after which the correlator outputs $V_0, V_1, \cdots, V_{2N-1}$ are compared and the largest output is chosen. As λ increases, the probability of making an error in synchronization decreases; however, the acquisition time increases. Thus λ is usually chosen as a compromise between the probability of a synchronization error and the time to acquire PN phase.

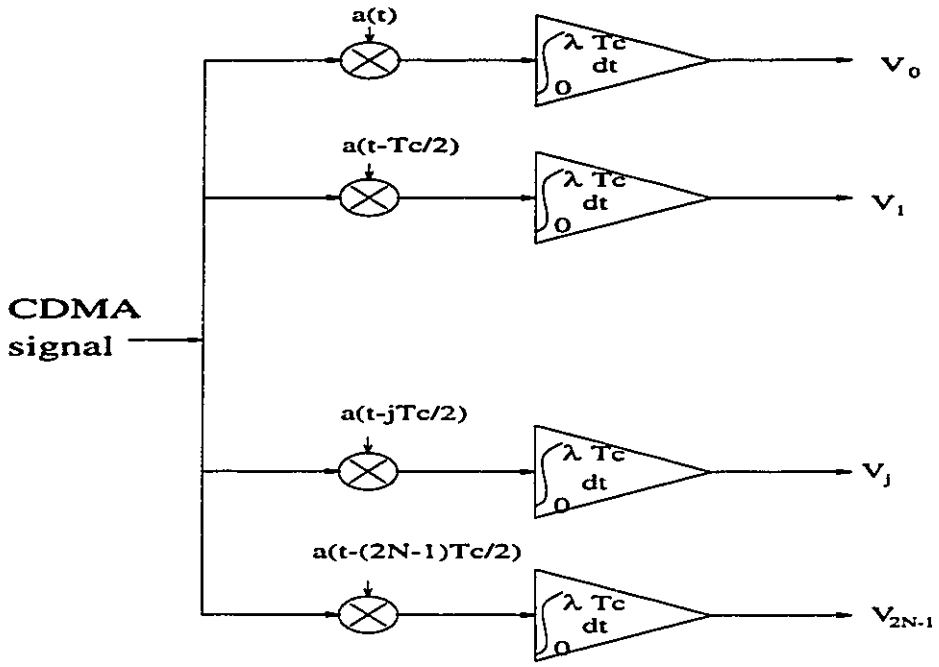

Figure 2.4: Parallel match filters for DS-CDMA systems

A second example, in which FH synchronization is employed, is shown in figure 2.5. Here the spread-spectrum signal hops over m distinct frequencies. Assume that the frequency-hopping sequence is $f_1, f_2, \cdots, f_m$ and then repeats. The correlator thus consists of m mixers, each followed by a bandpass filter and square law detector. The delays are inserted so that when the correct sequence appears, the voltages $V_1, V_2, \cdots, V_m$ will occur at the same instant of time at the adder and will, therefore, with high probability, exceed the threshold level indicating synchronization of the receiver to the signal.

While the above technique of using a bank of correlators or matched filters provides a means for rapid acquisition, a considerable reduction in complexity, size, and receiver cost can be achieved by using a single correlator or a single matched filter and repeating the procedure for each possible sequence shift. However, these reductions are paid for by the increased acquisition time needed when performing a serial rather than a parallel operation. There is a tradeoff between the number of parallel correlators(or matched filters) used and the cost and time to acquire.

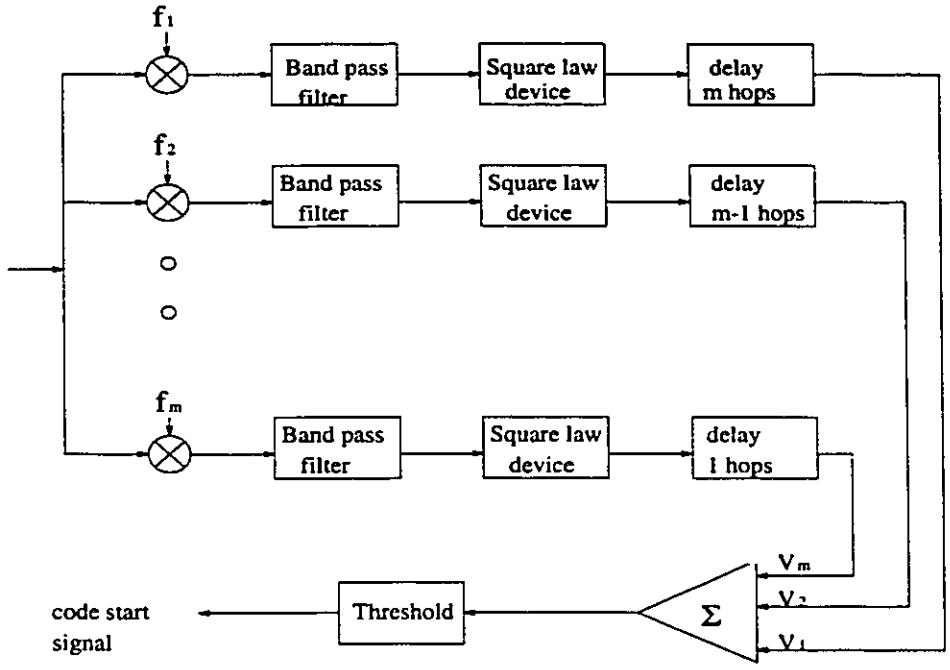

Figure 2.5: Passive correlator structure for a frequency-hopping coarse acquistion scheme

One popular method of acquisition is called the *sliding correlator* and is shown in figure 2.6. A single correlator is used rather than a correlator bank. Initially, the output phase k of the local PN generator is set to $k = 0$ and a partial correlation is performed by examining λ chips. If the integrator output falls below the threshold and therefore is deemed too small, k is set to $k = 1$, and the procedure is repeated. The determination that acquisition has taken place is made when the integrator output V_I exceeds the threshold voltage $V_T(\lambda)$.

It should be clear that in the worst case, we may have to set $k = 0, 1, 2, \cdots, 2M-1$ before finding the correct value of k. If, during each correlation, λ chips are examined, the worst case acquistion time is

$$\max\{T_{acq}\} = 2\lambda M T_c \tag{2.3}$$

In the $2M$-correlator system, $\max\{T_{acq}\} = \lambda T_c$, and so we see there is a time-complexity tradeoff.

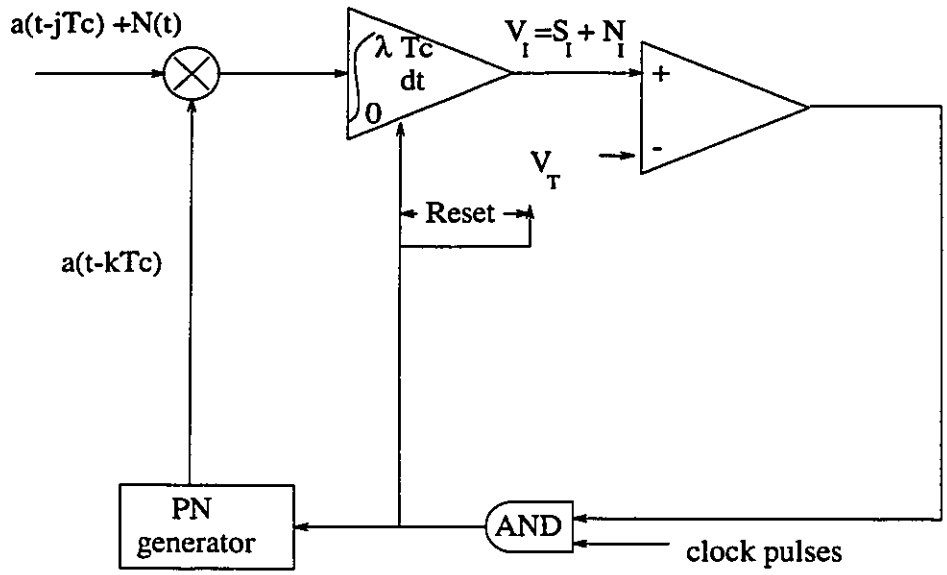

Figure 2.6: The sliding correlator

One can approximately calculate the mean acquistion time of a parallel search acquistion system, such as the system shown in figure 2.4, by noting that after integrating over λ chips, a correct decision will be made with probability P_D where P_D is the probability of detection. If, however, an incorrect output is chosen, we will, after examining an additional λ chips, again make a determination of the correct output. Thus, on the average, the acquistion time is

$$\begin{aligned} \overline{T}_{acq} &= \lambda T_c P_D + 2\lambda T_c P_D(1-P_D) + 3\lambda T_c P_D(1-P_D)^2 + \cdots \\ &= \frac{\lambda T_c}{P_D} \end{aligned} \tag{2.4}$$

Calculation of the mean acquistion time when using the "sliding correlator" shown in figur 2.6 can be accomplished in a similar way by noting that we are initially offset by a random number of chips Δ. After the correlator finally "slides" by these Δ chips, acquisition can be achieved with probability P_D. If, due to an incorrect decision, synchronization is not achieved at that time, M additional chips must then be examined before acquisition can be achieved(again with probability P_D).

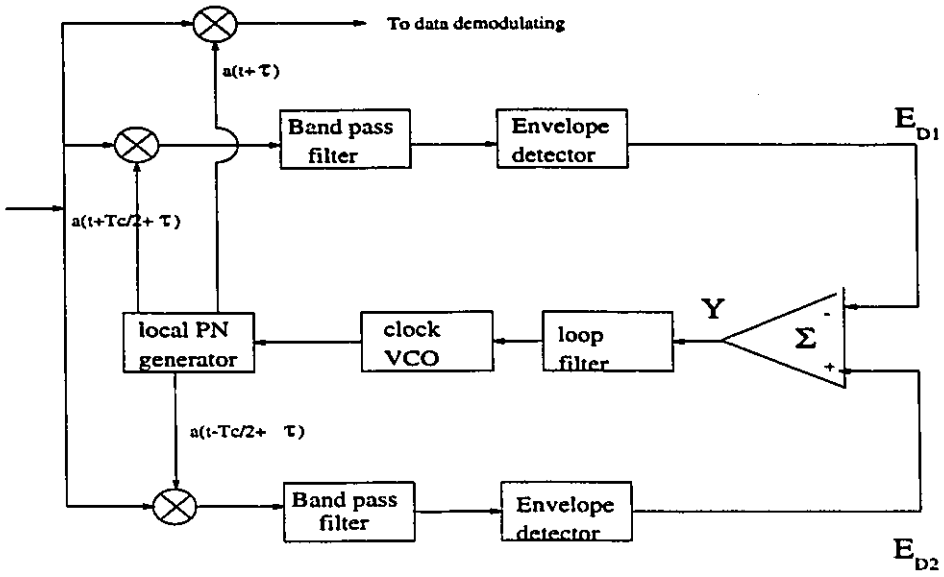

Figure 2.7: Delay locked loop for tracking direct-sequence PN signals

The mean time to acquire a signal can be written as(see Pickholtz, et. al. [65])

$$\overline{T}_{acq} = M(\lambda + \frac{1}{2})T_c + \frac{\lambda T_c P_F}{(1-P_F)^2} + \frac{1-P_D}{P_D}[2M(\lambda + \frac{1}{2})T_c + \frac{\lambda T_c P_F}{(1-P_F)^2}] \qquad (2.5)$$

where P_F is the false alarm probability.

Once acquisition, or coarse synchronization, has been accomplished, tracking, or fine synchronization, takes place. The basic tracking loop for a direct sequence spread spectrum system using PSK data transmission is shown in figure 2.7. The incoming carrier at frequency f_c is amplitude modulated by the product of the data $b(t)$ and the PN sequence $a(t)$. The tracking loop contains a local PN generator which is offset in phase from the incoming sequence $a(t)$ by a time τ which is less than one half the chip time. To provide "fine" synchronization, the local PN generator generates two sequences, delayed from each other by one chip. The two bandpass filters are designed to have a two sided bandwidth B equal to twice the chip rate,

$$B = 2/T_c \qquad (2.6)$$

In this way the data are passed, but the product of the two PN sequences $a(t)$ and $a(t \mp T_c/2 + \tau)$ is averaged. The envelope detector eliminates the data since $|a(t)| = 1$.

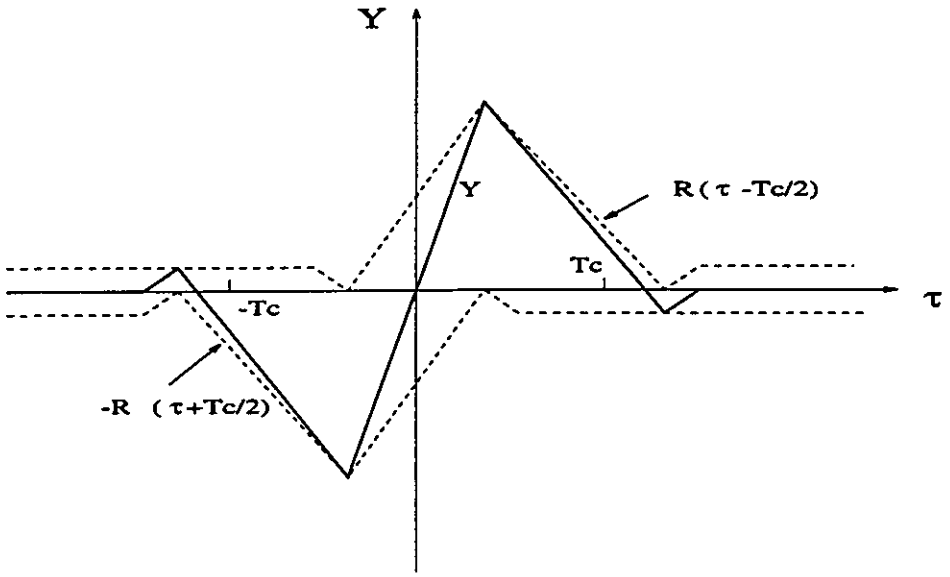

Figure 2.8: Variation of Y with τ

As a result, the output of each envelope detector is approximately given by

$$E_{D1,2} = \overline{|a(t)a(t \pm \frac{T_c}{2} + \tau)|} = |R(\tau \pm \frac{T_c}{2})| \tag{2.7}$$

where $R(x)$ is the autocorrelation function of the PN waveform. The output of the adder $Y(t)$ is shown in figure 2.8.

We see from this figure that, when τ is positive, a positive voltage, proportional to Y, instructs the VCO to increase its frequency, thereby forcing τ to decrease. On the other hand, when τ is negative, a negative voltage instructs the VCO to reduce its frequency, thereby forcing τ to increase toward 0.

When the tracking error τ is made equal to zero, an output of the local PN generator $a(t + \tau) = a(t)$ is correlated with the input signal $a(t)b(t)cos(\omega_c t + \theta)$ to form

$$a^2(t)b(t)cos(\omega_c t + \theta) = b(t)cos(\omega_c t + \theta) \tag{2.8}$$

This despread PSK signal is input to the data-demodulator where the data are detected.

2.3 Saving of acquisition

From the discussion in the previous section, we have shown that acquisition part is an essential part in a CDMA system for detecting the presence of a user's signal. This is the fundamental difference from TDMA or FDMA systems. The acquisition procedure can affect the performance of the system seriously, in the way of loss of efficiency when setting up a link.

Let's consider the case of using DS-CDMA for PCS systems. The assumed bandwidth for up-link (user to base station) is 50 MHz. The transmission bandwidth for users is 10 KHz. If one period of code sequence is embedded in one data bit, the period of code should equal to 5000, in order to spread over the whole bandwidth. If user's access is random, the uncertainty of delays is equal to the period of the code sequence, since the receiver has completely no knowledge about WHEN and WHERE the transmitter started signaling. By assuming an ideal case when $P_F = 0$ and $P_D = 1$, and $\lambda = M = N$ where N is the period of the code sequence, the mean acquisition time from equation (2.5) is

$$\overline{T}_{acq} \approx 5000 \times 5000 T_c \tag{2.9}$$

or equivalently, it will take the time of transmitting 5000 data symbols to finish acquisition on average. For some applications like data communications which has the bursty traffic, the overhead is too large to be acceptable.

If the receiver knows when the transmitter starts, it is possible to reduce the uncertainty region to $M < 1$ for the PCS systems. In this case, the uncertainty is caused by propagation delays, and the maximum delay is bounded by the size of the cell. If we can control the chip duration, we can effectively control the searching region for the phase of the code sequence. The idea is shown in figure (2.9). The observation to the above arguments is as follows: The spatial duration of a chip is $L = cT_c$ where c is the speed of light. Generally the users are randomly distributed inside the cell, with a mean distance of $\frac{R}{2}$ to the base station. Without knowing the

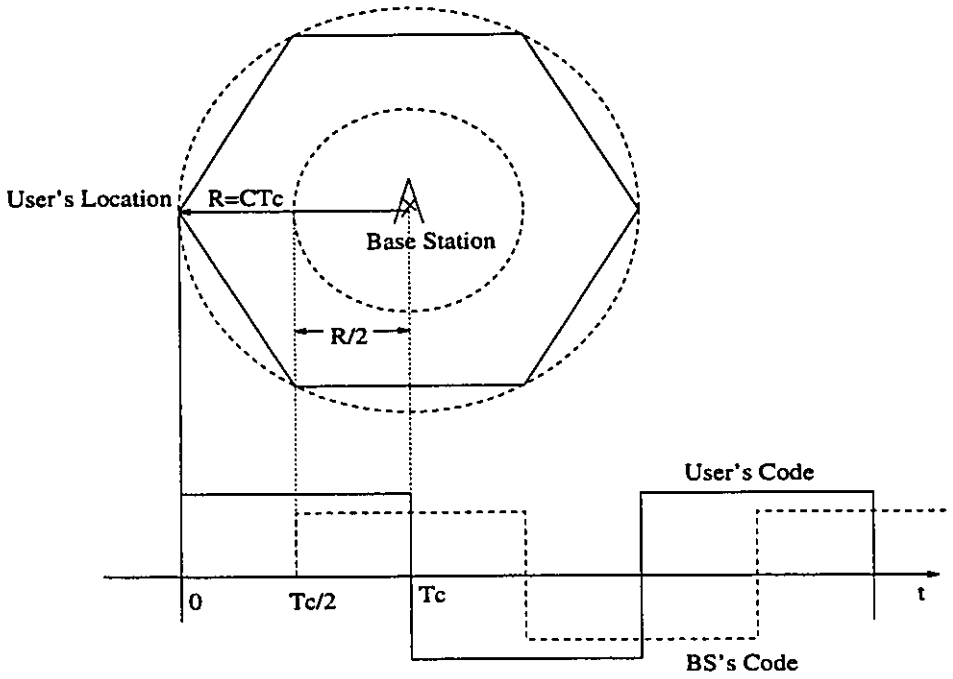

Figure 2.9: The maximum propagation delay caused by a user at the boundary. Base station always delays its code by $\frac{T_c}{2}$. If cT_c, the spatial duration of the chip, is equal to R, then the maximum phase difference will be less then $\frac{T_c}{2}$.

precise locations of users, the base station can assume that there is a mean delay of $\frac{R}{2c}$ and purposely postpone its locally generated codes by the mean delay time behind the common time reference. Suppose that L is made equal to the radius of the cell, R. In the extreme case, if a user is on the boundary of the cell, as shown in figure (2.9), the maximum delay between the received code sequence and the locally generated code sequence at the base station will be under $\frac{T_c}{2}$. On the other hand, if a user is very close to the base station, the delay can be $-\frac{T_c}{2}$, or actually the locally generated code sequence lags behind the received signal. In both extreme cases, the maximum phase error between the received sequence and the locally generated sequence is controlled under half of the chip duration.

The tracking loops can trace the phase error within the $\pm\frac{T_c}{2}$. Under such circumstances, the acquisition may not be necessary, and we can directly start the tracking process in setting up the communication. However, this sets the restriction of chip duration to be $T_c \geq \frac{R}{c}$, and the chip rate satisfying the above condition may not cover the whole spectrum. As we have discussed in chapter 1, the major advantages of CDMA such as the frequency diversity, voice activity cycle, etc, come from spreading each user's signal to excessively wide bandwidth. To make full use of these advantages, frequency hopping can be introduced to cover the total spectrum. As we will show later, only slow frequency hopping is needed, that is, the hopping interval can be longer than the data bit duration, and can be much longer than the chip duration. This makes the acquisition of hopping pattern even easier than that of direct sequence.

As a summary to this point, we can break a long and difficulty acquisition problem into two easy and parallel steps, namely the acquisition in direct sequences and the acquisition in hopping patterns, by introducing the hybrid DS/SFH techniques. Furthermore, we have found that by making the chip spatial duration comparable to the radius of small PCS cells, the maximum phase errors between the received direct sequence codes and frequency hopping patterns, and the locally generated counterparts

can be controlled to the level at which the tracking loops can be directly activated. Therefore virtually no acquisition is need in this hybrid system. On the other hand, a high processing gain is still kept.

2.4 Time Slot and Synchronous Access

Another crucial condition for eliminating the acquisition time is that the receiver and the transmitter must have the same time reference, or the receiver "knows" when to start the code generator. This is achievable through master-slave network architecture, by letting the clock of base station dictate the users' clock. A timing signal can be sent out from base station periodically to provide the time reference.

In a CDMA environment, it is much more beneficial to coordinate all the users using the same time reference, rather than to have the base station provide the time reference for each individual users. If all the users start a new period of code sequence at the same time, the orthogonality among the users' codes can be maintained, as required in equation (2.2). This is the optimum status of a CDMA system since the mutual interference among users is reduced to a minimum. Access in such a manner is called *synchronous access.*

Time slots should be implemented for a synchronous-access network. It is mandatory for transmitters to start transmitting only at the beginning of each time slot. There are some considerations in choosing time slot. The ratios of hopping interval, bit duration and chip duration must be integer numbers such that one time slot can manage synchronization at different levels. Data bit duration T can be a natural choice, such that one bit is transmitted in each time slot. Since each bit is multiplied by one period of code sequence, equation (2.2) is satisfied. Time slot can be as wide as T_h, the hopping time interval. It is easier to manage the hopping patterns so that the users having the same hopping pattern will always stay together in frequency. This will avoid the collision and near-far problem, as we will discuss in the next section.

In practice, even if time slots are employed, equation (2.2) can only be approximately satisfied for the up-link. First, some codes such as PN codes are not perfectly orthogonal. More on this will be discussed in chapter 3. More importantly, a residual in equation (2.2) still exists as the random propagation delays occur due to the random locations of transmitters, even for orthogonal codes. We call this case *quasi-synchronous access.* For the down-link (base station to users) communication, however, perfect synchronization is achievable in the time slot environment, since all signals transmitted from base station reach a particular user via the same route.

In the hybrid DS/FH CDMA system, each transmitter is identified by two codes. One is used for implementation of the direct sequence, while the other is used to control the frequency hopping pattern. The difference in any of them yields a different and ideally an orthogonal link. We call these two codes the ID codes for each transmitter. In CDMA system, the ID codes are only temporarily assigned to a user when a call is set up, and may be required to be changed during the communication. However, modern technology of shift register and microprocessor make such a change in code easy and fast.

We assume that narrow-band paging channels are available in the system, as in the case of cellular systems. The operating procedure of the proposed system is as follows: When a user wants to initiate a call, his handset signals the base station via the paging channels. The base station checks the traffic within the cell, and if the system is capable to accommodate this new user, the base station will send the ID codes through the paging channel for that user, and itself will start these codes within the next time slot with a delay of $\frac{R}{2C}$. After receiving the ID codes, the user's handset will activate its code generators at the begining of the next time slot. Ignoring the reaction time in the handset, in the case of $L = R$, the phase errors between the handset and the base station will be controlled below $\pm\frac{T_c}{2}$, so that the tracking loops in both sides can start immediately.

2.4.1 Saving the power control

Another serious problem in the implementation of the DS/CDMA systems is the so-called "near-far" problem. That is, the received power at base station from the users nearby is much stronger than that of the users in the far-end, so that the remote users may be invisible to base station since all user signals access the same bandwidth at the same time. The system capacity will be considerablely decreased by this effect. In the practical DS/CDMA systems, power control scheme is introduced to combat such a problem. The base station will monitor the power level of each signal and order the transmitters to adjust their signal such that all signals have the same power at the receiver. However, power control requires complicated hardware.

We propose a new scheme to solve this problem in this hybrid system, by taking advantage of frequency hopping. Such a scheme requires a little more complexity for base stations in the allocation of channels to the users. The allocation scheme works as following: The base station first scales the whole power range of signals to different levels. Ideally, users with the same power will have the same distance to base station, so that they are all located on a ring, as shown in figure (2.10). More users can be found on a larger ring if all users are uniformly distributed in the cell, and the number of users on each ring is proportional to the radius r. Therefore the number of hopping patterns on each ring should also be proportional to the radius in order to have relatively the same number of users in each hopping pattern. The base station measures the received power from a handset and allocates to the user the hopping pattern corresponding to that measured power level. Users having similar power will use the same hopping pattern and always stay together if the hopping interval equals to the length of time slots. If no coordinations exist among the hopping patterns, there are chances that two or more hopping patterns may hop into the same frequence slot. This is called a *collision* in frequency. During a collision period, near-far problem still exists. However, the chance is inversely proportional to the number of hopping patterns. Coordinated hopping patterns such as orthogonal hopping patterns can be

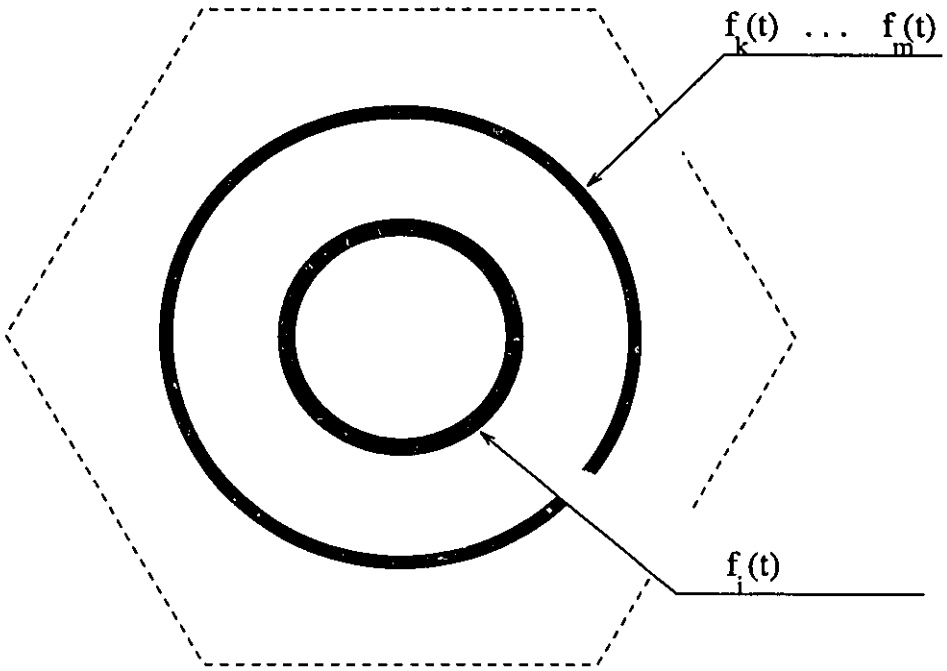

Figure 2.10: The frequency hopping patterns are associated with the power levels of the received signals, which, in turn, are determined by their distance to the base station. A larger ring will have more hopping pattern associated with it.

used to avoid the collisions. In this way, we can completely solve the near-far problem in the upper link channels.

User's power may change since they are moving, and the base station may ask the frequency hopping pattern to be changed if the power of the handset is not in the power range of the original frequency hopping pattern. Such switching or changing of code is fast, however, since there is essentially no acquisition time.

The same principle also works for the down-link channels. If we ignore the multi-path effect, by the reciprocity of the EM wave, two users will receive the same power from the base station if they deliver the same power to the base station, provided that base station uses the same transmission power for both of them.

2.5 System Design

The emerging PCS proposed uses the $1.8 \sim 2GHz$. Similar to the current cellular system, the total 200 MHz bandwidth is split for two licenses, with each taking 100 MHz. While both up-link and down-link have the same bandwidth. the total bandwidth of spread spectrum will be B_{ss} =50 MHz. The data rate is supposed to be R_b =10 kbps, and the cell size is supposed to be $R = 500$ in radius. Therefore to have the chip spatial duration no less than the cell radius, the chip time duration must be

$$T_c \geq \frac{R}{c} = 1.5\mu s \tag{2.10}$$

and the chip rate is:

$$R_c \leq 0.66Mbps \tag{2.11}$$

Hence we may take the $R_c = 0.63$ Mbps such that the process gain for direct sequence modulation equals

$$P_{ds} = \frac{R_c}{R_b} = 63 \tag{2.12}$$

We thus use a PN sequence of length 63 for direct sequence part. To achieve the total 50 MHz band, we use the slow frequency hopping method to obtain another process

gain:

$$P_{fh} = \frac{B_{ss}}{2R_c} \approx 40 \tag{2.13}$$

Therefore we have total 40 different frequency patterns. The total process gain is the product of the two,

$$P_{total} = P_{ds}P_{fh} = \frac{B_{ss}}{R_b} = 2500 \tag{2.14}$$

For each frequency hopping pattern, the number of users we can put in is limited by the DS modulation. As pointed out by Gilhousen *et al*[2], the capacity is about the same as the process gain of the direct sequence. If we use orthogonal hopping patterns, the total capacity is simply the capacity of DS modulation multiplied by the number of hopping frequencies, which is the same as the total process gain. In the particular case above, we can put approximately 2500 users in one cell based on that estimation.

A block diagram of a hybrid DS-FH system is shown in figure (2.11). In the transmitter, the CDMA modulation is realized by two steps. First, the data is modulated by the code sequence to get the DS modulation. Following that it is modulated again by a frequency hop sequence. A band pass filter removes the redundant frequency band. At the receiver, the demodulation is also realized by two steps, in the opposite order.

2.6 Spectrum of the Proposed System

It is interesting to examine the spectrum of above system. Using the system model given by fig. 2.11, the spectrum of the final output from transmitter is the convolution of the spectrum of DS-modulated signal with the spectrum of frequency hopping pattern. In the case $T_b \gg T_c$, the spectrum of DS signal is simply the same as that of PN sequence, i.e.:

$$S_{ds}(f) = \frac{T_c}{2}\{sinc^2[(f - f_0)T_c] + sinc^2[(f + f_0)T_c]\} \tag{2.15}$$

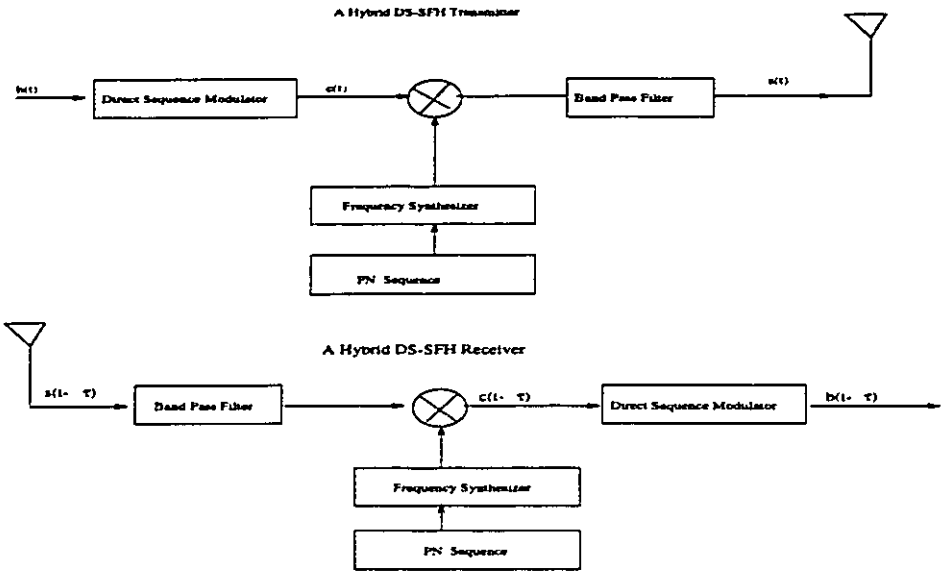

Figure 2.11: Transceiver models for DS-FH systems

It is much more complicated to evaluate the spectrum of hopping patterns. For a periodic deterministic hopping, the same frequency will be used every $T_0 = NT_h$ seconds, where N is the total number of frequencies. For one period of T_0, the hopping sequence is:

$$g(t) = \sum_{i=1}^{N} 2P_{T_h}(t - iT_h)cos(2\pi f_i t + \phi_i) \tag{2.16}$$

here pulse $P_{T_h}(t) = 1$ for $0 \leq t < T_h$ and $P_{T_h}(t) = 0$, otherwise. If ϕ_i is the same for each period when the frequency returns to f_i, the PSD function of $g(t)$ is given as:

$$S_h(f) = \frac{1}{T_0^2} \sum_{n=-\infty}^{\infty} |G(\frac{n}{T_0})|^2 \delta(f - \frac{n}{T_0}) \tag{2.17}$$

where $G(f)$ is the Fourier transform of $g(t)$ given as:

$$\begin{aligned} G(\frac{n}{T_0}) &= \frac{T_h}{2} \sum_{i=1}^{N} \{sinc[(\frac{n}{T_0} - f_i)T_h]exp[-j2\pi(\frac{n}{T_0} - f_i)(2i-1)T_h]exp(j\phi_i) \\ &\quad + \{sinc[(\frac{n}{T_0} + f_i)T_h]exp[-j2\pi(\frac{n}{T_0} + f_i)(2i-1)T_h]exp(j\phi_i) \end{aligned} \tag{2.18}$$

However, if ϕ_i is random for different period, $g(t)$ is not a periodic function, and the PSD of frequency hopping is given as:

$$S_h(f) = T_h \sum_{i=1}^{N} \{sinc^2[(f - f_i)T_h] + sinc^2[(f + f_i)T_h]\} \tag{2.19}$$

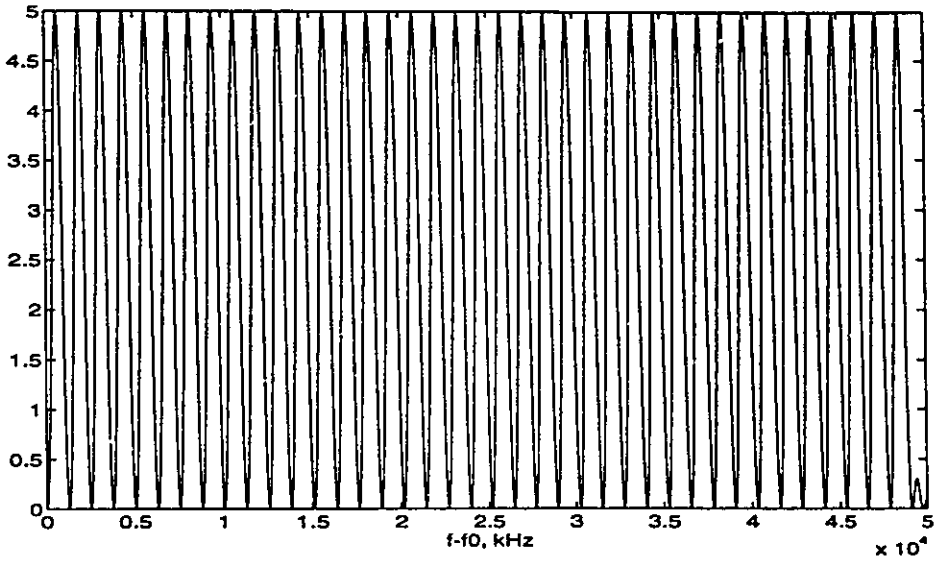

Figure 2.12: Spectrum of DS-SFH systems

where N is the total number of frequencies. Since $T_h \gg T_c$, each sinc function inside the $S_h(f)$ is just like a δ function compared with the sinc function of S_{ds}. If the minimum interval of the two adjacent frequencies in S_h is about the same width of S_{ds}, then the S_{ds} is just like a comb of δ functions.

The spectrum of the final modulated signals is the convolution of the two power spectral density functions,

$$S(f) = S_h(f) \bigotimes S_{ds}(f) \tag{2.20}$$

In the positive frequency part, it is

$$S(f) = T_c T_h \sum_{i=1}^{N} sinc^2[(f - f_i)T_h] \bigotimes sinc^2[(f - f_0)T_c] \tag{2.21}$$

The spectrum is shown in figure 2.12, from which we can see that it indeed covers the whole 50 MHz band. However, the spectrum is not fully filled due to the shape of sinc function. This is the result of rectangular pulse shape. Other kind of pulse such as the raise cosine pulse will give a different spectrum.

2.7 Summary of the chapter

One major objective in our design is to make the acquisition of code sequence easier in the receiver such that the received signal can be directly sent to the tracking loop. This is achievable due to the small cell size in PCS and carefully selected chip duration. Another necessary condition is the synchronization between transmitter and receiver. We have argued that by using time slots, not only that the condition is satisfied, but also the orthogonality among users' access is also maintained. In practice, it is required to deliver integer number of data bits in each hopping interval. Thus the hopping interval provides a natural time slot for the system.

On the other hand, to keep a high processing gain, we have used the technology of hybrid DS/FH CDMA. To spread over the same bandwidth we need lower chip rate and hopping rate compared to the systems using only either of these technologies. Solving the "near-far" problem is an important application of this hybrid technology. This system also has some other advantages. It inherits essentially all the advantages of CDMA systems such as the immunity to multi-path interference and frequency selective fading. Fast hand-off from cell to cell is an advantage which follows directly from the fast acquisition feature. Such an advantage is more appreciated for small cells where the hand-off happens more often. Fast hand-off also makes it easier to implement more effective hand-off algorithms.

Other advantages include the flexibility of the system. Since we have a two stage spectrum spreading, we gain more room to manoeuver the fitting of different system configurations. Such a system can easily solve the problem of coexisting with the fixed microwave users whose transmission bands overlap with the allocated spectrum of PCS, by simply skipping these occupied bands in the frequency hopping.

We list the major features of this system as follows:

- Fast acquisition
- No power control

- Synchronous multi-user access at chip level

The system capacity discussed in this chapter, however, is a rough estimation. A system plan requires far more detailed estimation based on the received signal quality. In digital communications, system capacity is evaluated as the maximum number users at a given ratio of signal bit energy to noise power density, and the bit error rate. This is the major objective we will explore in the following chapters.

Chapter 3

Code Properties

In CDMA systems, especially for DS-CDMA systems, mutual interferences depend on the orthogonality among user's codes, which in turn, depend on the cross-correlation property of the codes. However, in the situation of imperfect synchronous access, cross-correlation of codes often evaluated only in part of the period. In this chapter, we will introduce the basic concepts for evaluating the quality of codes which affects the performance of CDMA systems.

3.1 Model of a DS-CDMA system

Consider a simple PSK-CDMA system model shown in figure 3.1 for K simultaneously transmitting users. Since in PSK modulation, the ONE is represented by phase 0° and MINUS ONE is represented by phase 180°, it is equivalent to multiply ONE or MINUS ONE directly to the amplitude of the carrier. The ith user's data signal $b_i(t)$ is a sequence of positive and negative pulses of duration T and unit amplitude

$$b_i(t) = \sum_{l=-\infty}^{\infty} b_l^{(i)} P_T(t - lT) \tag{3.1}$$

where $b_l^{(i)} \in \{+1, -1\}$ denotes the ith user's information bit stream and pulse $P_T(t) = 1$ for $0 \leq t < T$ and $P_T(t) = 0$, otherwise.

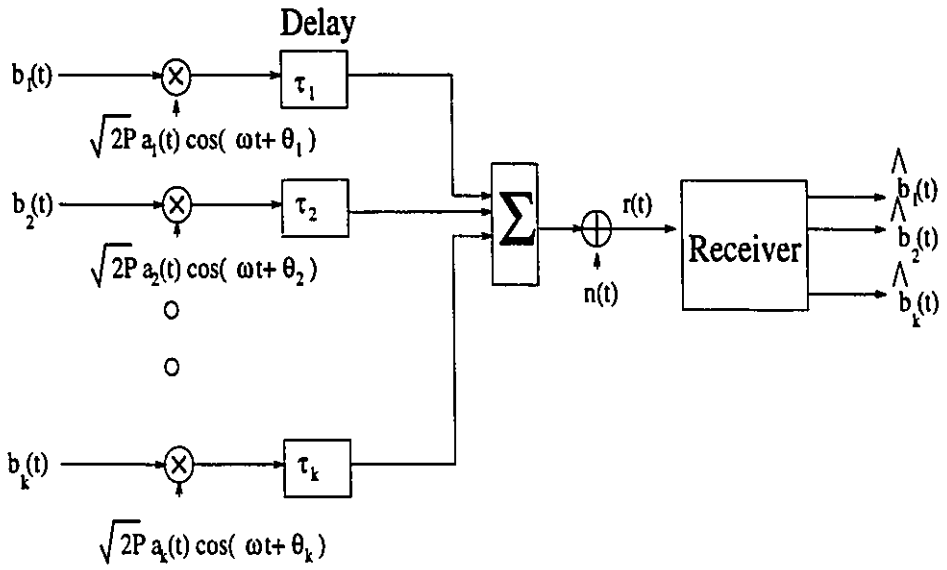

Figure 3.1: A model of DS-CDMA system

The code wave form which binary phase modulates the user's RF carrier frequency can be expressed as

$$a_i(t) = \sum_{j=-\infty}^{\infty} a_j^{(i)} P_{T_c}(t - jT_c) \tag{3.2}$$

where $\{a_j^{(i)}\}$ represents the discrete code sequence of the ith user, and has period $N = T/T_c$ and elements of $\{+1, -1\}$.

For an asynchronous system where no timing reference for the K users is assumed, the received signal at the message destination can be expressed as

$$r(t) = \sum_{i=1}^{K} \sqrt{2P} a_i(t - \tau_i) b_i(t - \tau_i) \cos(\omega t + \phi_i) + n(t) \tag{3.3}$$

Here $n(t)$ represents the channel noise which we assume to be a white gaussian process with two-sided spectral density $N_0/2$, ω represents the common RF center frequency and P the common signal power.

If the received signal $r(t)$ is the input to a synchronized correlation receiver matched to the ith user signal, the output at sample moment $t = T$ is

$$\begin{aligned} Z_i(T) &= \int_0^T r(t)a_i(t)\cos\omega t dt \\ &= \sqrt{\frac{P}{2}}\{b_{i,0}T + \sum_{k=1,k\neq i}^{K} I_{k,i}(\tau_k)cos\phi_k\} + \int_0^T n(t)a_i(t)\cos\omega t dt \end{aligned} \tag{3.4}$$

where $\phi_k = \theta_k - \omega\tau_k$, and $I_{k,i}(\tau_k)$ equals

$$I_{k,i}(\tau_k) = b_{k,-1}R_{k,i}(\tau_k) + b_{k,0}\hat{R}_{k,i}(\tau_k) \tag{3.5}$$

here $b_{k,0}$ denotes the current data bit of the kth user, and $b_{k,-1}$ denotes the former data bit of the kth user. Since $b_{k,0}$ and $b_{k,-1}$ may have difference signs, the correlation may have to be broken into two parts. $R_{k,i}$ and $\hat{R}_{k,i}$ are the continuous-time partial cross-correlation functions

$$R_{k,i}(\tau) = \int_0^\tau a_k(t-\tau)a_i(t)dt \tag{3.6}$$

$$\hat{R}_{k,i}(\tau) = \int_\tau^T a_k(t-\tau)a_i(t)dt \tag{3.7}$$

and can be written as:

$$R_{k,i}(\tau) = C_{k,i}(l-N)T_c + [C_{k,i}(l+1-N) - C_{k,i}(l-N)](\tau - lT_c) \tag{3.8}$$

and

$$\hat{R}_{k,i}(\tau) = C_{k,i}(l)T_c + [C_{k,i}(l+1) - C_{k,i}(l)](\tau - lT_c) \tag{3.9}$$

where l is defined by $0 \leq lT_c \leq \tau \leq (l+1)T_c \leq T$, and the aperiodic cross-correlation function $C_{k,i}$ for the sequences $(a_j^{(k)})$ and $(a_j^{(i)})$ is defined by

$$C_{k,i}(l) = \begin{cases} \sum_{j=0}^{N-1-l} a_j^{(k)}a_{j+l}^{(i)}, & 0 \leq l \leq N-1 \\ \sum_{j=0}^{N-1+l} a_{j-l}^{(k)}a_j^{(i)}, & 1-N \leq l \leq 0 \\ 0, & |l| \geq N \end{cases} \tag{3.10}$$

It is clear now that the interference contributed from the kth signal to the output Z_i is $I_{k,i}(\tau_k)cos\phi_k$ If the synchronization of access is achievable, that is, all $\tau_k = 0$, then $\hat{R}_{k,i}$ will disappear from equation (3.4). The interference is then caused only by the residual of the cross-correlation functions $R_{k,i}$. It can be expressed in discrete form

$$\theta_{k,i}(l) = \sum_{j=0}^{N-1} a_j^{(k)} a_{j+l}^{(i)} \tag{3.11}$$

Notice that $\theta_{k,i}(l) = C_{k,i}(l) + C_{k,i}(l-N)$, for any integer l so that $0 \leq l < N$. To reduce the inter-user interference, we need to choose the "good" codes such that $\theta_{k,i}$ can be as small as possible. Orthogonal codes are the optimum codes, whose $\theta_{k,i} = 0$.

However, in land mobile radio communications, the perfectly synchronous access is not generally feasible for up-link. First, the users may initiate their call randomly, if no time reference is provided. Secondly, even if there is time reference, random propagation delays still exist at the receiver side due to the random location of users. In the completely asynchronous systems, where τ_k is randomly distributed in the interval $[0, T]$, the interference is the result of both $R_{k,i}$ and $\hat{R}_{k,i}$. We may define the odd cross-correlation function

$$\hat{\theta}_{k,i}(l) = C_{k,i}(l) - C_{k,i}(l-N) \tag{3.12}$$

Thus, if $b_{k,-1}$ and $b_{k,0}$ has the same polarity,

$$I_{k,i}(\tau_k) = b_{k,-1}\{\theta_{k,i}(l_k)T_c + [\theta_{k,i}(l_k+1) - \theta_{k,i}(l_k)](\tau_k - l_k T_c)\} \tag{3.13}$$

and if $b_{k,-1}$ and $b_{k,0}$ has the opposite polarity,

$$I_{k,i}(\tau_k) = b_{k,-1}\{\hat{\theta}_{k,i}(l_k)T_c + [\hat{\theta}_{k,i}(l_k+1) - \hat{\theta}_{k,i}(l_k)](\tau_k - l_k T_c)\} \tag{3.14}$$

Since the both cases happen with the same probability, $\hat{\theta}_{k,i}$ is as important as $\theta_{k,i}$. By the same token, the good codes in asynchronous access systems are small not only in $\theta_{k,i}$, but also in $\hat{\theta}_{k,i}$.

It is interesting to examine the statistical properties of those functions. By assuming that the code sequences are i.i.d random sequences within a period, we have

$$\begin{aligned}\overline{C^2_{k,i}(N-|l|)} &= \mathrm{E}\{[\sum_{j=0}^{|l|-1} a_j^{(k)} a_{j+|l|}^{(i)}]^2\} \\ &= \sum_{j=0}^{|l|-1} \mathrm{E}\{(a_j^{(k)})^2 (a_{j+|l|}^{(i)})^2\} \\ &= |l| \end{aligned} \tag{3.15}$$

and obviously, for $l \neq m$

$$\mathrm{E}\{C_{k,i}(l) C_{k,i}(m)\} = 0 \tag{3.16}$$

As a consequence of the foregoing,

$$\overline{\theta^2_{k,i}(l)} = \overline{C^2_{k,i}(l)} + \overline{C^2_{k,i}(l-N)} \tag{3.17}$$

The important properties of the codes, $\theta_{k,i}$ and $\hat{\theta}_{k,i}$, are determined by those $C_{k,i}(l)$'s. Depending on the application, one may choose the favourable codes for a system. In the system we designed in chapter 2, we have chosen the chip spatial length to be no less than the radius of the cell. The quasi-synchronization can be achieved since the maximum of uncertainty to τ_k is less than $0.5T_c$. Therefore, in the home cell, the important parameters are $C_{k,i}(0), C_{k,i}(1)$, and $C_{k,i}(1-N)$. If the interference of the adjacent cells up-to the first tier is included, then those $C_{k,i}(l)$ with l up-to 3 (we will explain this in chapter 5) are important in our system. In the following sections, we will investigate these parameters for different codes.

3.2 Maximum Length Code

Historically, the spread spectrum communication was originated from anti-jamming and anti-interference problems. That is, the transmitter tries to hide its signal from being detected in a hostile environment. To have a low probability of interception, the codes should be noise-like. However, they can never be purely random for the

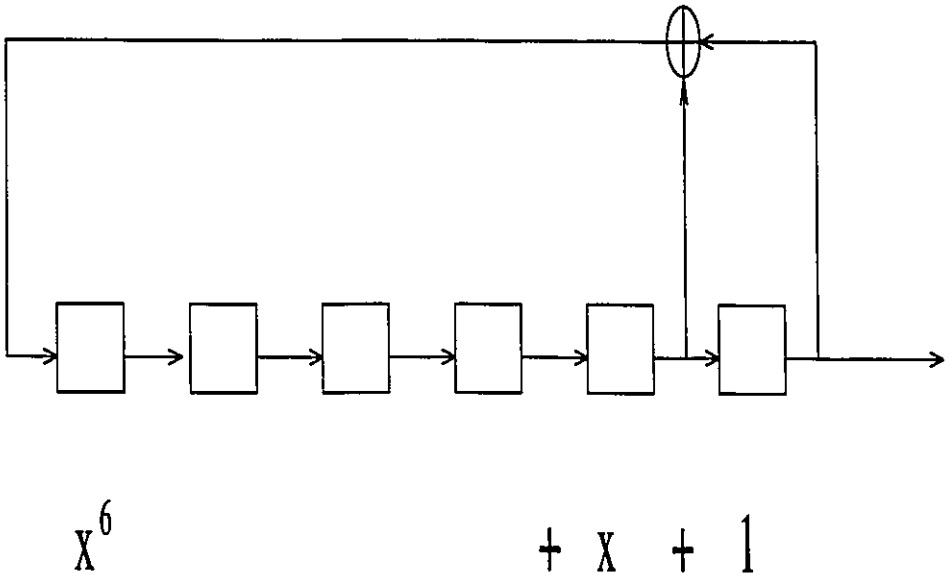

Figure 3.2: An example of shift register

purpose of despreading at the receiver. In practice, we use the pseudo-noise(PN) sequences so that the following properties are satisfied. They

- are easy to generate
- have random properties
- have long periods

Linear feedback shift register(LFSR) sequences possess those properties. Figure 3.2 shows an example of a binary LFSR with six elements. The shift register consists of binary storage elements(boxes) which transfer their contents to the right after each clock pulse (not shown). The binary (code) sequence $a(n)$ clearly satisfies the recursion

$$a(n+6) = a(n) \oplus a(n+1) \tag{3.18}$$

where $\oplus$ denotes the mod-2 adder or EXCLUSIVE-OR gate. Generally, for a LFSR with n boxes containing a 0 or 1, there are 2^n possible states for this shift register.

However, the zero state 00...0 cannot occur unless the sequence is all zeros. Thus, the maximum possible period is $2^n - 1$. The PN sequence with the period of $2^n - 1$ is called maximum length PN sequence (m-sequence).

The sequence generated by LFSR can have the polynomial representation.

$$a(x) = \sum_{i=0}^{\infty} a(i)x^i \leftrightarrow (a(0), a(1), a(2), ...) \tag{3.19}$$

and the structure of the LFSR can be represented by

$$h(x) = \sum_{i=0}^{n} h_i x^i \tag{3.20}$$

These h_i's are 1 or 0 depending on if there is a feed back or not, with h_0 and h_n always equal to 1. In the example shown in figure 3.2, the polynomial $h(x) = x^6 + x + 1$.

Let $N = 2^n - 1$, if $h(x)$ is primitive and can divide the polynomial $x^N + 1$, it is sufficient that $a(x)$ obtained by

$$a(x) = \frac{x^N + 1}{h(x)} \tag{3.21}$$

is a m-sequence.

In our system design, we are interested in the m-sequence with $N = 63$. and six sequences can be found by computer search. They are listed in Table 3.1. Those polynomials can also be represented by $h_n h_{n-1} \cdots h_0$. For example, the first polynomial can be written as 1000011, or in short form by translating into octonal number, as 103. Therefore it is also called $pn103$, as frequently appeared in the literatures, e. g., [77].

The most important property of the m-sequences is their auto-correlation function, which is defined by

$$\theta_a(i) = \sum_{j=0}^{N-1} (-1)^{a(j)+a(j+i)} \tag{3.22}$$

Then

$$\theta_a(i) = \begin{cases} N & i = 0 \\ -1 & 1 \leq i \leq N-1 \end{cases} \tag{3.23}$$

Table 3.1: Six m-sequences with period of 63

No.	h(x)
pn103	x^6+x+1
pn133	x^6+x^5+1
pn141	$x^6+x^5+x^2+x+1$
pn147	$x^6+x^5+x^3+x^2+1$
pn155	$x^6+x^4+x^3+x+1$
pn163	$x^6+x^5+x^4+x+1$

This auto-correlation function has the very desirable property that the sidelobe is very low, especially when N is large.

If more than one sequence is used, the cross-correlation functions which will play an important role in mutual interference is defined as,

$$\theta_{x,y}(l) = \sum_{i=0}^{N-1} x(i)y(i+l). \tag{3.24}$$

For each value of $\theta_{x,y}(l)$, it dependents on the relative phase shift l of the two binary sequences x, y. However, it can be shown that[78]

$$\sum_{l=0}^{N-1} |\theta_{x,y}(l)|^2 = \sum_{l=0}^{N-1} \theta_x(l)\theta_y(l). \tag{3.25}$$

As a consequence of this identity, if both x, y are the m-sequence, then the averaged $\overline{|\theta_{x,y}(l)|^2}$ is

$$\overline{|\theta_{x,y}(l)|^2} = N + \frac{N-1}{N} \tag{3.26}$$

This result is important to the interference analysis, as we will see later. For the worst case of $|\theta_{x,y}(l)|$, an upper bound can be given as

$$\begin{aligned} |\theta_{x,y}(l)| &= |\langle x, Q^l y\rangle| \\ &\leq \|x\| \cdot \|Q^l y\| \\ &= \|x\| \cdot \|y\| \\ &= \sqrt{\theta_x(0)\theta_y(0)} \end{aligned} \tag{3.27}$$

where Q is a unitary rotation matrix which causes a 1-bit left shift to the sequence y, as shown in the following:

$$\begin{bmatrix} 0 & 1 & 0 & \cdots & 0 \\ 0 & 0 & 1 & \cdots & 0 \\ \vdots & \vdots & \vdots & \ddots & \vdots \\ 1 & 0 & 0 & \cdots & 0 \end{bmatrix}. \tag{3.28}$$

As we can see from equation (3.27), if x, y are arbitrary sequences, for the worst case, $\theta_{x,y}(l)$ is equal to N, which is too large to be useful. In many cases, especially if the system is not fully loaded, one may want to improve equation (3.27) by having an optimal set of sequences with the lower cross-correlation. The search for the optimal sets is largely dependent on the properties of the m-sequences. Besides the auto-correlation property listed above, they have some other important properties:

Shift-and-add property[29]: Let u denote the m-sequence. Given distinct integers i and j, $0 \leq i, j < N$, there is a unique integer k, distinct from both i and j, such that $0 \leq k < N$ and

$$Q^i u \oplus Q^j u = Q^k u \tag{3.29}$$

Let q denote a positive integer, and consider the sequence v formed by taking every qth bit of u. The sequence v is said to be a decimation by q of u, and will be denoted by $u[q]$. Let $\gcd(a, b)$ denote the greatest common divisor of the integers a and b, we have:

Decimation property: Assume that $u[q]$ is not identically zero. Then, $u[q]$ has period $N/\gcd(N, q)$, and is generated by the polynominal $\hat{h}(x)$ whose roots are the qth powers of the roots of $h(x)$.

For $N = 63$, the decimation relationships between the six m-sequences listed in Table 3.1 is shown in figure 3.3.

If u denotes an m-sequence generated by the polynomial 103, then $v = u[5]$, $w = u[11]$, $x = u[31]$, $y = u[23]$, and $z = u[13]$ are generated by the polynomials 147, 155, 141, 163, and 133. All of the values of q above have the property $\gcd(63, q) = 1$,

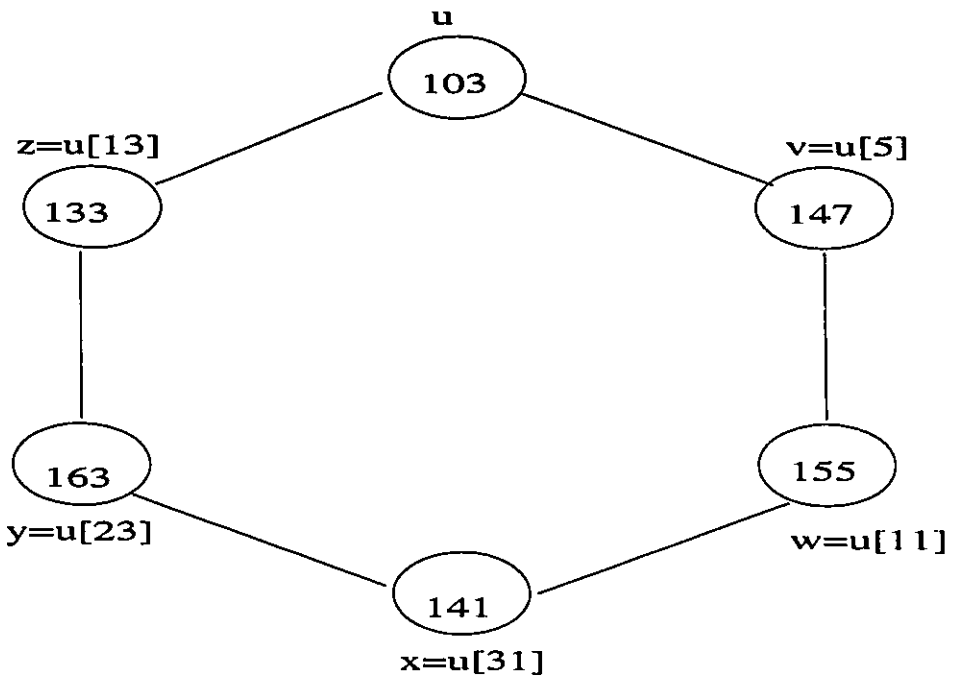

Figure 3.3: Decimation relations for m-sequence of period 63

which is called *proper decimation.* Only the sequences generated by *proper decimation* can have the period N.

Given a set χ of periodic sequences, define θ_c, the *peak cross-correlation magnitude*, by

$$\theta_c = \max\{|\theta_{x,y}(l)| : 0 \leq l \leq N-1, x, y \in \chi\} \tag{3.30}$$

and θ_a, the *peak out-of-phase autocorrelation magnitude*, by

$$\theta_a = \max\{|\theta_x(l)| : 1 \leq l \leq N-1, x \in \chi\} \tag{3.31}$$

Then Sarwate[79] has shown that if χ contains K sequences,

$$\frac{2N-1}{N}\left(\frac{\theta_c^2}{N}\right) + \frac{2(N-1)}{N(K-1)}\frac{\theta_a^2}{N} \geq 1 \tag{3.32}$$

This formula shows the trade-off relation for θ_c and θ_a in selecting the binary sequence sets.

We already know that for the m-sequence, the autocorrelation spectrum is two valued

$$\begin{array}{llll} N & \text{occurs} & 1 & \text{time} \\ -1 & \text{occurs} & N-1 & \text{times} \end{array} \tag{3.33}$$

It is much more complex for the cross-correlation spectrum, which takes on at least three values. We cite the following theorem without proof from [78], which exhibits specific decimations which produce three-valued cross-correlation spectra except when n is a power of 2.

Theorem 1: Let u and v denote m-sequence of period $2^n - 1$. If $v = u[q]$, where either $q = 2^k + 1$ or $q = 2^{2k} - 2^k + 1$, and if $e = \gcd(n, k)$ is such that n/e is odd, then the spectrum of $\theta_{u,v}$ is three valued and

$$\begin{array}{llll} -1 + 2^{(n+e)/2} & \text{occurs} & 2^{n-e+1} + 2^{(n-e-2)/2} & \text{times} \\ -1 & \text{occurs} & 2^n - 2^{n-e} - 1 & \text{times} \\ -1 - 2^{(n+e)/2} & \text{occurs} & 2^{n-e-1} - 2^{(n-e-2)/2} & \text{times} \end{array} \tag{3.34}$$

Notice that if e is large, $\theta_{u,v}(l)$ takes on large values but only very few times while if e is small, $\theta_{u,v}(l)$ takes on smaller values more frequently. In most instances, small values of e are desirable. For the example we mentioned before, let u denotes the sequence by the polynomial 105, and $v = u[5]$, then the three valued cross-correlation spectra will be:

$$\begin{array}{llll} 15 & \text{occurs} & 10 & \text{times} \\ -1 & \text{occurs} & 47 & \text{times} \\ -17 & \text{occurs} & 6 & \text{times} \end{array} \tag{3.35}$$

If we define $t(n)$ as:

$$t(n) = 1 + 2^{\lfloor (n+2)/2 \rfloor} \tag{3.36}$$

where $\lfloor \alpha \rfloor$ denotes the integer part of the real number α. Then if $n \not\equiv 0 \mod 4$, there exist pairs of m-sequences with cross-correlation functions taking on the values $-1, -t(n)$ and $t(n) - 2$. These pairs are called *preferred pair* of m-sequence. For $n = 6$, it can be shown that every pair of the sequences on the two adjacent vertices

in figure 3.3 is a preferred pair. A connected set of m-sequences is a collection of m-sequences which has the property that each pair in the collection is a preferred pair. A largest possible connected set is called a *maximal connected set* and the size of such a set is denoted by M_n. For $n = 6$, $M_n = 2$, θ_c takes on the value of 17 for maximal connected set, compared with the value of 23 for set of of all m-sequences. The difference is more significant for $n = 7$, in which case $\theta_c = 17$ for maximal connected set and $\theta_c = 41$ for the set of all m-sequence, and $M_n = 6$.

Maximal connected sets of m-sequences are useful in those applications which require only a few sequences with excellent cross-correlation and autocorrelation properties. However, some applications require larger sets of sequences. For instance, even if we assign each user a different phase of one m-sequence in one cell, we still need 3 m-sequences in order to take the advantage of voice activity circle. This is the motivation for seeking the alternatives such as the Gold sequences.

When n is even, the lower cross-correlation can be reached for reciprocal pairs of m-sequences, which yield $\theta_c = t(n) - 2$.

The aperiodic correlation functions satisfy identities analogous to those presented for θ_a and θ_c. We just list them as follows:

$$\sum_{l=1-N}^{N-1} |C_{x,y}(l)|^2 = \sum_{l=1-N}^{N-1} C_x(l)C_y(l) \tag{3.37}$$

Similarly, we have the bound

$$|C_{x,y}(l)| \leq \sqrt{C_x(0)C_y(0)} \tag{3.38}$$

For a set χ of periodic sequences, the peak aperiodic cross-correlation magnitude C_c is defined by

$$C_c = \max\{|C_{x,y}(l)| : 0 \leq l \leq N-1, x, y \in \chi\} \tag{3.39}$$

and the peak aperiodic autocorrelation magnitude is

$$C_a = \max\{|C_x(l)| : 1 \leq l \leq N-1, x \in \chi\} \tag{3.40}$$

Table 3.2: Mean value of important parameters of m-sequence(pn103) with period of 63

Paramters	Mean value	Paramters	Mean value
$\overline{C_{k,i}(N-1)}$	0.0	$\overline{C^2_{k,i}(N-1)}$	1.0
$\overline{C_{k,i}(1)}$	0.0323	$\overline{C^2_{k,i}(1)}$	63.9355
$\overline{C_{k,i}(0)}$	-1.0	$\overline{C^2_{k,i}(0)}$	1.0
$\overline{CC_{k,i}(N-1)}$	-0.0159	$\overline{CC^2_{k,i}(N-1)}$	1.0
$\overline{CC_{k,i}(N-2)}$	-0.0317	$\overline{CC^2_{k,i}(N-2)}$	1.9683
$\overline{CC_{k,i}(N-3)}$	-0.0476	$\overline{CC^2_{k,i}(N-3)}$	2.9048
$\overline{CC_{k,i}(0)}$	0.0159	$\overline{CC^2_{k,i}(0)}$	63.9841
$\overline{CC_{k,i}(1)}$	0.0317	$\overline{CC^2_{k,i}(1)}$	62.9206
$\overline{CC_{k,i}(2)}$	0.0476	$\overline{CC^2_{k,i}(2)}$	61.8254
$\overline{CC_{k,i}(3)}$	0.0635	$\overline{CC^2_{k,i}(3)}$	60.6984

Then if χ contain K sequences, it has been shown by Sarwate that

$$\frac{(2N-1)}{N}\left(\frac{C_c^2}{N}\right)+\frac{2(N-1)}{N(K-1)}\left(\frac{C_a^2}{N}\right)\geq 1 \tag{3.41}$$

For the odd cross-correlation function, similarly

$$\sum_{l=1-N}^{N-1}|\hat{\theta}_{x,y}(l)|^2=\sum_{l=1-N}^{N-1}\hat{\theta}_x(l)\hat{\theta}_y(l) \tag{3.42}$$

As a complement, we evaluated the function $C_{k,i}$. In table 3.2, we considered the case when only a single m-sequence (pn103) is employed for all users, a case we will analyse in chapter 4. The functions $\overline{C_{k,i}(l)}$ are evaluated within the home cell, where k took on 62 different values. The function $\overline{CC_{k,i}(l)}$ are the same functions but evaluated from the adjacent cells, so k took on 63 different values. The mean values of those functions are very close to zero, except $C_{k,i}(0)$ whose value is the value of out-of-phase autocorrelation function for pn103. However, those functions have different distributions such that their mean square values are very different from zero, which result in major contributions to the interference. Figures 3.4–3.13 show the distributions of those functions.

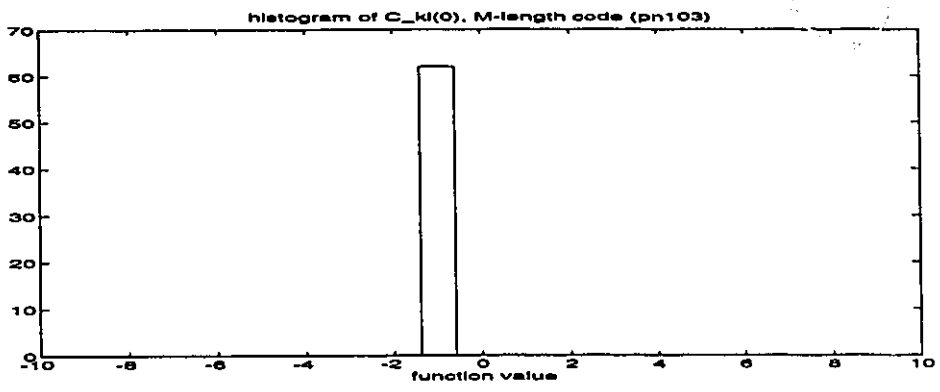

Figure 3.4: Distribution of $C_{k,i}(0)$ of pn103

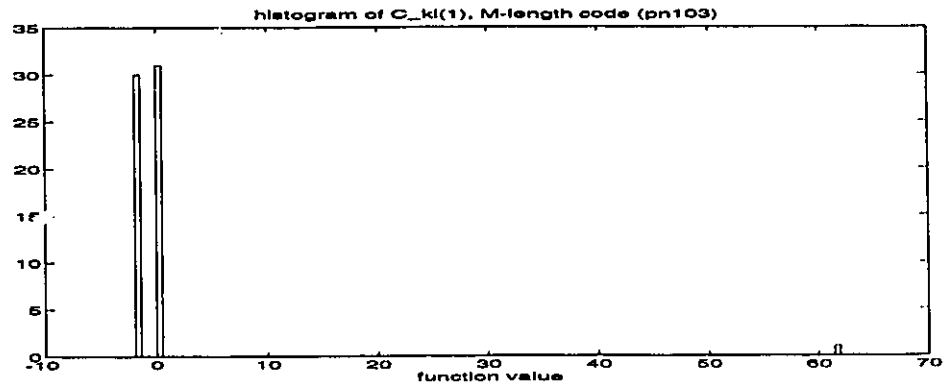

Figure 3.5: Distribution of $C_{k,i}(1)$ of pn103

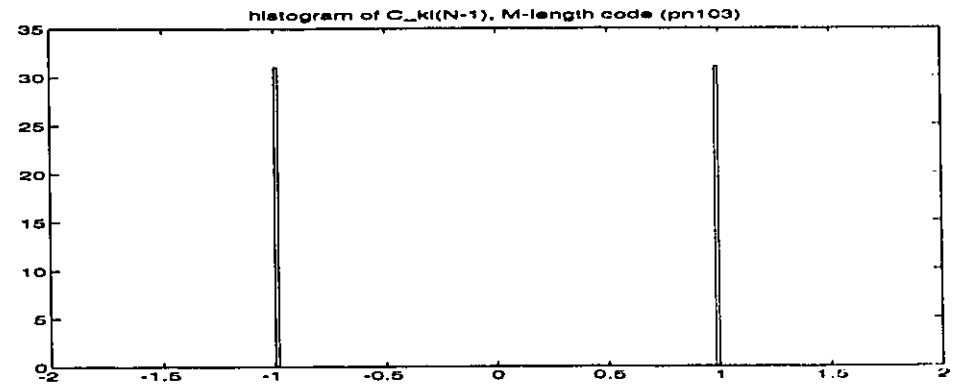

Figure 3.6: Distribution of $C_{k,i}(N-1)$ of pn103

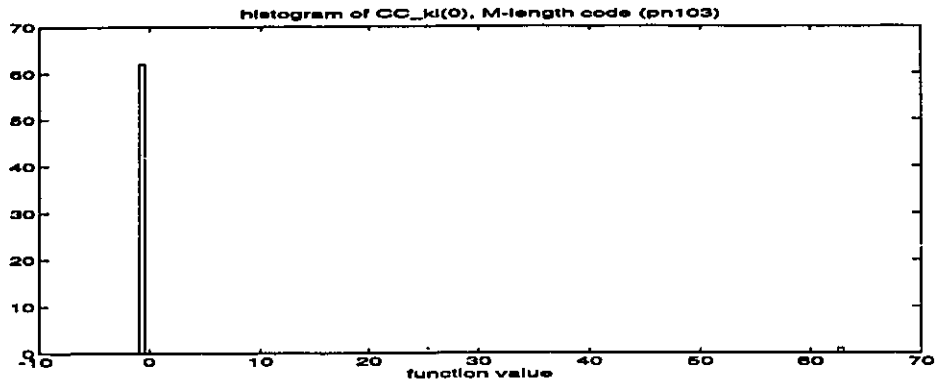

Figure 3.7: Distribution of $CC_{k,i}(0)$ of pn103

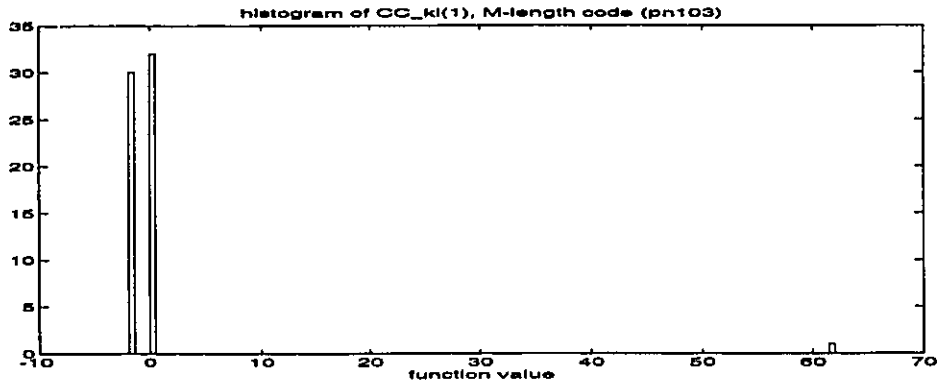

Figure 3.8: Distribution of $CC_{k,i}(1)$ of pn103

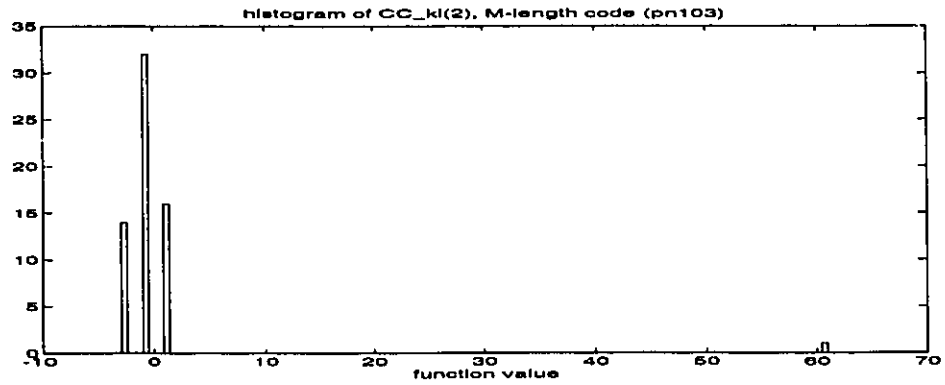

Figure 3.9: Distribution of $CC_{k,i}(2)$ of pn103

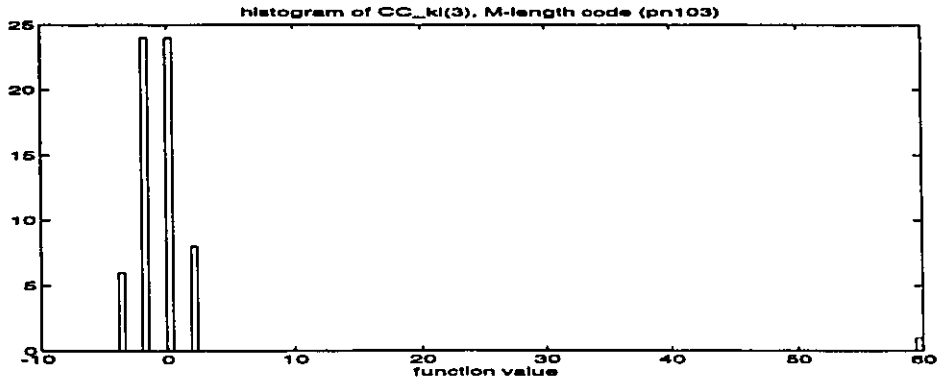

Figure 3.10: Distribution of $CC_{k,i}(3)$ of pn103

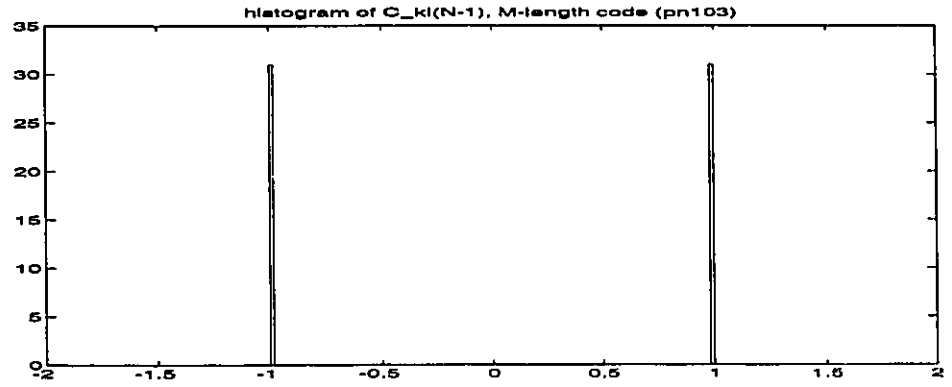

Figure 3.11: Distribution of $CC_{k,i}(N-1)$ of pn103

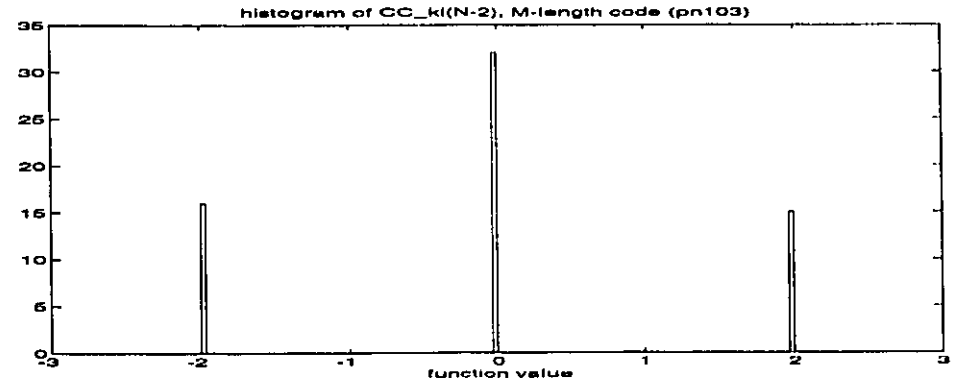

Figure 3.12: Distribution of $CC_{k,i}(N-2)$ of pn103

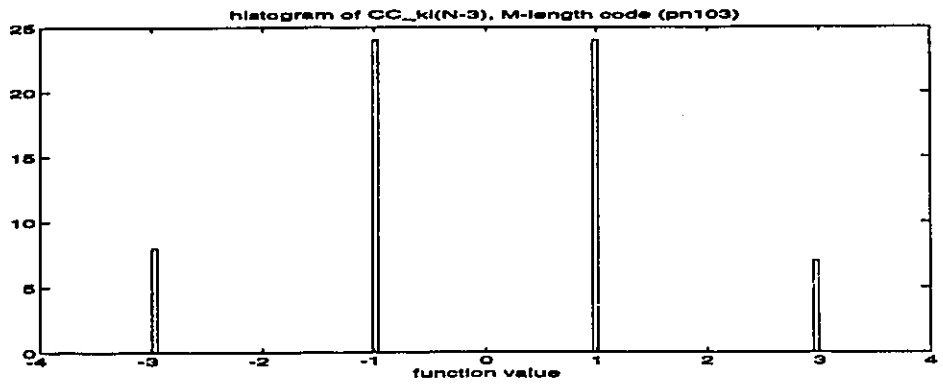

Figure 3.13: Distribution of $CC_{k,i}(N-3)$ of pn103

3.3 Gold Code

As pointed out earlier, only very small sets of m-sequences can have good periodic cross-correlation properties. It is therefore desirable to obtain larger sets of sequences of period $N = 2^n - 1$ which have the same bound $\theta_c \leq t(n)$on the peak periodic cross-correlation as for the maximal connected sets. Since the larger sets must contain some non-m-sequences, then their peak periodic autocorrelation θ_a must exceed 1.

One important class of periodic sequences which provides larger sets of sequences with good periodic cross-correlation is the class of Gold sequences. A set of Gold sequences of period $N = 2^n - 1$, consisting of $N+2$ sequences for which $\theta_c = \theta_a = t(n)$, can be constructed from appropriately selected m-sequences as described below.

Suppose a shift register polynomial $f(x)$ factors into $h(x)\hat{h}(x)$ where $h(x)$ and $\hat{h}(x)$ have no factor in common. Then the set of all sequences generated by $f(x)$ is just the set of all sequences of the form $a \oplus b$ where a is some sequence generated by $h(x)$, b is some sequence generated by $\hat{h}(x)$, and we do not make the usual restriction that a and b are nonzero sequences. Now suppose that $h(x)$ and $\hat{h}(x)$ are two different primitive binary polynominals of degree n that generate the m-sequence u and v, respectively, of period N. If y denotes a nonzero sequence generated by $f(x) = h(x)\hat{h}(x)$, then we get either

$$y = Q^i u \tag{3.43}$$

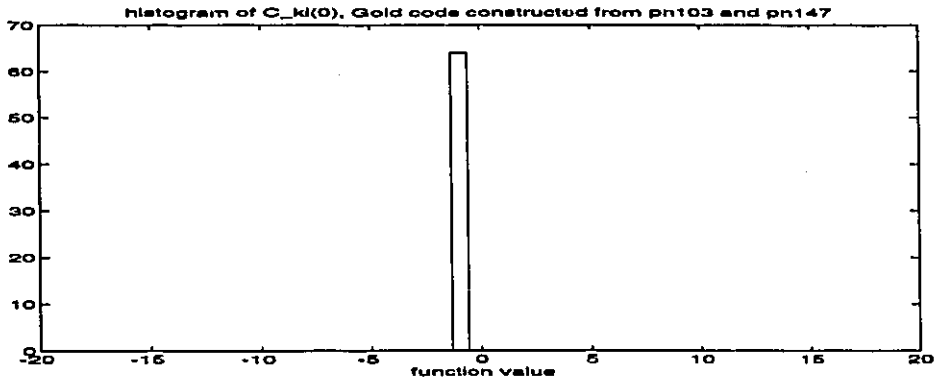

Figure 3.14: Distribution of $C_{k,i}(0)$ of Gold code

or

$$y = Q^j v \tag{3.44}$$

or

$$y = Q^i u \oplus Q^j v \tag{3.45}$$

where $0 \leq i, j \leq N - j$, and where, as before, $Q^i u \oplus Q^j v$ denotes the sequence whose kth element is $u_{i+k} \oplus v_{j+k}$. From this it follows that y is some phase of some sequence in the set $G(u, v)$ defined by

$$G(u, v) \equiv \{u, v, u \oplus v, u \oplus Qv, u \oplus Q^2 v, \ldots, u \oplus Q^{N-1} v\} \tag{3.46}$$

Note that $G(u, v)$ contains $N + 2$ sequences of period N. Gold[27][28] has shown the peak correlation parameters θ_c and θ_a for $G(u, v)$ satisfy

$$\theta_c = \theta_a = \max\{|\theta_{u,v}| : 0 \leq l \leq N - 1\} \tag{3.47}$$

Therefore if $\{u, v\}$ is any preferred pair of m-sequences then $G(u, v)$ has the peak correlation parameters $\theta_c = \theta_a = t(n)$. In this case, the cross-correlation functions for sequences belonging to $G(u, v)$ take on the three preferred values only, i.e., $\{-1, -t(n), t(n) - 2\}$. This is shown in figure 3.17, since $\theta_c = CC_{k,i}(0)$.

Again, we listed the numerical results of mean values of the important functions in table 3.3. Their distributions are shown in figure 3.14–3.23.

Table 3.3: Mean value of important parameters of Gold code with period of 63

Paramters	Mean value	Paramters	Mean value
$\overline{C_{k,i}(N-1)}$	0.0	$\overline{C_{k,i}^2(N-1)}$	1.0
$\overline{C_{k,i}(1)}$	0.2500	$\overline{C_{k,i}^2(1)}$	66.0
$\overline{C_{k,i}(0)}$	-1.0	$\overline{C_{k,i}^2(0)}$	1.0
$\overline{CC_{k,i}(N-1)}$	-0.0308	$\overline{CC_{k,i}^2(N-1)}$	1.0
$\overline{CC_{k,i}(N-2)}$	0.0462	$\overline{CC_{k,i}^2(N-2)}$	2.0308
$\overline{CC_{k,i}(N-3)}$	-0.0154	$\overline{CC_{k,i}^2(N-3)}$	3.0923
$\overline{CC_{k,i}(0)}$	-0.0154	$\overline{CC_{k,i}^2(0)}$	62.0462
$\overline{CC_{k,i}(1)}$	-0.0308	$\overline{CC_{k,i}^2(1)}$	61.1077
$\overline{CC_{k,i}(2)}$	0.2000	$\overline{CC_{k,i}^2(2)}$	62.6615
$\overline{CC_{k,i}(3)}$	-0.0615	$\overline{CC_{k,i}^2(3)}$	59.3231

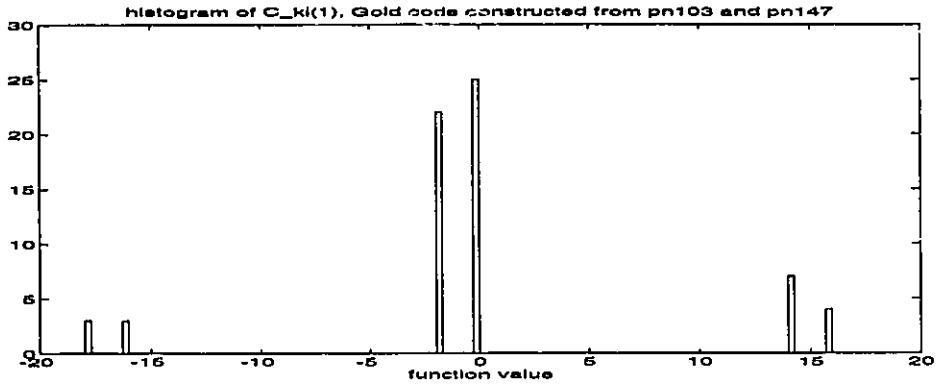

Figure 3.15: Distribution of $C_{k,i}(1)$ of Gold code

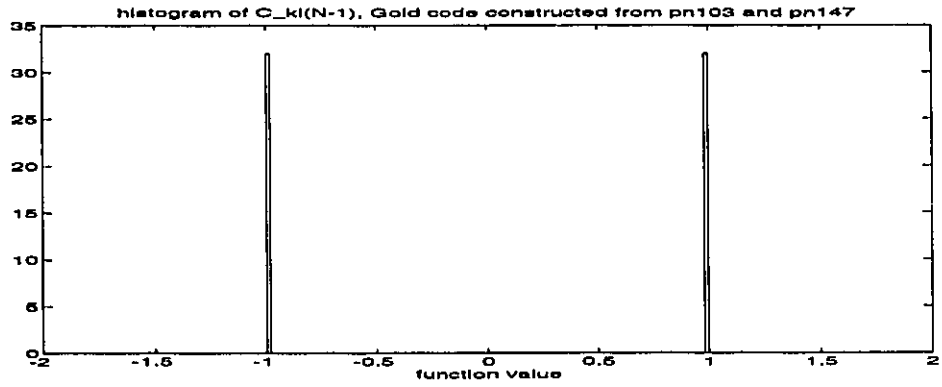

Figure 3.16: Distribution of $C_{k,i}(N-1)$ of Gold code

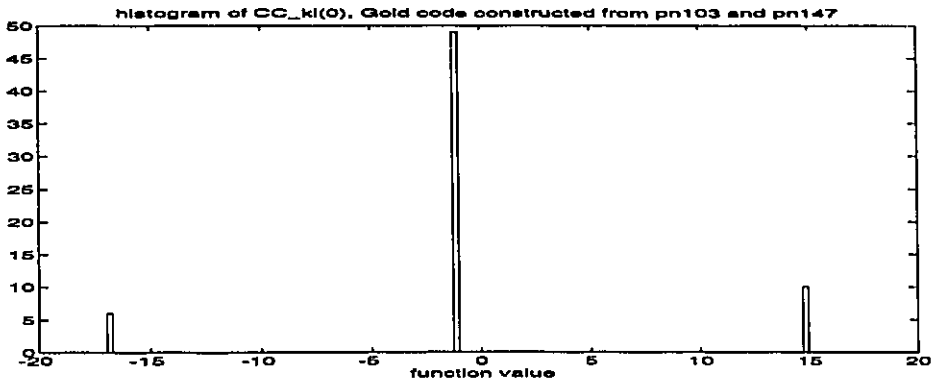

Figure 3.17: Distribution of $CC_{k,i}(0)$ of Gold code

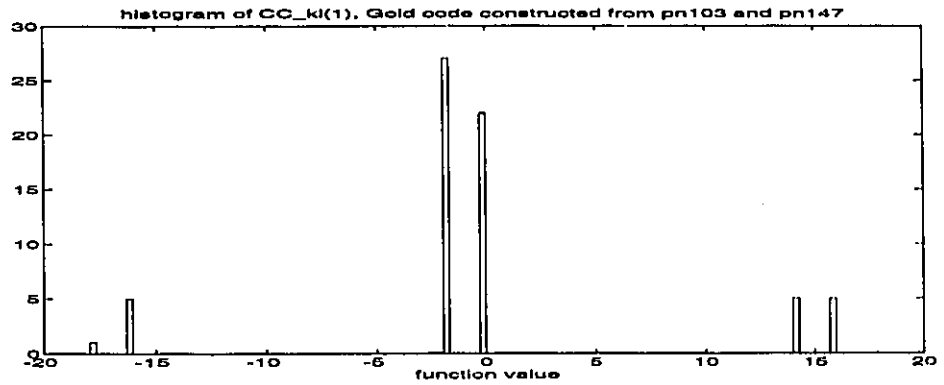

Figure 3.18: Distribution of $CC_{k,i}(1)$ of Gold code

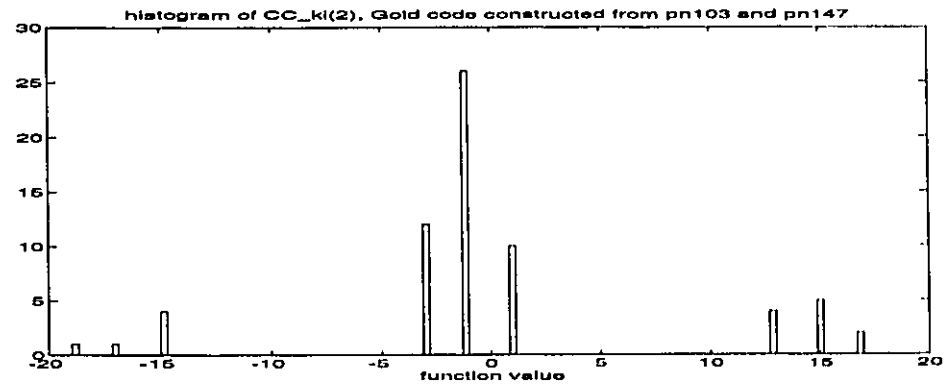

Figure 3.19: Distribution of $CC_{k,i}(2)$ of Gold code

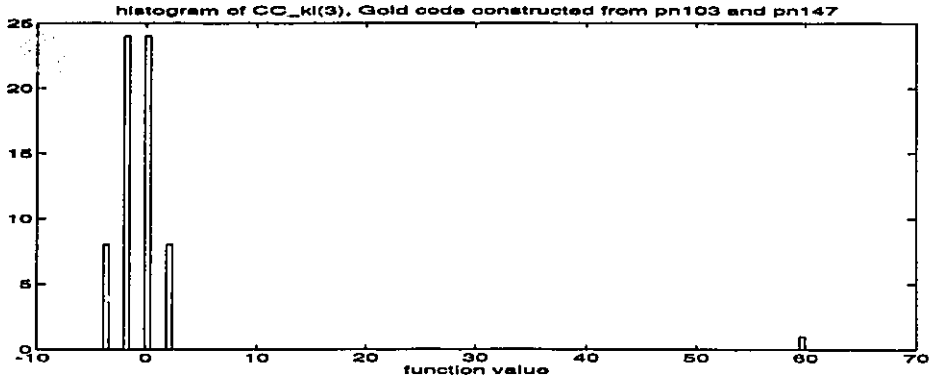

Figure 3.20: Distribution of $CC_{k,i}(3)$ of Gold code

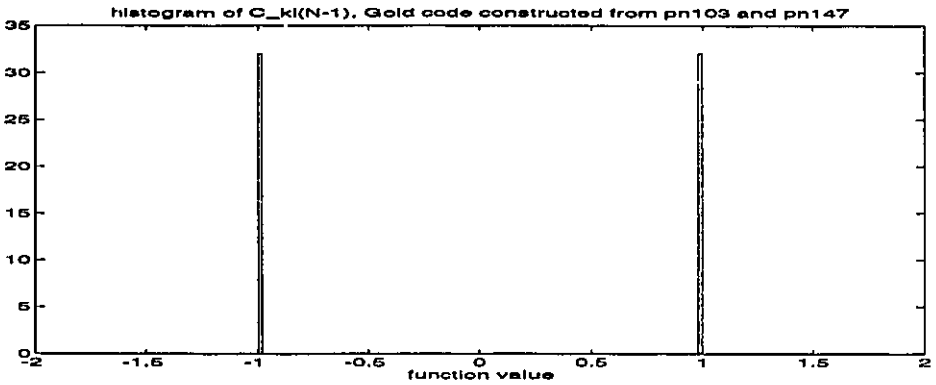

Figure 3.21: Distribution of $CC_{k,i}(N-1)$ of Gold code

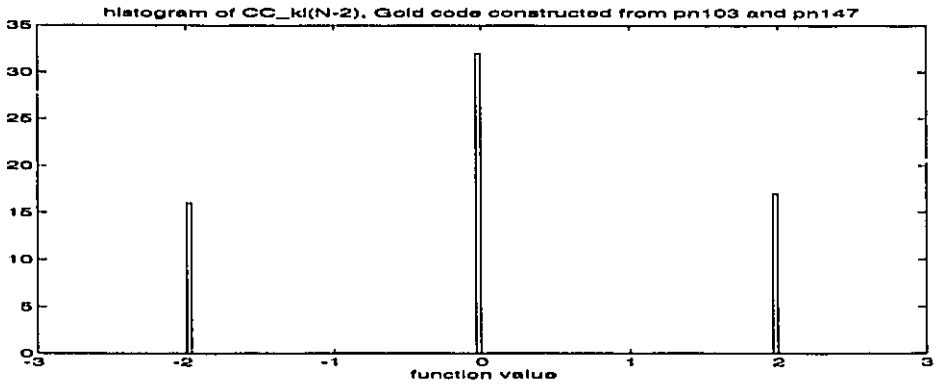

Figure 3.22: Distribution of $CC_{k,i}(N-2)$ of Gold code

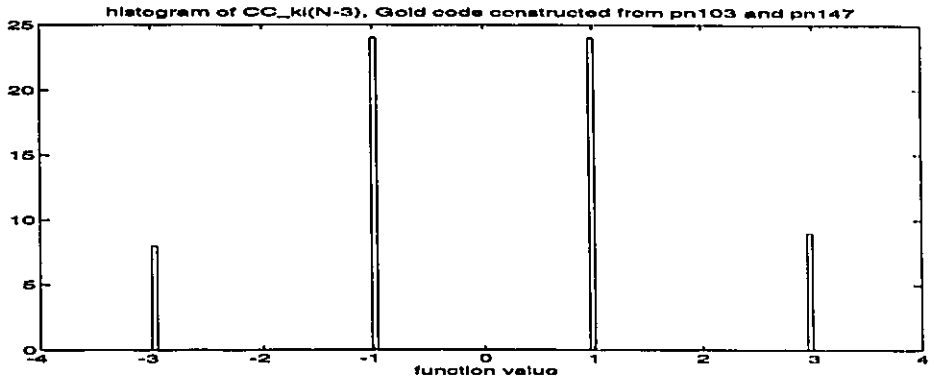

Figure 3.23: Distribution of $CC_{k,i}(N-3)$ of Gold code

3.4 Orthogonal sequences

For the system we designed, time slots can help us to achieve the synchronous access, or at least quasi-synchronous access, in which case the maximum uncertainty of the phase error is less than $0.5T_c$. Under such a circumstance it is advantageous to use orthogonal codes which can eliminate or reduce the cross-correlation residuals.

The orthogonal codes can be taken from the column vectors of the *Hadamard* Matrices. Recall that a Hadamard matrix is a real $N \times N$ matrix H_N of $+1$'s and -1's which satisfies

$$H_N^T H_N = NI \tag{3.48}$$

where the superscribe T denotes transpose and I is an $N \times N$ identity matrix.

One type of Hadamard matrices is called Walsh-Hadamard matrices which is constructed by the following way:

$$\begin{aligned} H_1 &= 1 \\ H_{2N} &= \begin{bmatrix} H_N & H_N \\ H_N & -H_N \end{bmatrix} \end{aligned} \tag{3.49}$$

Where N must be the power of 2. For instance, when $N = 8$, the H_8 is:

$$\begin{bmatrix} 1 & 1 & 1 & 1 & 1 & 1 & 1 & 1 \\ 1 & -1 & 1 & -1 & 1 & -1 & 1 & -1 \\ 1 & 1 & -1 & -1 & 1 & 1 & -1 & -1 \\ 1 & -1 & -1 & 1 & 1 & -1 & -1 & 1 \\ 1 & 1 & 1 & 1 & -1 & -1 & -1 & -1 \\ 1 & -1 & 1 & -1 & -1 & 1 & -1 & 1 \\ 1 & 1 & -1 & -1 & -1 & -1 & 1 & 1 \\ 1 & -1 & -1 & 1 & -1 & 1 & 1 & -1 \end{bmatrix} \tag{3.50}$$

Observation to matrix (3.50) shows that the row or column vectors exhibit much shorter period than N. Therefore they are not ideal candidates for CDMA codes since we need to spread the spectrum to the maximum. The remedy we pointed out is to randomly permute the rows of H_N if we use the column vectors as the codes. Suppose $X = \{x_1, x_2, \ldots x_N\}$ is a binary random sequence, then let I_x denotes the diagonal matrix in which $I_x(i,i) = x_i$ and all $I_x(i,j) = 0$ for $i \neq j$. Then the new matrix Y

$$Y = H_N^T I_x \tag{3.51}$$

will be a random like orthogonal matrix, whose column vectors can be used as the orthogonal sequences. Those sequences therefore have the random apparence under the maximum period which equals to N. X can be arbitrary binary sequences and should be chosen to generate the lowest cross-correlation in case when only quasi-synchronization can be achieved, there will be minimum interference.

Another way to construct a Hadamard matrices is by taking advantage of the auto-correlation property of the m-sequence. Recall that the $\theta_a(l) = -1$ for all $l \neq 0$, so we may use one signal m-sequence to construct a circulant matrix, and for every row we add a $+1$ as the first element, then add a first row of all $+1$. As an example,

Table 3.4: Mean values of important parameters of orthogonal codes with period of 64

Paramters	Mean value	Paramters	Mean value
$\overline{C_{k,i}(N-1)}$	0.0	$\overline{C^2_{k,i}(N-1)}$	1.0
$\overline{C_{k,i}(1)}$	1.0323	$\overline{C^2_{k,i}(1)}$	65.0
$\overline{C_{k,i}(0)}$	0.0	$\overline{C^2_{k,i}(0)}$	0.0
$\overline{CC_{k,i}(N-1)}$	-0.0159	$\overline{CC^2_{k,i}(N-1)}$	1.0
$\overline{CC_{k,i}(N-2)}$	-0.0317	$\overline{CC^2_{k,i}(N-2)}$	1.9683
$\overline{CC_{k,i}(N-3)}$	-0.0476	$\overline{CC^2_{k,i}(N-3)}$	2.9048
$\overline{CC_{k,i}(0)}$	1.0159	$\overline{CC^2_{k,i}(0)}$	65.0159
$\overline{CC_{k,i}(1)}$	1.0317	$\overline{CC^2_{k,i}(1)}$	63.9841
$\overline{CC_{k,i}(2)}$	1.0476	$\overline{CC^2_{k,i}(2)}$	62.9206
$\overline{CC_{k,i}(3)}$	1.0635	$\overline{CC^2_{k,i}(3)}$	61.8254

an 8×8 Hadamard matrix constructed in this way is as follows:

$$\begin{bmatrix} 1 & 1 & 1 & 1 & 1 & 1 & 1 & 1 \\ 1 & 1 & 1 & -1 & 1 & -1 & -1 & -1 \\ 1 & 1 & -1 & 1 & -1 & -1 & -1 & 1 \\ 1 & -1 & 1 & -1 & -1 & -1 & 1 & 1 \\ 1 & 1 & -1 & -1 & -1 & 1 & 1 & -1 \\ 1 & -1 & -1 & -1 & 1 & 1 & -1 & 1 \\ 1 & -1 & -1 & 1 & 1 & -1 & 1 & -1 \\ 1 & -1 & 1 & 1 & -1 & 1 & -1 & -1 \end{bmatrix} \tag{3.52}$$

This matrix automatically has the random appearance except the first row and the first column. Of course, it can be further scrambled by another random binary sequence, as we did for the Walsh-Hadamard matrices.

The mean values of the important functions is listed in table 3.4. The statistical properties of equation (3.15)–(3.17) are closely maintained. The distributions of those functions are shown in figures (3.24)–(3.33).

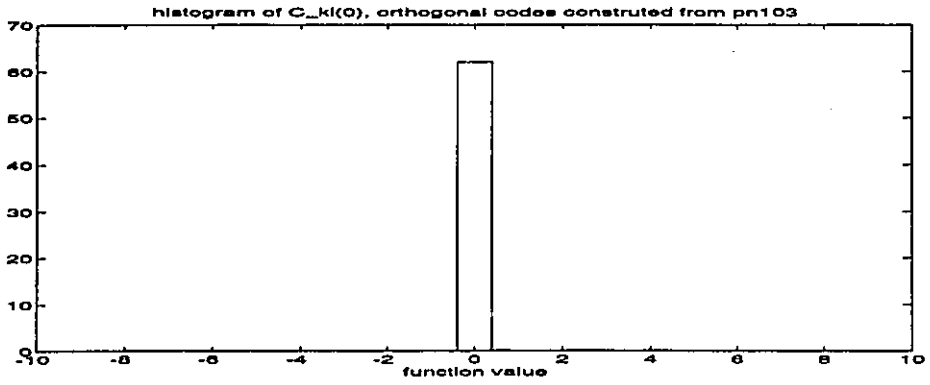

Figure 3.24: Distribution of $C_{k,i}(0)$ of orthogonal code

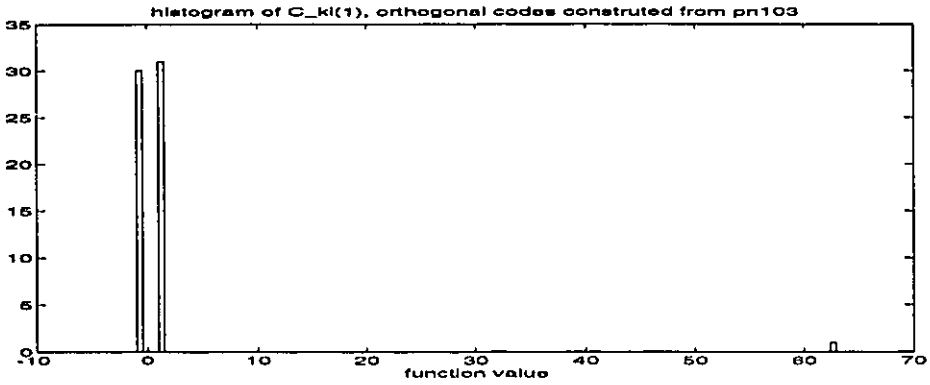

Figure 3.25: Distribution of $C_{k,i}(1)$ of orthogonal code

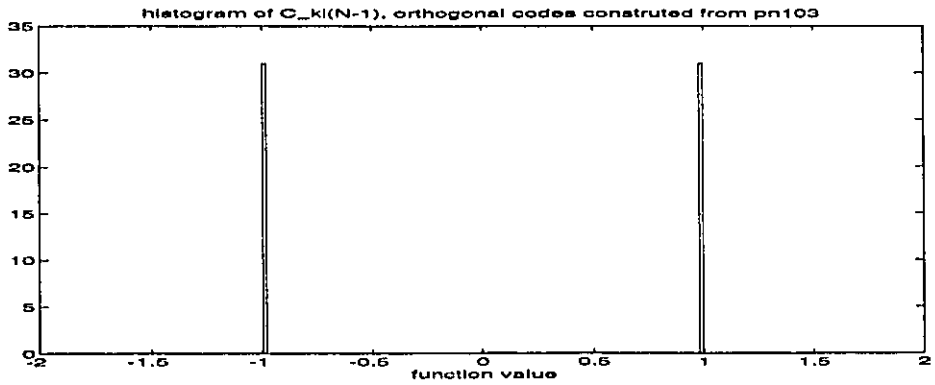

Figure 3.26: Distribution of $C_{k,i}(N-1)$ of orthogonal code

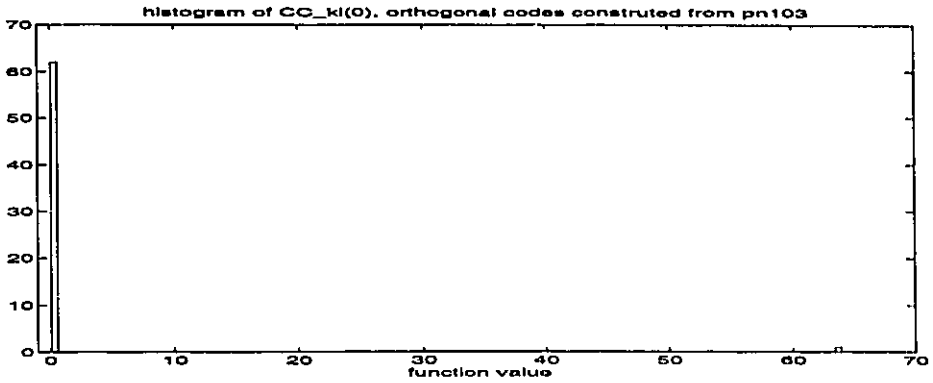

Figure 3.27: Distribution of $CC_{k,i}(0)$ of orthogonal code

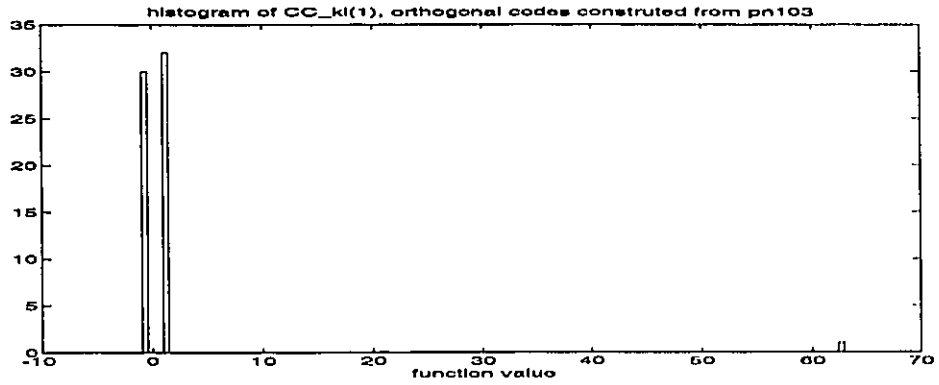

Figure 3.28: Distribution of $CC_{k,i}(1)$ of orthogonal code

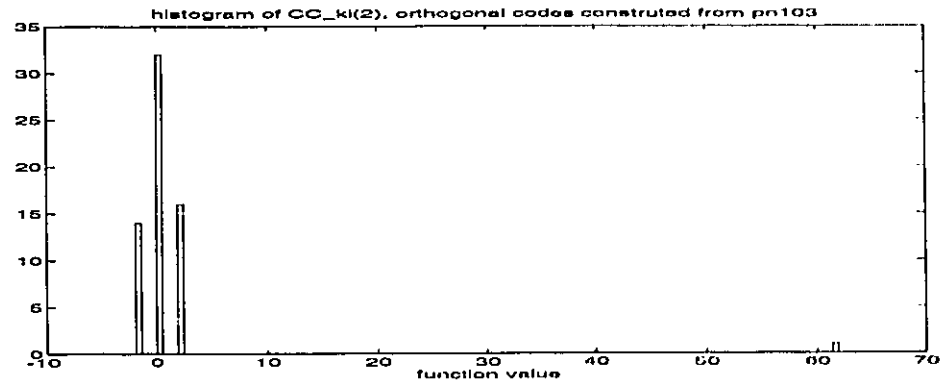

Figure 3.29: Distribution of $CC_{k,i}(2)$ of orthogonal code

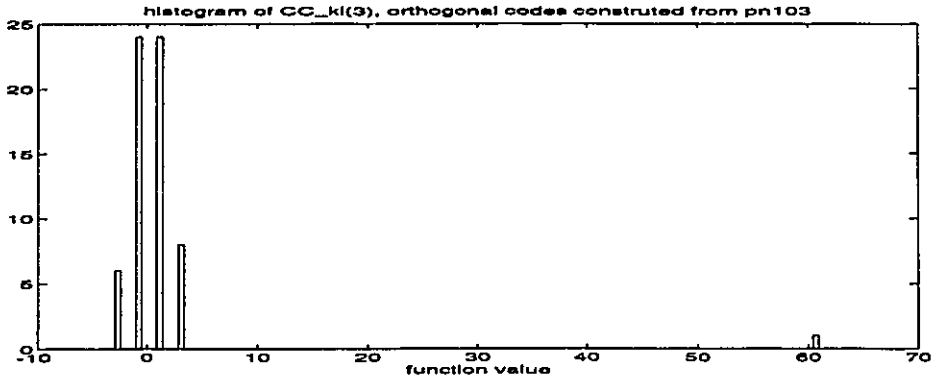

Figure 3.30: Distribution of $CC_{k,i}(3)$ of orthogonal code

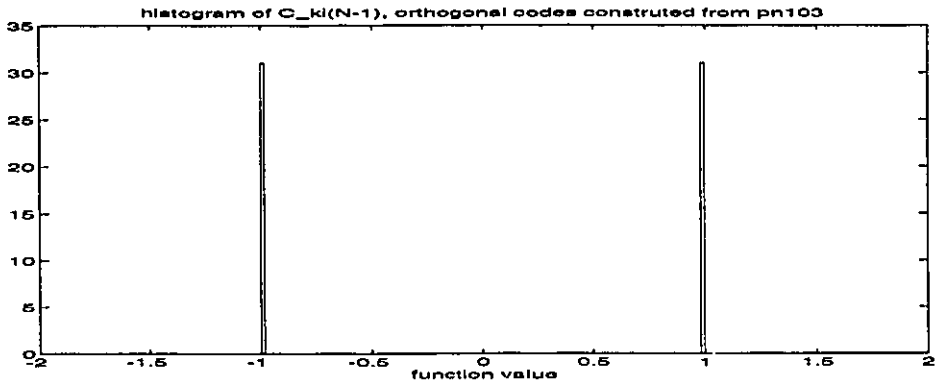

Figure 3.31: Distribution of $CC_{k,i}(N-1)$ of orthogonal code

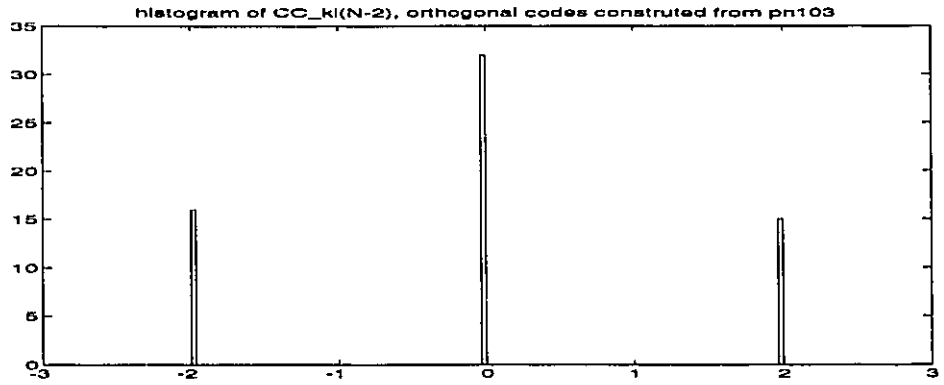

Figure 3.32: Distribution of $CC_{k,i}(N-2)$ of orthogonal code

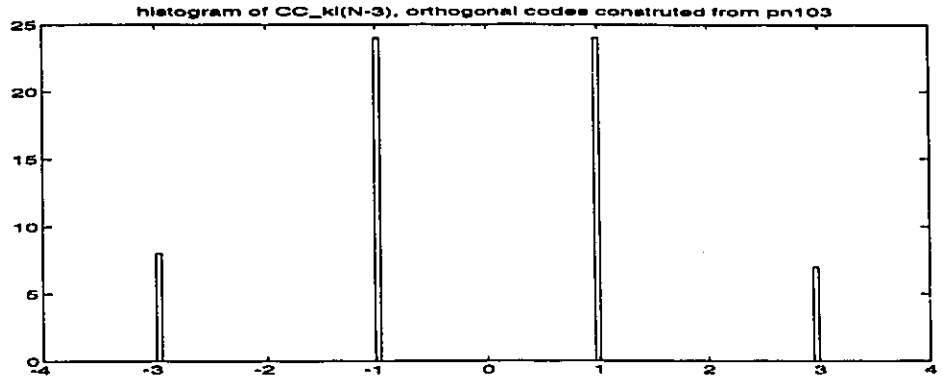

Figure 3.33: Distribution of $CC_{k,i}(N-3)$ of orthogonal code

3.5 Summary of chapter

In this chapter, we have shown that the performance of a CDMA system depends on the properties of codes employed in the system, and on the asychronous access. Three major types of codes are discussed, namely the m-length codes, Gold codes, and orthogonal codes. Their relative merit is summarized as follows:

- m-length codes:
  - Advantages:
    - Easy to generate.
    - Random appearance.
    - Very low sidelobe in autocorrelation.
  - Disadvantages:
    - Smaller variety.
    - Cross-correlation can be high.
- Gold codes:
  - Advantages:
    - greater variety.

    * Relatively easy to generate.
    * Random appearance.
    * Controlled cross-correlation values.
  - Disadvantages:
    * High sidelobe in autocorrelation.

- Orthogonal codes:
  - Advantages:
    * Greater variety.
    * Optimum for synchronous access.
  - Disadvantages:
    * Complex in construction.
    * May need scrambling to have random appearance

A choice of codes depends on the environment of communication. More on this will be discussed in the following chapters.

Chapter 4

Capacity Analysis in Home Cell

In chapter 3, we have shown how mutual interferences arise in CDMA systems, and studied the properties of different type of codes. We concluded that orthogonal codes are the optimum codes in the strict synchronous access environment. However, as pointed out in chapter 2, we can only have quasi-synchronous access at best for uplink, and the system configurations will affect the performance, in addition to the code properties. To maximize the system capacity, a type of suitable code should be chosen such that the bit-error-rate (BER) of the final output is minimum among all the available codes. This requires adequate modeling of the system. In this chapter, we will describe the system model for calculating the BER. However, attention will be focused on the cases in which only interferences from users in the home cell are considered.

4.1 Modulation scheme for hybrid system

In the system performance analysis, we focus on the situation in which the receiver can acquire synchronization with the desired signal but not a phase reference, therefore only non-coherent demodulation is feasible. This is because there exists an abrupt change of phase as a result of frequency hopping. We have used slow frequency hop-

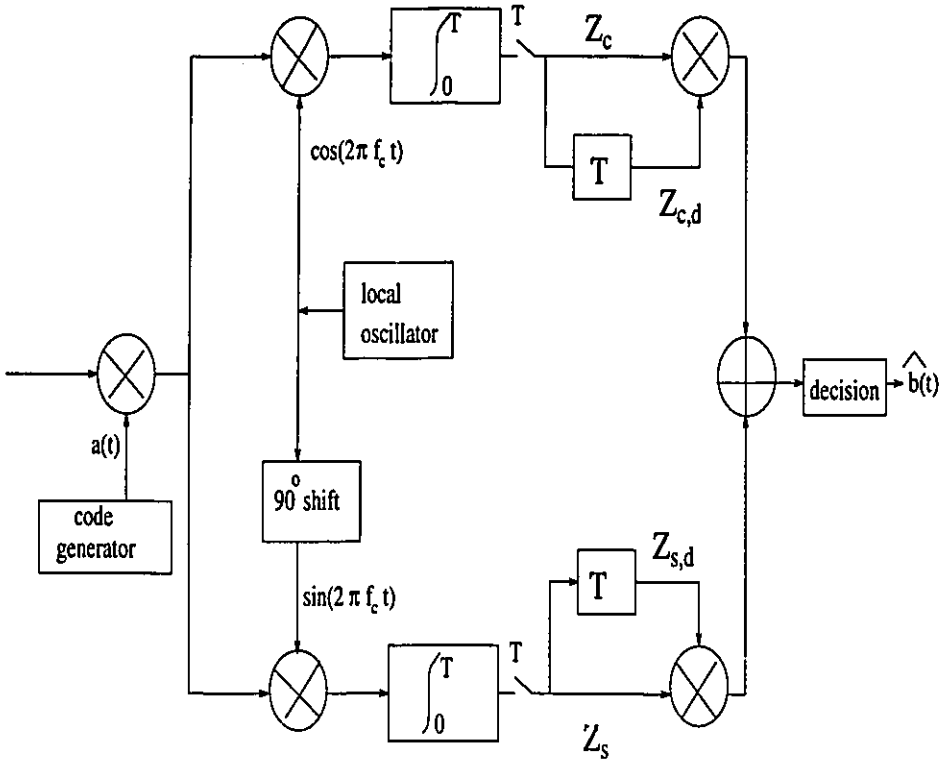

Figure 4.1: The DPSK non-coherent detection model

ping, so several data bits (assumed 10 bits) are transmitted during each hopping interval. As shown in figure 2.7, we can dehop the received signals by correlating it with the locally generated frequency hopping patterns. Following that, we still need to restore the data bits scrambled by the direct sequence. To employ the non-coherent demodulation, the modulation scheme of interest is differential-phase-shift-keying(DPSK) because of its relatively lower BER.

An implementation of DPSK demodulation is shown in figure 4.1. We still let $b(t)$ denote the data stream and $a(t)$ denote the code stream, the same as that in chapter 3. As shown in section 3.1, the received signal, after dehopping, is

$$r(t) = \sum_{k=1}^{K} \sqrt{2P} a_k(t-\tau_k) b_k(t-\tau_k) \cos(2\pi f_c t + \phi_k) + n(t) \qquad (4.1)$$

Both the inphase and the quadrature branches of the demodulator have two sub-branches: the first utilizes the received signal, the second a delayed version of it.

Once again we assume the ith signal to be the desired signal. In the in-phase component the signal is multiplied by $a_i(t)\cos(2\pi f_c t)$, and in the quadrature component it is multiplied by $a_i(t)\sin(2\pi f_c t)$. The output of the inphase components of the two branches of the receiver matched to the ith signal are given by

$$Z_c = \int_0^T r(t)a_i(t)\cos(2\pi f_c t)dt \tag{4.2}$$

and

$$Z_{c,d} = \int_0^T r(t-T)a_i(t)\cos(2\pi f_c t)dt \tag{4.3}$$

where $r(t)$ is the received signal. The outputs of the quadrature components of the two branches are defined by eqs. (4.2) and (4.3) with the $\cos(\cdot)$ terms replaced by $\sin(\cdot)$. The receiver forms the statistic $Z_c Z_{c,d} + Z_s Z_{s,d}$ and compares it with a zero threshold. ONE is assumed if it is great than zero and MINUS ONE is assumed if it is less than zero. The $\hat{b}_0^{(i)}$ must then be differentially decoded from the decisions.

The performance measure is the *average probability of error* at the output of the correlation receiver. If we denotes the power of inphase component and quadrature component for the desired signal by D_c and D_s respectively, and the branch output statistics by $Z_c, Z_{c,d}, Z_s$, and $Z_{s,d}$, then the probability of error P_e is given by[85]:

$$P_e = \frac{1}{2}\left[1 - \tilde{\sigma}^2(\sigma_c^2)^{-1}\right]\exp\{-\frac{1}{2}(D_c^2 + D_s^2)(\sigma_c^2)^{-1}\} \tag{4.4}$$

The second order moments are $\sigma_c^2 = \mathrm{Var}\{Z_c\}$, $\tilde{\sigma}^2 = \mathrm{Cov}\{Z_c, Z_{c,d}\}$. Equation (4.4) is valid if $\sigma_c^2 = \sigma_{c,d}^2 = \mathrm{Var}\{Z_{c,d}\}$.

Besides the average error probability another performance measure is considered. It is termed *multiple-access capability* and is defined as the maximum number of signals transmitted from different stations simultaneously that can be tolerated in the neighborhood of a receiver so that the error probability for the reception of a particular signal does not exceed a prespecified maximum value.

4.2 Performance of Noncoherent Direct-Sequence CDMA Systems

Before we start to explore the performance of our system, we first give the performance of the classical spread spectrum systems. Direct-sequence(DS) multi-access is the most popular way to implement so far. Frequency-hopping(FH) multi-access provides an alternative. However, the fast frequency hopping(many hops in one data bit), as desired in most application, are not technologically feasible for high speed data transmission.

Let consider a DS/SSMA system using the demodulation model shown in figure 4.1. We assume that the receiver matched to the ith signal can acquire time synchronization. We can therefore set $\tau_i = 0$ and justify our consideration of the time delays relative to the delay of the ith signal. We do not require knowledge of the phase but, for DPSK communication, we require that the phase θ_i does not change over the duration of two adjacent data bits. Since $f_c \gg T^{-1}$ in practical spread-spectrum systems, the double frequency ($2f_c$) terms may be ignored, and the output of the integrator at the sampling instant is then given for *asynchronous* system by

$$Z_i(T) = N_c + D_c + \sum_{k=1,k\neq i}^{K} I_c^{(k,i)} \tag{4.5}$$

where N_c is the result of $\int_0^T n(t)a_i(t)\cos\omega_c t dt$, which is zero-mean Gaussian with variance $N_0T/4$. The random variables D_c and $I_c^{(k,i)}$ are defined by

$$D_c = \sqrt{\frac{P}{2}} T b_{i,0} \cos(\theta_i) \tag{4.6}$$

and

$$I_c^{(k,i)} = T^{-1}\left[b_{k,-1}R_{k,i}(\tau_k) + b_{k,0}\hat{R}_{k,i}(\tau_k)\right]\cos(\phi_k) \tag{4.7}$$

where

$$\phi_k = \theta_i + \theta_k - 2\pi f_c \tau_k \tag{4.8}$$

In the *synchronous* case it is assumed that $\tau_k = 0$ for all k and time synchronization can be acquired at the chip level. In this case the multiple-access interference term $I_c^{(k,i)}$ takes the form

$$I_c^{(k,i)} = b_{k,0}[\theta_{k,i}(0)/N]cos(\phi_k) \tag{4.9}$$

where $\theta_{k,i}(l)$ is the even cross-correlation function of the code sequences $a_k(j)$ and $a_i(j)$.

We now proceed on to the evaluation of the error probability for noncoherent asynchronous DS/SSMA systems. We approximate $\sum_{k=1,k\neq i}^{K} I_c^{(k,i)}$ by Gaussian random variables. The resulting approximation to the average probability of error is given by

$$\overline{P}_e = \frac{1}{2}(1 - \tilde{v}v^{-1})\exp(-\frac{1}{2v}) \tag{4.10}$$

The normalized moments $v, \tilde{v}$ are defined by

$$v = (2E_b/N_0)^{-1} + \sum_{k=1,k\neq i}^{K} \sigma_{k,i}^2 \tag{4.11}$$

$$\tilde{v} = \sum_{k=i,k\neq i}^{K} \tilde{\sigma}_{k,i}^2 \tag{4.12}$$

where $E_b = PT$ is the average energy per bit for the transmitted signals. The quantities $\sigma_{k,i}^2, \tilde{\sigma}_{k,i}^2$ are defined as $\mathrm{Var}\{I_c(k,i)\}, \mathrm{Cov}\{I_c(k,i)\}$, and are given by the expressions

$$\sigma_{k,i}^2 = \frac{1}{2}T^{-3}\int_0^T \left[R_{k,i}^2(\tau) + \hat{R}_{k,i}^2(\tau)\right] d\tau \tag{4.13}$$

$$\tilde{\sigma}_{k,i}^2 = \frac{1}{2}T^{-3}\int_0^T R_{k,i}(\tau)\hat{R}_{k,i}(\tau)d\tau \tag{4.14}$$

Throughout this thesis, we suppose that the code sequences are random like within their periods, that is, for each k, $(a_k(l))$ consists of a sequence of mutually independent random variables taking on values in $[+1, -1]$ with equal probability, and that code sequences assigned to different users are mutually independent. Modeling the code sequences as random may be desirable for analytical purposes, or for purposes of satisfactory representation of code sequences that are unknown or hard to model.

In particular, we need to evaluate the average of $\sigma_{k,i}^2$ and $\tilde{\sigma}_{k,i}^2$. We first write $\sigma_{k,i}^2$ as

$$\int_0^T \left[R_{k,i}^2(\tau) + \hat{R}_{k,i}^2(\tau)\right] d\tau = \left[\frac{2}{3}\sum_{l=1-N}^{N-1} C_{k,i}(l)^2 + \frac{1}{6}\sum_{l=1-N}^{N-1} C_{k,i}(l)C_{k,i}(l+1)\right] T_c^3 \quad (4.15)$$

Similarly one can show that

$$\begin{aligned}\int_0^T \left[R_{k,i}^2(\tau)\hat{R}_{k,i}^2(\tau)\right] d\tau \quad &= \left\{\tfrac{2}{3}\textstyle\sum_{l=0}^{N-1}\left[C_{k,i}(l)C_{k,i}(l-N) + C_{k,i}(l+1)C_{k,i}(l+1-N)\right]\right. \\ &\left. +\tfrac{1}{6}\textstyle\sum_{l=0}^{N-1}\left[C_{k,i}(l)C_{k,i}(l+1-N) + C_{k,i}(l-N)C_{k,i}(l+1)\right]\right\} T_c^3\end{aligned} \quad (4.16)$$

If E denotes expected value of the ensemble of random signature sequences of length N, then

$$\mathrm{E}\{C_{k,i}(l)C_{k,i}(m)\} = \begin{cases} N-|l| & \text{for} \quad l=m \\ 0 & \text{for} \quad l\neq m \end{cases} \quad (4.17)$$

Therefore, equations (4.15) and (4.16) reduce to

$$\mathrm{E}\left\{\int_0^T \left[R_{k,i}^2(\tau) + \hat{R}_{k,i}^2(\tau)\right] d\tau\right\} = \frac{2}{3}N^2T_c^3 \quad (4.18)$$

and

$$\mathrm{E}\left\{\int_0^T \left[R_{k,i}^2(\tau)\hat{R}_{k,i}^2(\tau)\right] d\tau\right\} = 0 \quad (4.19)$$

Thus for asynchronous access,

$$\sigma_{k,i}^2 = \frac{1}{3N} \quad (4.20)$$

$$\tilde{\sigma}_{k,i}^2 = 0 \quad (4.21)$$

For synchronous systems, the analysis is much simpler since $\hat{R}_{k,i} = 0$. We have

$$\sigma_{k,i}^2 = \frac{1}{2}\left[\theta_{k,i}(0)/N\right]^2 = \frac{1}{2N} \quad (4.22)$$

$$\tilde{\sigma}_{k,i}^2 = 0 \quad (4.23)$$

In the last step of equation 4.22, we have used the fact that $\overline{\theta_{k,i}^2(0)} = N$ for random sequences, as given by [77].

Then we can obtain the averaged bit error rate for asynchronous systems

$$\overline{P}_e = \frac{1}{2}\exp\left\{-\frac{1}{2\left[(2E_b/N_0)^{-1} + (K-1)/(3N)\right]}\right\} \tag{4.24}$$

and for synchronous system

$$\overline{P}_e = \frac{1}{2}\exp\left\{-\frac{1}{2\left[(2E_b/N_0)^{-1} + (K-1)/(2N)\right]}\right\} \tag{4.25}$$

In both equations (4.24) and (4.25), there exists an interference term arising from the multiple-access. That is the major difference from the performance of DPSK modulation if Gaussian noise is the only source for bit error. When the number of signals K is large, both systems have large BER since the multiple-access interference term will rapidly become the dominate source for bit error. In figure 4.2, we plot the average bit error rate (BER) vs. the E_b/N_0 for the case of $N = 63, K = 30$. For the same bandwidth, we can put 63 users in both TDMA or FDMA systems, and still obtain the same performance as DPSK modulation with only Gaussian thermal noise characterized by N_0. However, 30 users in the random access CDMA systems already generate excessive mutual interference, and make such kinds of systems unusable. The reasonable performance curve in which the BER reaches 10^{-3} when $E_b/N_0 = 10$dB is found at the total number of user $K = 7$, which is only about $\frac{1}{9}$ of the hard limit. That is considerably below the system capacity given by TDMA or FDMA. Therefore it has been concluded in the late 70's that asynchronous CDMA systems with random codes are not efficient multiple access methods, neither in spectrum nor in capacity, although it had been found some application in satellite communications[70][98]. In the early of 90's, it has been found[24] that by taking advantage of the voice activity cycle and splitting the cells into three sectors, the capacity can increase by ninefold approximately in the environment of mobile cellular systems. Therefore in a single cell, it is already approaching the hard limit. In addition, its frequency reuse pattern is

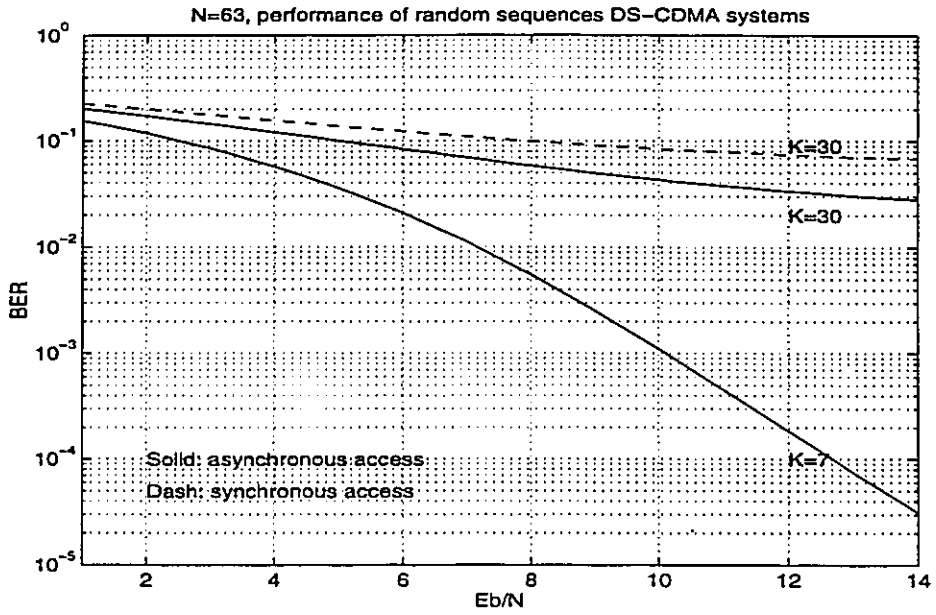

Figure 4.2: The classical DS-SSMA performance

one. therefore it has been argued by Gilhousen,*et al*[24], Lee[50] that CDMA systems can increase the capacity of digital cellular by four folds.

It is interesting to note that the case of synchronous access performs even worse than the asynchronous access. This is because of the fact that the cross-correlation functions of the random sequences take on both positive and negative values, including zeros when they cross the horizontal axis. For synchronous access, $\overline{\theta^2_{k,i}(\tau)}$ is always evaluated at the integer number of τ and no zero-crossing values will be taken which always happen between two integer numbers of τ unless it happen to be zero at an integer number. However, for the case of asynchronous access, $\overline{\theta^2_{k,i}(\tau)}$ is averaged by including those zero-cross points and therefore get lower averaged values.

4.3 Performance of a general noncoherent hybrid DS-FH CDMA systems

The hybrid DS/FH has long been known as a way of spread-spectrum. The performance analysis for a system with random signature sequences and random hopping patterns can be shown as follows. The difference from the previous section is that there is a frequency dehopping part which correlates the locally generated hopping patterns to the received signals. The signal after the frequency dehopping is

$$r_d(t) = \sum_{k=1}^{K} \sqrt{\frac{1}{2}} P \delta[f_k(t-\tau_k), f_1(t-t_k)] a_k(t-\tau_k) cos[2\pi f_c t + \Phi_k(t)] + \hat{n}(t) \quad (4.26)$$

where $\hat{n}(t)$ is a band-limited version of $n(t)$ which can be treated as WGN with spectral density $N_0/8$. The phase waveform $\Phi_k(t)$ is defined as

$$\Phi_k(t) = \theta_k - 2\pi[f_c + f_k(t-\tau_k)]\tau_k + \alpha_k(t-\tau_k) - \beta_i(t) \quad (4.27)$$

where $\alpha(t)$ and $\beta(t)$ are the random phase offsets caused by the frequency hopper from the transmitter and the frequency dehopper at the receiver, respectively.

The outputs of the inphase components of the receiver during the reception of the λth data bit(where $\lambda = j_i N_b + n_i$, i.e., for the n_ith data bit of the j_ith hop) are

$$Z_c = \int_{\lambda T}^{(\lambda+1)T} r_d(t) a_i(t) \cos(2\pi f_c t) dt \quad (4.28)$$

The outputs of the quadrature components can be obtained from (4.28) by replacing $\cos(\cdot)$ with $\sin(\cdot)$. As before, we assume that the receiver matched to the ith signal can acquire time synchronization. We can therefore set $\tau_i = 0$ and consider time delays relative to the delay of the first signal. We do not require the knowledge of the phase, but for DPSK communication, we require than the phase θ_i does not change over the duration of two adjacent data bits. It is assumed that the number of data bits transmitted during each dwell time is strictly larger than 1 ($N_b > 1$) and that there is not going to be a decision on the first data bit of the j_ith dwell time; it

will be used for acquiring the phase reference. Thus, any two adjacent bits of the j_ith dwell interval, say the n_ith and (n_i+1)th(where $0 < n_i < N_b$), will have phase $\theta_i + \alpha_{j_i}^{(i)} - \beta_{j_i}^{(i)}$. If we put the form of $r_d(t)$ into equation (4.28), we have

$$Z_c = D_c + N_c + \sqrt{P/8}T \sum_{k=1,k\neq i}^{K} I_c^{(k,i)} \tag{4.29}$$

where N_c is a zero mean Gaussian random variable with variance $N_0T/16$, and the desired signal component D_c is defined by

$$D_c = \sqrt{P/8}Tb_\lambda^{(i)} cos[\theta_i + \alpha_{j_i}^{(i)} - \beta_{j_i}^{(i)}] \tag{4.30}$$

The term $I_c^{(k,i)}$ denotes the multiple-access interference due to the kth signal and is defined as follows. Let $j_k = \lfloor \tau_k/T_h \rfloor$ and $n_k = \lfloor (\tau_k - j_kT_h)/T \rfloor$, where $\lfloor u \rfloor$ denotes the integer part of the real number u. Also define for $0 \leq j < N$ and $0 \leq n < N_b$

$$d(j) = \delta(f_{j_i-j}^{(k)}, f_{j_i}^{(i)}) \tag{4.31}$$

and $L(j,n) = (j_i - j)N_b + n_i - n$. Recall that for the λth data bit $\lambda = j_iN_b + n_i$ where $1 \leq n_i < N_b$. Note that if $d(j_k) = 1$, then during the $(j_i - j_k)$th dwell time of the kth signal and the j_ith dwell time of the ith signal, the same frequency is occupied (a hit occurs). If $d(j_k) = 0$, then there is no interference during the j_ith dwell time of the ith signal caused from the $(j_i - j_k)$th dwell time of the kth signal.

For $0 \leq n_k < n_i$ we can write

$$I_c^{(k,i)} = d(j_k)[e(j_k, n_k) + \hat{e}(j_k, n_k)] \cos[\psi(j_k)] \tag{4.32}$$

This corresponds to a possible full hit during the $(j_i - j_k)$th dwell time of the kth signal. For $n_k = n_i$ we have

$$I_c^{(k,i)} = d(j_k+1)e(j_k, n_k) \cos[\psi(j_k+1)] + d(j_k)\hat{e}(j_k, n_k) \cos[\psi(j_k)] \tag{4.33}$$

which corresponds to possible partial hits during either the $(j_i - j_k - 1)$th or $(j_i - j_k)$th dwell time of the kth signal, or to a possible full hit when $f_{j_i-j_k-1}^{(k)} = f_{j_i-j_k}^{(k)} = f_{j_i}^{(i)}$. Finally, for $n_i < n_k < N_b$

$$I_c^{(k,i)} = d(j_k+1)[e(j_k, n_k) + \hat{e}(j_k, n_k)] \cos[\psi(j_k+1)] \tag{4.34}$$

which corresponds to a possible full hit during the $(j_i - j_k - 1)$th dwell time of the kth signal. In (4.32)-(4.34) the quantities $e, \hat{e}$ and ψ are defined as

$$e(j,n) = b^{(k)}_{L(j,n+1)} R_{k,i}(\tau_k - jT_h - nT)/T \tag{4.35}$$

$$\hat{e}(j,n) = b^{(k)}_{L(j,n+1)} \hat{R}_{k,i}(\tau_k - jT_h - nT)/T \tag{4.36}$$

and $\psi(j) = \theta_k - 2\pi[f_c - f^{(k)}_{j_i - j_k - 1}]\tau_k + \alpha^{(i)}_{j_i} - \beta^{(i)}_{j_i}$. To obtain the output of the lower branch $Z_{c,d}$ we need to replace $b^{(i)}_{\lambda}$ by $b^{(i)}_{\lambda-1}$ in (4.30) and n_i with $n_i - 1$ in the definition of the quantity $L(j,n)$. Finally, to obtain the outputs of the quadrature components Z_s and $Z_{s,d}$ we only need to replace $\cos(\cdot)$ with $-\sin(\cdot)$.

Next step is to evaluate the average error probability at the output of the receiver of the hybrid SSMA systems. The technique used here is to decouple the effect of hits from other users due to frequency hopping from the multiple-access interference due to the direct sequence spread spectrum signals. This is done by first evaluating the conditional probability of error, given the number of full hits and the number of partial hits, and then averaging with respect to the distribution of the full hits and partial hits. Given that a number of full hits from other users has occurred, the hybrid SSMA systems under consideration are equivalent to the DS/SSMA analyzed in section 4.2. A slight modification can be adopted to the partial hits cases. Here only the random hopping patterns are considered.

The bit error rate of the hybrid SSMA system $\overline{P}_e$ can be written as

$$\overline{P}_e = \sum_{k_f=0}^{K-1} \sum_{k_p=0}^{K-k_f-1} P_h(k_f, k_p) \overline{P}_e(k_f, k_p) \tag{4.37}$$

$P_h(k_f, k_p)$ denotes the probability of the occurrence of k_f full hits and k_p partial hits from the other $K-1$ users. $\overline{P}_e(k_f, k_p)$ denotes the conditional error probability of the system, given that k_f full hits and k_p partial hits occurred. For independent hopping patterns the joint probability of k full hits and k' partial hits is given by

$$P_h(k,k') = \begin{pmatrix} K-1 \\ k \end{pmatrix} \begin{pmatrix} K-1-k \\ k' \end{pmatrix} P_f^k P_p^{k'} (1 - P_f - P_p)^{K-1-k-k'} \tag{4.38}$$

where $0 \leq k < K, 0 \leq k' < K - k$, and P_f and P_p denote the probability of a full and a partial hit from other users, respectively. For the first order Markov random hopping patterns, these probabilities are

$$P_f = (1 - N_b^{-1})q^{-1} \tag{4.39}$$

$$P_p = 2N_b^{-1}q^{-1} \tag{4.40}$$

q is the total number of distinct frequencies to hop. For partial hits, in the case of random signature sequences,

$$\sigma_p^2 = \frac{1}{6N} \tag{4.41}$$

$$\tilde{\sigma}_p^2 = 0 \tag{4.42}$$

and

$$\overline{v_1} = (2E_b/N_0)^{-1} + k_f\sigma_f^2 + k_p\sigma_p^2 \tag{4.43}$$

$$\overline{\tilde{v}_1} = k_f\tilde{\sigma}_f^2 + k_p\tilde{\sigma}_p^2 = 0 \tag{4.44}$$

then using the equation (4.20), we have

$$\overline{P}_e = \frac{1}{2}\exp\left\{-\frac{1}{2\left[(2E_b/N_0)^{-1} + (k_f + \frac{1}{2}k_p)/(3N)\right]}\right\} \tag{4.45}$$

For synchronous access, only full hit happens with the probability

$$P_h = q^{-1} \tag{4.46}$$

The computation of bit error rate is considerablely easier in this case

$$\overline{P}_e = \sum_{k=0}^{K-1} \begin{pmatrix} K-1 \\ k \end{pmatrix} P_h^k (1 - P_h)^{K-1-k} \overline{P}_e(k) \tag{4.47}$$

where $\overline{P}_e(k)$ is given as

$$\overline{P}_e = \frac{1}{2}\exp\left\{-\frac{1}{2\left[(2E_b/N_0)^{-1} + k/(2N)\right]}\right\} \tag{4.48}$$

which is the special case of equation (4.25) for $K = k$.

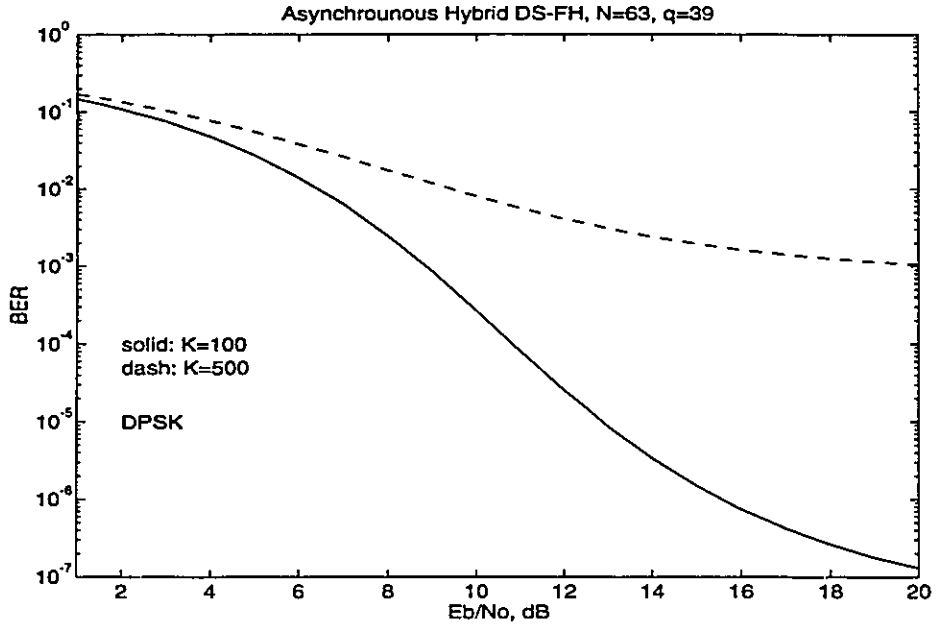

Figure 4.3: The asynchronous DS/FH-SSMA performance

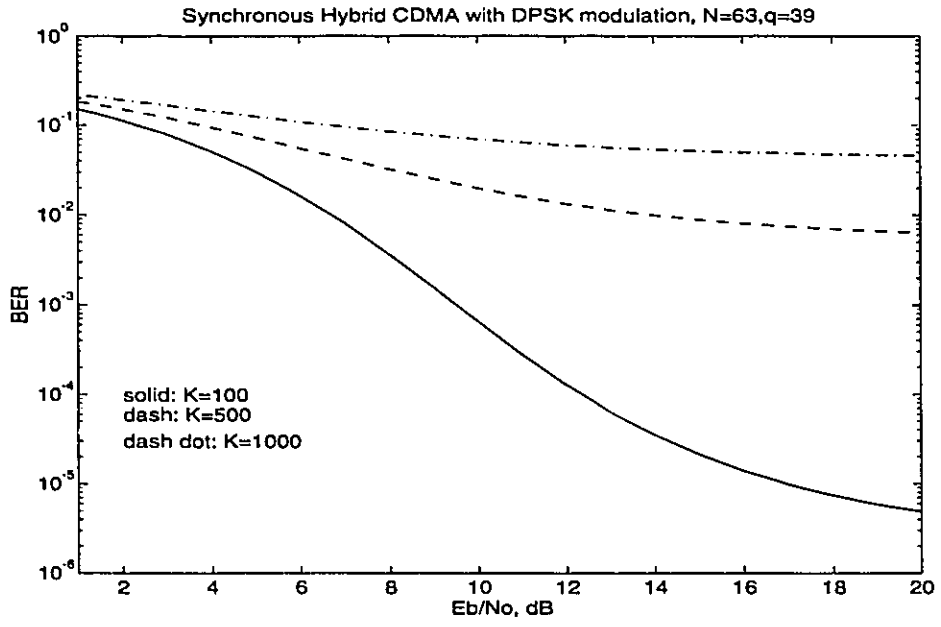

Figure 4.4: The synchronous DS/FH-SSMA performance

In figure 4.3, we plotted the performance of the asynchronous hybrid DS/FH SSMA systems. In figure 4.4, we plotted the performance curves of the synchronous hybrid DS/FH SSMA systems

Ideally, the bandwidth in both cases should be able to accommodate $63 \times 80 \approx 5000$ users without mutual interference if the systems are operated by TDMA or FDMA. However, for these two hybrid systems, at the user number $K = 500$, or at about 10% of the hard limit of capacity, they already generate excessive interferences which causes the BER to be higher than 10^{-3}. We can see that the performance of the hybrid systems is worse than that of DS systems, for which a similar performance curve is achieve at $K = 30$ or 50% of the hard limit. The main reason for this degradation is the collision in the frequency domain, caused by the random hopping. For the hybrid systems using random hopping patterns and random code sequence, the asynchronous access method performs slightly better than the synchronous access method, because of the reduced collisions by partial hits.

4.4 BER for deterministic hopping

As we have shown in section 4.3, a random hopping system cannot have satisfactory performance. A solution to this is to introduce the deterministic periodic frequency hopping, and the hopping patterns are coordinated such that no collision will happen. For example, one may choose a signal PN sequence to control all the hopping patterns, and each hopping pattern is associated with a unique phase of this sequence. Since the hopping patterns are separated by the fixed phase offset on this sequence, there is no collision even though the hopping patterns exhaust all possible states of the PN sequence.

Another important advantage from no collision of hopping patterns is that, by associating the hopping patterns with the user's transmission power, the system can get rid of the near-far problem. Under such circumstance, within a signal cell, the

performance of the hybrid system is the same as that of the DS system. Thus the analysis conducted in section 4.2 is valid for this hybrid system also. However, we still want to seek the possibility of enhancing the system performance by taking the advantage of the configurations of our system.

4.4.1 Synchronous access with a single maximum length code

First, we propose to use a single maximum length sequence to generate the codes for all the users in the home cell. Each code is identified by starting from a unique phase of this sequence. An obvious advantage is that, the cross-correlations of different codes are equal to the sidelobe of the auto-correlation of this sequence, which are all equal to -1. This is conditioned on the synchronous access. If the random access happens, such an assignment is not possible, since the random phase delay will cause code ambiguities.

In our system plan, time slots are implemented for users to transmit signals synchronously. Since there are still propagation delays, although no longer than half a chip duration, the strictly synchronous access to the receiver is achievable for up-link. However, for downlink, it is possible to achieve perfect synchronization since all user signals are transmitted from the base station according to the same time slot, and go through the same route to a particular user. We first analysis the case of strictly synchronous access, so all the τ's are equal to 0.

The cross-correlation of two codes $\theta_{k,i}(0)$ equals the auto-correlation $\theta_a(l)$ where l is the phase offset of these two codes in integer numbers. Since $l > 1$, so $\theta_a(l) = -1$ for all the l, therefore,

$$\begin{aligned} \sigma_{k,i}^2 &= \frac{1}{2} E\{[\theta_{k,i}(0)/N]^2\} \\ &= \frac{1}{2N^2} \end{aligned} \tag{4.49}$$

and

$$\tilde{\sigma}_{k,i}^2 = 0 \tag{4.50}$$

so

$$\begin{aligned} v &= (2E_b/N_0)^{-1} + \sum_{k=1,k\neq i}^{K} \sigma_{k,i}^2 \\ &= (2E_b/N_0)^{-1} + \frac{K-1}{N^2} \end{aligned} \tag{4.51}$$

$$\tilde{v} = 0 \tag{4.52}$$

such that

$$\overline{P}_e = \frac{1}{2}\exp\left\{-\frac{1}{(\frac{2E_b}{N_0})^{-1} + \frac{(K-1)}{N^2}}\right\} \tag{4.53}$$

By comparing with equation (4.25), we find the interferences from the co-channel users are reduced by a factor of N. This shows the great advantage of using time slots to enforce the synchronous access. More importantly, as N increases, the interference term approaches to zero asymptotically, so long as the total number of user K is no more than the system hard limit, which is given by N. In other words, the codes used in such a way are asymptotically orthogonal as N increases.

To verify the above result, we also conducted the Monte-Carlo simulations. In the simulations, we assigned each of the K users a code uniquely segmented from the same m-length sequence. All the users transmitted independent message sequence in the synchronous way, such that each information bit started at the same time for all the users. In addition, we also introduced the Gaussian random noise with the power spectrum density N_0, and added it to the channel. After DPSK demodulator, we compared the output message with the transmitted message for the desired user, and countered the number of wrong bits. The ratio of that to the total length of message would approximately give the BER. We repeated each experiment 50 times and get the mean value of them as the expected BER.

In figure 4.5, we shown the BER curves when there are 50 users on each hopping pattern, calculated from equation (4.53) (dashed curve) and simulated result (solid

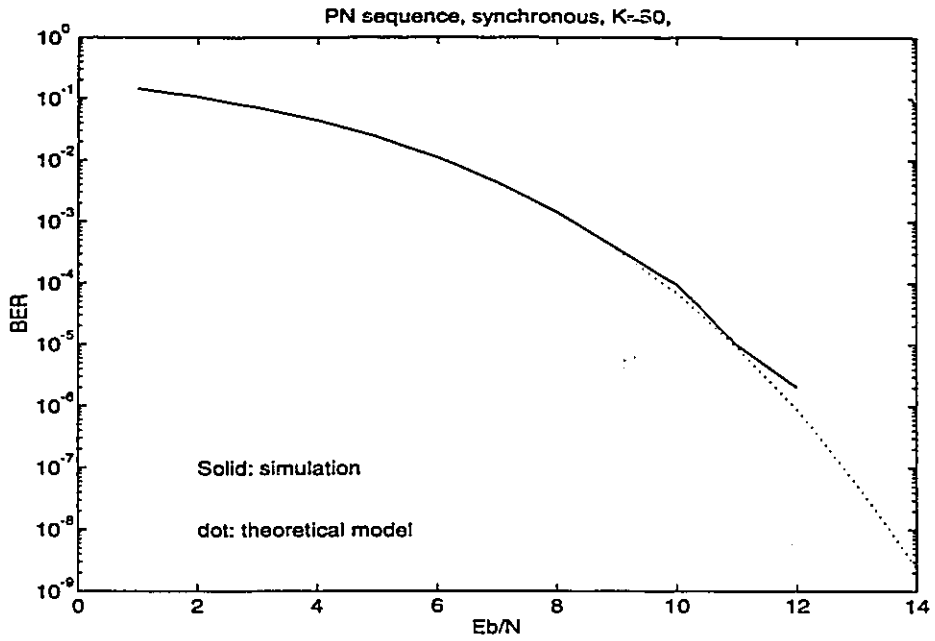

Figure 4.5: The synchronous DS/FH-CDMA bit error rate for a signal m-sequence employed as the codes for all users

curve). The simulation results are in good agreement with the theoretical analysis. More results are shown in table 4.1. Those results show the great improvement over the CDMA systems with random sequences. Moreover, the mutual interferences have been suppressed so much that the capacity of this system can reach the hard limit, i.e., $K = N = 63$.

Such an implementation cannot accommodate more than N users, otherwise at least a pair of users would have the identical code. If this happens, the performance degrades dramatically, as shown in figure 4.6. To take advantage of voice activity cycle, two or three sequences may be needed. The rule is to choose the sequences with the lowest cross correlation, such as the *preferred pairs*. Nevertheless this will still increase the mutual interference considerably, and we do not expect to triple the capacity at the same performance.

Table 4.1: BER performance for single PN sequence used as codes for all the users in the downlink

$\frac{E_b}{N_0}$	K=40		K=50	
dB	theory	simulation	theory	simulation
1	0.1442	0.1443	0.1447	0.1451
2	0.1050	0.1054	0.1056	0.1061
3	0.0706	0.0700	0.0713	0.0710
4	0.0431	0.0437	0.0437	0.0441
5	0.0233	0.0236	0.0238	0.0238
6	0.0108	0.0105	0.0112	0.0110
7	0.0042	0.0041	0.0045	0.0044
8	0.0013	0.0014	0.0014	0.0014
9	0.0003	0.0003	0.0004	0.0004
10	5.6E-5	8.2E-5	6.8E-5	9.4E-5
11	6.8E-6	0.0000	9.3E-6	1.0E-5
12	1.6E-6	0.0000	8.8E-7	2.0E-6
13	1.3E-7	0.0000	5.6E-8	0.0000
14	7.9E-9	0.0000	2.4E-9	0.0000

$\frac{E_b}{N_0}$	K=63		K=64
dB	theory	simulation	simulation
1	0.1455	0.1449	0.3196
2	0.1065	0.1068	0.3129
3	0.0722	0.0722	0.3046
4	0.0450	0.0450	0.3006
5	0.0246	0.0253	0.2932
6	0.0118	0.0116	0.2885
7	0.0048	0.0046	0.2845
8	0.0016	0.0017	0.2831
9	0.0004	0.0005	0.2791
10	8.8E-5	1.1E-4	0.2761
11	1.3E-5	6.0E-6	0.2748
12	1.5E-6	4.0E-6	0.2718
13	1.2E-7	0.0000	0.2723
14	7.3E-9	0.0000	0.2708

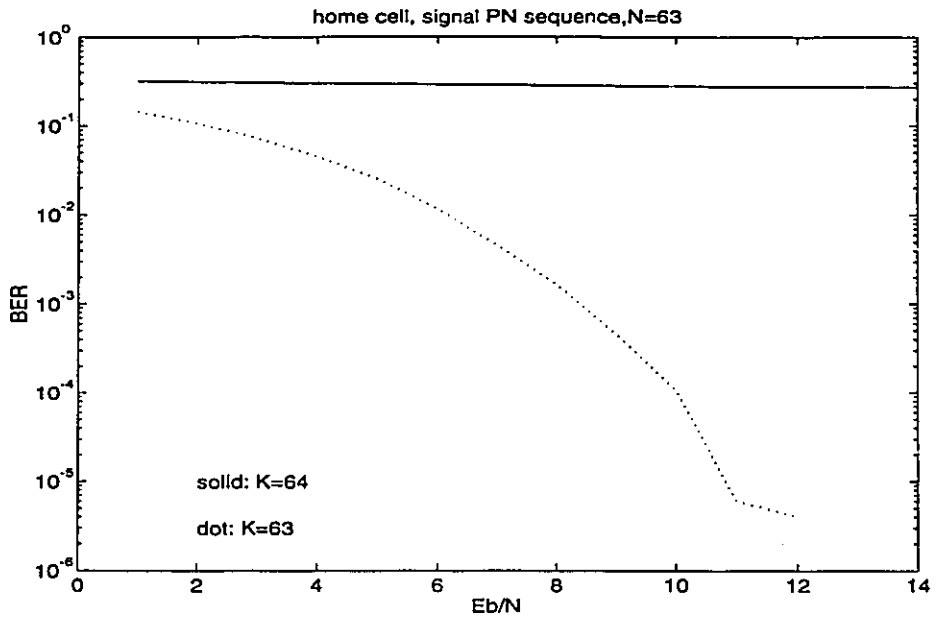

Figure 4.6: The performance of synchronous access using a single m-length sequence, when the hard limit is broken.

4.4.2 Quasi-synchronous access with a signal maximum length code

If synchronous access cannot be guaranteed, then there is hardly any benefit gained from the use of a single m-sequence to provide codes for all users. We can show this point by evaluating the cross-correlation of two codes at zero relative time delay is zero.

$$\begin{aligned} \theta_{k,i}(0) &= \int_0^T a_k(t)a_i(t)dt \\ &= \int_0^T a(t)a(t-\tau)dt \\ &= R_a(\tau) \end{aligned} \tag{4.54}$$

For random access, τ is a continuous variable, uniformly distributed within $[0, T]$.

Hence,

$$R_a(\tau) = \begin{cases} N(1 - \frac{1+\frac{1}{N}}{T_c}\tau) & 0 \le \tau < T_c \\ -1 & T_c \le \tau < (N-1)T_c \\ N(\frac{1+\frac{1}{N}}{T_c}\tau - N) & (N-1)T_c \le \tau < NT_c \end{cases} \tag{4.55}$$

The PDF of τ is:

$$f(\tau) = \begin{cases} \frac{1}{T} & 0 \le \tau < T_c \\ 0 & \text{otherwise} \end{cases} \tag{4.56}$$

Thus the PDF of $R(\tau)$ can be expressed as

$$f(R) = \begin{cases} \frac{2}{N^2+N} & -1 < R < N \\ A\delta(R+1) & R = -1 \\ 0 & \text{otherwise} \end{cases} \tag{4.57}$$

The constant A can be determined as following:

$$\begin{aligned} 1 &= \int_{-1}^{N} f(R)dR \\ &= \int_{-1^+}^{N} \frac{2}{N^2+N}dR + \int_{-1^-}^{-1^+} A\delta(R+1)dR \\ &= \frac{2}{N} + A \end{aligned} \tag{4.58}$$

so that

$$A = \frac{N-2}{N} \tag{4.59}$$

Therefore

$$\begin{aligned} E\{\theta_{k,i}^2(0)\} &= E\{R_a^2(\tau)\} \\ &= \int_{-1^+}^{N} \frac{2}{N^2+N}R^2dR + \int_{-1^-}^{-1^+} \frac{N-2}{N}\delta(R+1)R^2dR \\ &= \frac{2}{N^2+N}\frac{1}{3}(N^3+1) + \frac{N-2}{N} \\ &= \frac{2}{3}N - \frac{1}{3} \\ &\approx \frac{2}{3}N \end{aligned} \tag{4.60}$$

This shows when random access happens, the cross-correlation of these special codes is about the same as that of the random codes.

It is more interesting to examine the performance of systems with the quasi-synchronous access. It is the case in which perfect synchronization cannot be maintained, however, the maximum deviation of the delay-time caused by propagation or other reasons is under one chip duration, say it αT_c where α is a number in $[0,1)$. Then we can evaluate the error performance as follows:

$$\begin{aligned}
o_{k,i}^2 &= \mathrm{Var}\{I_c^{(k,i)}\} \\
&= \mathrm{Var}\{T^{-1}\left[b_{n-1}^{(k)}\int_0^{\alpha T_c} a_k(t-\alpha T_c)a_i(t)dt + b_n^{(k)}\int_{\alpha T_c}^{T} a_k(t-\alpha T_c)a_i(t)dt\right]\cos\phi_k\} \\
&= \frac{1}{2T^2}\mathrm{E}\{[b_{n-1}^{(k)}\int_0^{\alpha T_c} a_k(t-\alpha T_c)a_i(t)dt + b_n^{(k)}\int_{\alpha T_c}^{T} a_k(t-\alpha T_c)a_i(t)dt]^2\} \\
&= \frac{1}{2T^2}\mathrm{E}\{[(b_{n-1}^{(k)}-b_n^{(k)})\int_0^{\alpha T_c} a_k(t-\alpha T_c)a_i(t)dt + b_n^{(k)}\int_0^{T} a_k(t-\alpha T_c)a_i(t)dt]^2\} \\
&= \frac{1}{2T^2}\mathrm{E}\{[(b_{n-1}^{(k)}-b_n^{(k)})a_k(N-1)a_i(0)\alpha T_c + b_n^{(k)}R_a(\alpha T_c)]^2\} \\
&= \frac{1}{2T^2}\mathrm{E}\{(b_{n-1}^{(k)}-b_n^{(k)})^2\alpha^2T_c^2 + T_c^2R_a^2(\alpha T_c)\} \\
&= \frac{1}{2T^2}\{2\alpha^2T_c^2 + T_c^2\mathrm{E}[R_a^2(\alpha T_c)]\}
\end{aligned} \tag{4.61}$$

For a delay uniformly distributed within $[-\alpha T_c, +\alpha T_c]$, the PDF of τ is

$$f(\tau) = \begin{cases} \frac{1}{2\alpha T_c} & -\alpha T_c \le \tau < \alpha T_c \\ 0 & \text{otherwise} \end{cases} \tag{4.62}$$

As it is shown in figure 4.7, the PDF for $R(\tau_k)$ is

$$f(R) = \begin{cases} \frac{2}{N^2+N} & -1 < R < \alpha N + \alpha - 1 \\ A\delta(R+1) & R = -1 \\ 0 & \text{otherwise} \end{cases} \tag{4.63}$$

and the constant A is determined by

$$\begin{aligned}
1 &= \int_{-1}^{\alpha N+\alpha-1} f(R)dR \\
&= \int_{-1^+}^{\alpha N+\alpha-1} \frac{2}{N^2+N}dR + \int_{-1^-}^{-1^+} A\delta(R+1)dR \\
&= \frac{2\alpha}{N} + A
\end{aligned} \tag{4.64}$$

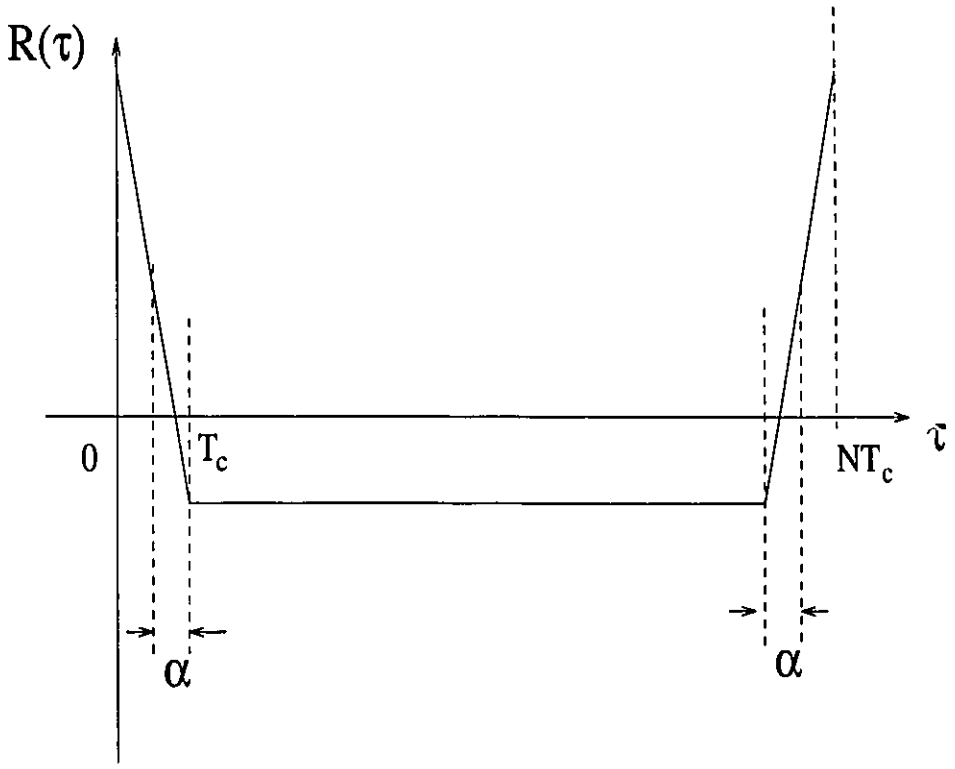

Figure 4.7: The cross correlation property of quasi-synchronous access performance, by using a single m-length sequence.

Thus,

$$A = \frac{N - 2\alpha}{N} \tag{4.65}$$

and we have

$$f(R) = \begin{cases} \frac{2}{N^2+N} & -1 < R < \alpha N + \alpha - 1 \\ \frac{N-2\alpha}{N}\delta(R+1) & R = -1 \\ 0 & \text{otherwise} \end{cases} \tag{4.66}$$

Therefore

$$\begin{aligned} \mathrm{E}\{R^2\} &= \int_{-1^+}^{\alpha N+\alpha-1} \frac{2}{N^2+N} R^2 dR + \frac{N-2\alpha}{N} \int_{-1^-}^{-1^+} \delta(R+1) R^2 dR \\ &= \frac{2}{3}\frac{1}{N^2+N}[(\alpha N + \alpha - 1)^3 + 1] + \frac{N-2\alpha}{N} \\ &= \frac{1}{3(N^2+N)}\left\{2\alpha^3 N^3 + 3(2\alpha^3 - 2\alpha^2 + 1)N^2 + 3(2\alpha^3 - 4\alpha^2 + 1)N + 2\alpha^3 - 6\alpha^2\right\} \end{aligned} \tag{4.67}$$

Thus we have

$$\begin{aligned} \sigma_{k,i}^2 &= \frac{1}{2T^2}\{2\alpha^2 T_c^2 + T_c^2 \mathrm{E}[R_a^2(\alpha T_c)]\} \\ &= \frac{1}{6N^3(N+1)}[2\alpha^3 N^3 + 3(2\alpha^3 + 1)N^2 + 3(2\alpha^3 - 2\alpha^2 + 1)N + 2\alpha^3 - 6\alpha^2] \end{aligned} \tag{4.68}$$

and the average error probability is

$$\overline{P}_e = \frac{1}{2}\exp\left\{-\frac{1}{2\left[(\frac{2E_b}{N_0})^{-1} + (K-1)\sigma_{k,i}^2\right]}\right\} \tag{4.69}$$

In comparison with the synchronous access case, we can see the degraded performance. For example, for the case $K = 50$, the 10^{-3} BER is reached when E_b/N_0 is about 11 dB in table 4.2, while for the synchronous case, similar performance can be reached when E_b/N_0 is about 8 dB, as shown in table 4.1.

If voice activity cycle is taken into consideration, two or three sequences will be used. This will further increase the cross-correlation among user's codes. Still we

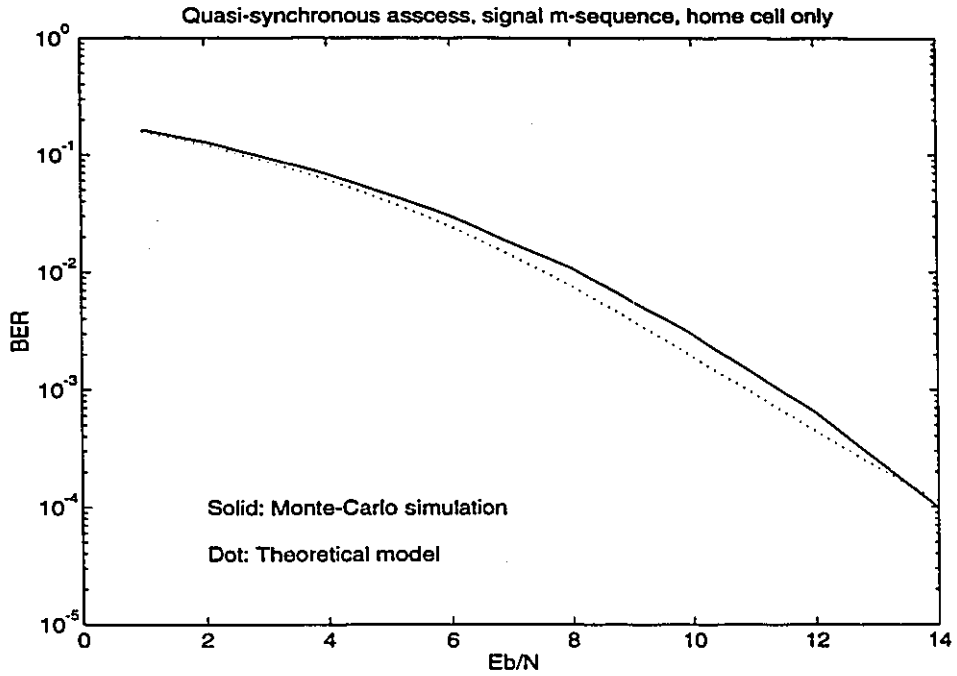

Figure 4.8: The performance of quasi-synchronous access using a single m-length sequence, with K=50, N=63.

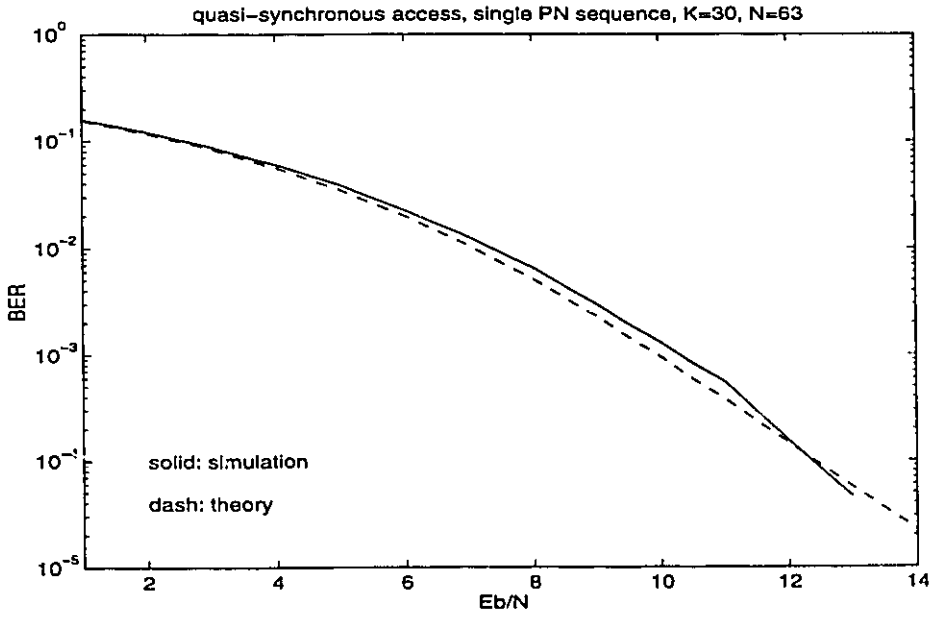

Figure 4.9: The performance of quasi-synchronous access using a single m-length sequence, with K=30, N=63.

Table 4.2: BER performance for single PN sequence used as codes for all the users in the up-link

$\frac{E_b}{N_0}$	K=30		K=40		K=50	
dB	theory	simulation	theory	simulation	theory	simulation
1	0.1523	0.1586	0.1557	0.1623	0.1591	0.1648
2	0.1143	0.1215	0.1183	0.1268	0.1223	0.1297
3	0.0806	0.0879	0.0850	0.0948	0.0892	0.0956
4	0.0528	0.0601	0.0572	0.0664	0.0615	0.0683
5	0.0318	0.0388	0.0358	0.0449	0.0399	0.0455
6	0.0174	0.0226	0.0207	0.0282	0.0242	0.0298
7	0.0863	0.0127	0.0111	0.0165	0.0138	0.0176
8	0.0038	0.0065	0.0055	0.0093	0.0074	0.0110
9	0.0015	0.0030	0.0025	0.0046	0.0038	0.0056
10	5.5E-4	1.3E-3	0.0011	0.0022	1.9E-3	2.9E-3
11	1.8E-4	5.6E-4	4.2E-4	9.4E-3	9.1E-4	1.3E-3
12	5.6E-5	1.6E-4	1.8E-4	4.3E-4	4.4E-4	6.4E-4
13	1.7E-5	4.6E-5	7.2E-5	1.4E-4	2.2E-4	2.5E-4
14	4.8E-6	0.0000	3.0E-5	4.8E-5	1.1E-4	9.8E-5

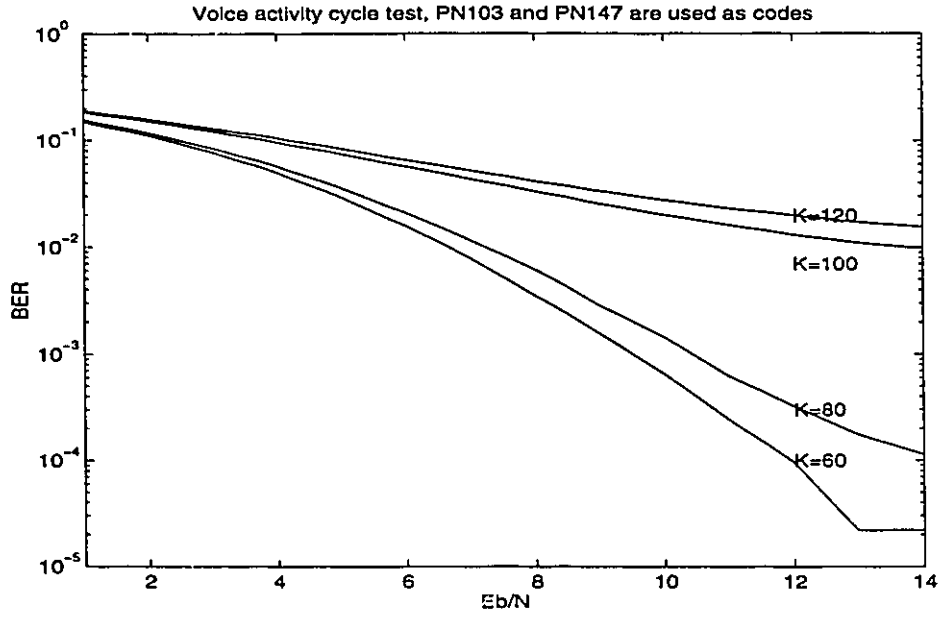

Figure 4.10: Simulated performance of quasi-synchronous access, with the consideration of voice activity cycle. PN103 and PN147 are used

Table 4.3: Voice activity cycle test in the uplink

$\frac{E_b}{N_0}$	K=60	K=80	K=100	K=120
1	0.1490	0.1561	0.1844	0.1900
2	0.1120	0.1184	0.1527	0.1587
3	0.0773	0.0841	0.1227	0.1301
4	0.0502	0.0575	0.0966	0.1056
5	0.0293	0.0359	0.0748	0.0836
6	0.0158	0.0210	0.0571	0.0655
7	0.0079	0.0116	0.0436	0.0523
8	0.0035	0.0062	0.0335	0.0416
9	0.0016	0.0028	0.0256	0.0336
10	6.5e-4	0.0015	0.0202	0.0278
11	2.4e-4	6.3e-4	0.0163	0.0233
12	9.6e-5	3.2e-4	0.0131	0.0200
13	2.2e-5	1.8e-4	0.0110	0.0173
14	2.2e-5	1.1e-4	0.0097	0.0156

will see the increased capacity, although it is far less than the tripled capacity. For $K = 60$, only one sequence is used as codes. For K above 63, the second sequence (PN147) is used to provide codes for the rest of users. We can see a sharp increase in BER from $K = 80$ to $K = 120$. The reason is the relatively big cross correlation values between the PN103 and PN147, although they are the *preferred pairs*. If K is modestly higher than 63, most users still use PN103 as code sequence. Only 17 users use PN147 as code, for $K = 80$. Thus the effect of that higher value of cross-correlation between PN103 and PN147 is not severe. However, as K increases, the cross-correlation between PN103 and PN147 will quickly become the dominated term for generating mutual interferences, as shown in the cases of $K = 100$ and $K = 120$.

4.4.3 Performance of system with Gold codes

It is interesting to examine the performance of Gold codes in the case of synchronous access. As we have discussed in chapter 3, the cross correlation of Gold codes in the same set equals to -1, if there is no relative phase shift (cf. the function $C(0)$ in

Table 4.4: Simulated BER performance for Gold codes in the downlink

$\frac{E_b}{N_0}$	K=30	K=40	K=50
1	0.1432	0.1435	0.1451
2	0.1040	0.1050	0.1061
3	0.0696	0.0707	0.0710
4	0.0427	0.0432	0.0441
5	0.0229	0.0231	0.0238
6	0.0102	0.0107	0.0110
7	0.0040	0.0044	0.0044
8	0.0012	0.0014	0.0014
9	0.0003	0.0003	0.0004
10	6.6E-5	4.4E-5	9.4E-5
11	1.8E-5	0.0000	1.0E-5
12	0.0000	8.0E-6	2.0E-6
13	0.0000	0.0000	0.0000
14	0.0000	0.0000	0.0000

Table 3.3 and Figure 3.14). Therefore the performance of Gold codes should be the same as that of single m-length codes for downlink. In Table 4.4 we list the simulated results only since the theoretical results can be found in Table 4.1 for synchronous access. It confirms our expectation and show close agreements with the theoretical prediction.

The performance of Gold codes in the uplink is shown in Figure 4.12 and Table 4.5. Gold codes have slightly better results than the code generated from a single m-length sequence.

4.4.4 Synchronous Access With Orthogonal Codes

The performance evaluation for such a case is straight forward. Since

$$\theta_{k,i}(0) = \int_0^T a_k(t)a_i(t)dt = 0 \tag{4.70}$$

Therefore the mutual interference terms are all equal to zero. Thus we have

$$\overline{P}_e = \frac{1}{2}\exp\left\{-\frac{E_b}{N_0}\right\} \tag{4.71}$$

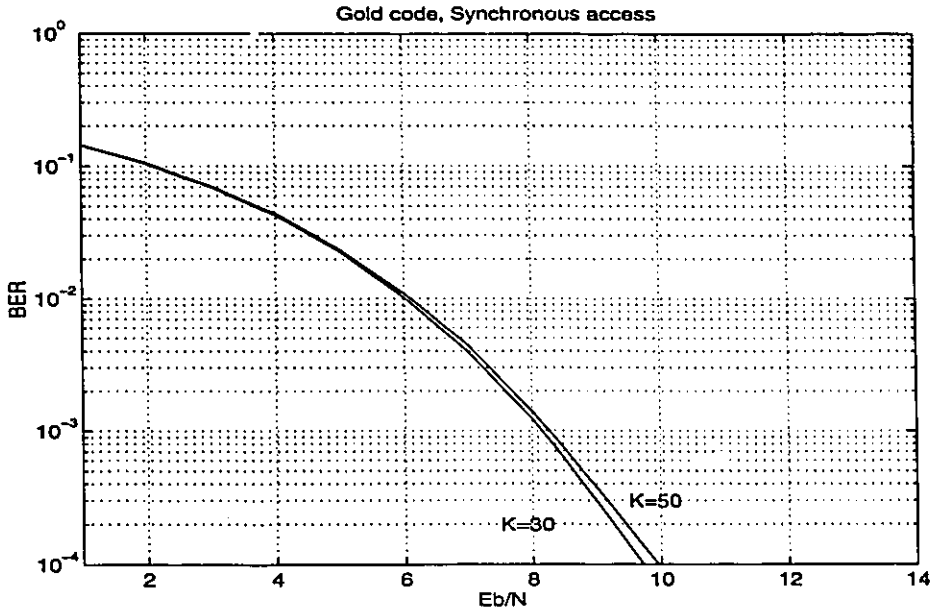

Figure 4.11: The performance of synchronous access using Gold codes

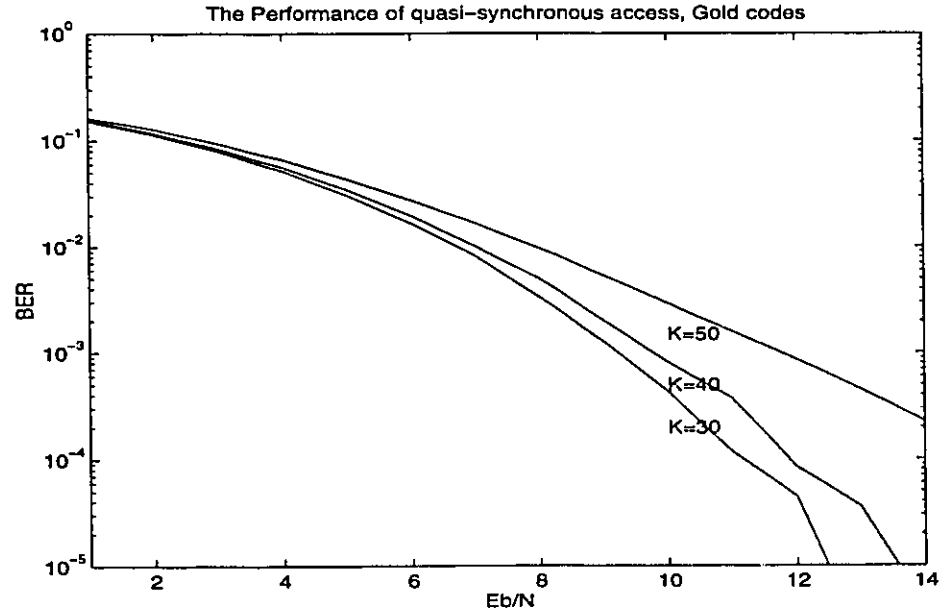

Figure 4.12: Simulated performance of quasi-synchronous access, Gold codes generated from PN103

Table 4.5: BER performance for Gold codes for all the users in the uplink

$\frac{E_b}{N_0}$	K=30	K=40	K=50
1	0.1517	0.1545	0.1618
2	0.1132	0.1171	0.1275
3	0.0795	0.0839	0.0933
4	0.0518	0.0559	0.0660
5	0.0309	0.0348	0.0437
6	0.0166	0.0196	0.0273
7	0.0082	0.0100	0.0167
8	0.0033	0.0050	0.0096
9	0.0013	0.0020	0.0053
10	4.3e-4	8.1e-4	0.0029
11	1.1e-4	3.7e-4	0.0015
12	4.4e-5	8.4e-5	8.6e-4
13	2.0e-6	3.6e-5	4.5e-4
14	8.0e-6	4.0e-6	2.2e-4

which is the error perfomace of DPSK modulation. The simulation results are shown in Figure 4.13, and Table 4.6.

4.4.5 Quasi-synchronous Access with Orthogonal Codes

Again, the more practical case in the uplink is the quasi-synchronous access. For the delays $\tau_k = \alpha T_c$ is bounded, and $0 \leq |\alpha| < 1$, we have

$$\begin{aligned} R_{k,i} &= \int_0^T b_k(t-\tau_k)a_k(t-t_k)a_i(t)dt \\ &= b_k^{(n)}\sum_{l=1}^{N}\{a_i(l)a_k(l-1)\alpha + a_i(l)a_k(l)(1-\alpha)\}T_c + (b_k^{(n-1)} - b_k^{(n)})a_i(1)a_k(N)\alpha T_c \\ &= (b_k^{(n-1)} - b_k^{(n)})a_i(1)a_k(N)\alpha T_c + b_k^{(n)}T_c\sum_{l=1}^{N}\alpha a_i(l)a_k(l-1) \end{aligned} \tag{4.72}$$

where in the last step we have used the fact that

$$\sum_{l=1}^{N}\alpha a_i(l)a_k(l) = 0 \quad \text{for} \qquad k \neq i \tag{4.73}$$

(4.74)

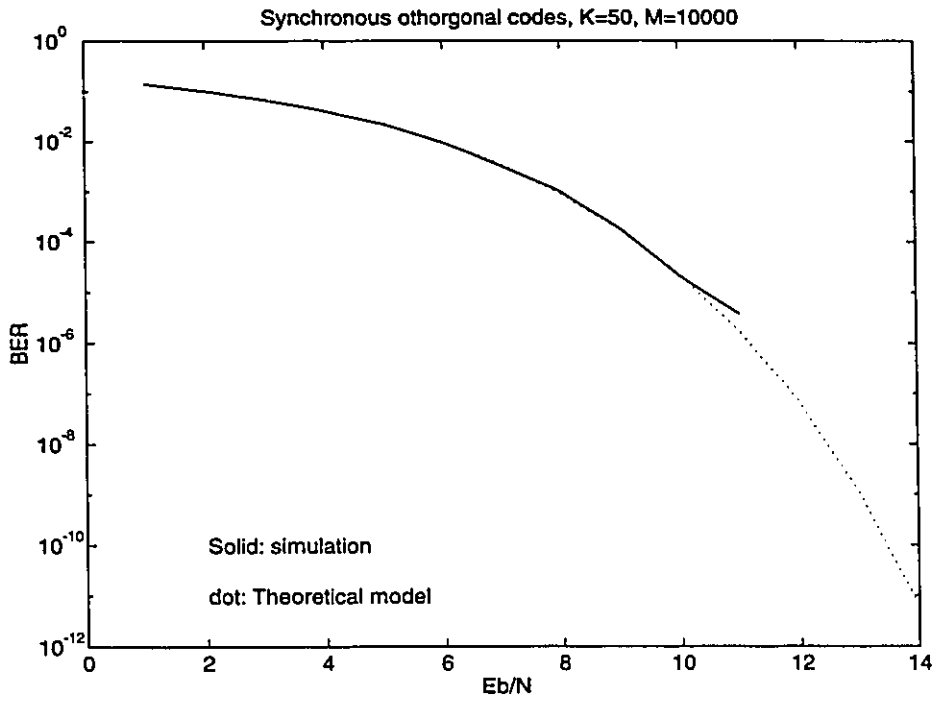

Figure 4.13: The synchronous access performance with orthogonal codes

Table 4.6: BER performance for Orthogonal codes in the uplink

$\frac{E_b}{N_0}$		K=40	K=50
dB	theory	simulation	simulation
1	0.1420	0.1390	0.1408
2	0.1025	0.1017	0.1013
3	0.0680	0.0683	0.0682
4	0.0406	0.0411	0.0406
5	0.0212	0.0209	0.0215
6	0.0093	0.0091	0.0091
7	0.0033	0.0033	0.0032
8	9.0e-4	0.0010	9.9e-4
9	1.7e-4	2.1e-4	1.8e-4
10	2.2e-5	1.1e-5	2.1e-5
11	1.7e-6	2.5e-6	3.7e-6
12	6.5e-8	0.0e+0	0.0e+0
13	1.0e-9	0.0e+0	0.0e+0
14	6.1e-12	0.0e+0	0.0e+0

Hence,

$$\begin{aligned}\overline{R_{i,k}^2(\alpha T_c)} &= \overline{\{(b_k^{(n-1)} - b_k^{(n)})a_i(1)a_k(N)\alpha T_c\}^2} \\ &\quad \overline{+ \{b_k^{(n)} T_c \sum_{l=1}^{N} \alpha a_i(l)a_k(l-1)\}^2} \\ &= 2\alpha^2 T_c^2 + \alpha^2 T_c^2 N \end{aligned} \tag{4.75}$$

Therefore

$$\overline{P_e} = \frac{1}{2}\exp\left\{-\frac{1}{(\frac{2E_b}{N_0})^{-1} + \alpha^2\frac{(K-1)(N+2)}{N^2}}\right\} \tag{4.76}$$

In figures 4.14 and 4.15, we show the performance of both the theoretical results as well as the simulated results. We see the degradation of performance due to the imperfection of synchronization. In table 4.7, we listed the results for different number of users.

To have the comparison more apparent, we reproduced the curves of $K = 50$ for all the three codes, for synchronous access (figure 4.16) and asynchronous access (figure 4.17). We can see that for the down-link, orthogonal codes are the best choice. In the quasi-synchronous access environment such as the uplink, the difference between them is small, with orthogonal codes slightly outperforming the m-length codes and Gold codes.

4.5 Summary of the chapter

The major concern in this chapter is to explore ways of maximizing the system capacity, by only considering the interference from other users in the home cell. Several points are important in the understanding of the capacity of CDMA systems, and they are listed as following:

- We used the classical DS/FH hybrid systems to show that they are inefficient and cannot satisfy our requirement of high capacity. We pointed out that the solution is to use coordinated deterministic hopping patterns. Without

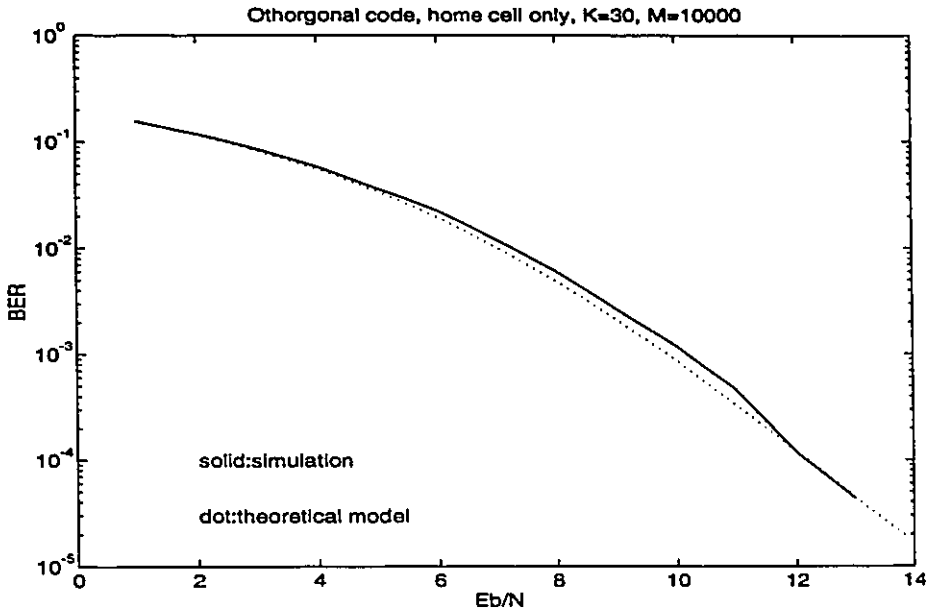

Figure 4.14: The quasi-synchronous access performance with orthogonal codes

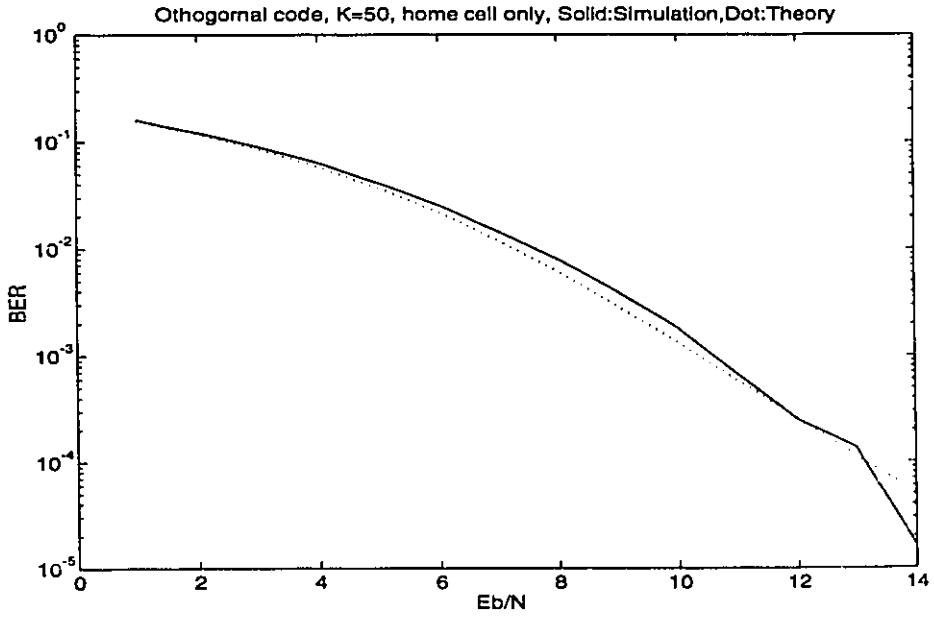

Figure 4.15: The quasi-synchronous access performance with orthogonal codes

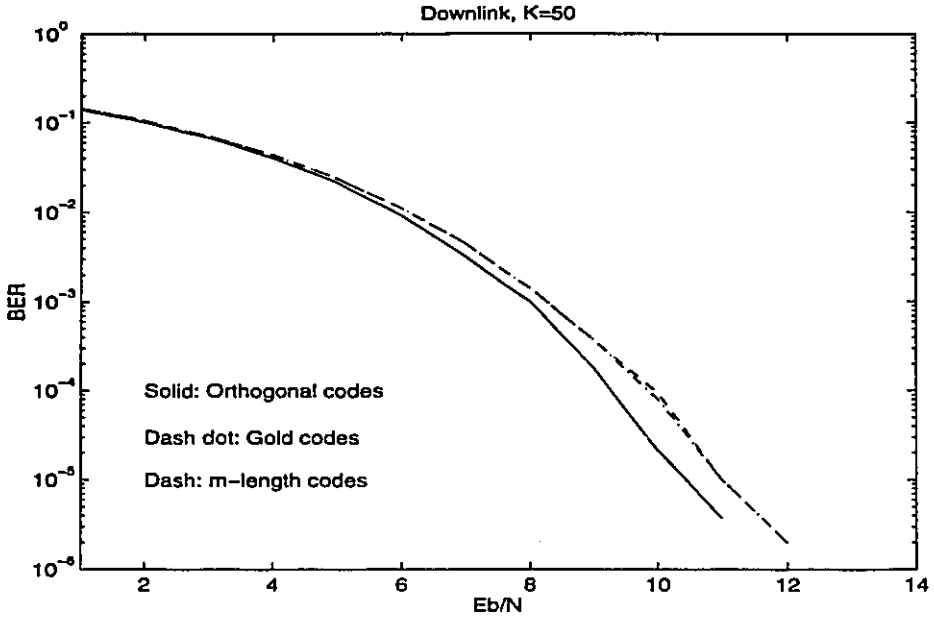

Figure 4.16: Simulated performance of synchronous access, Orthogonal codes, Gold codes and m-length code

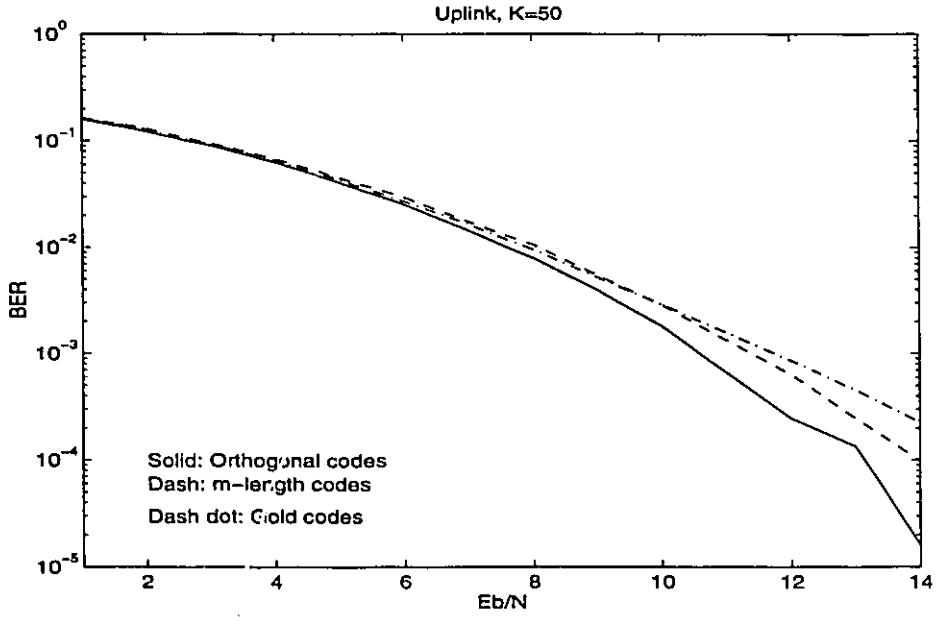

Figure 4.17: Simulated performance of quasi-synchronous access, Orthogonal codes, Gold codes and m-length code

Table 4.7: BER performance for Orthogonal codes in the uplink

$\frac{E_b}{N_0}$	K=30		K=40		K=50	
dB	theory	simulation	theory	simulation	theory	simulation
1	0.1559	0.1561	0.1568	0.1572	0.1574	0.1601
2	0.1185	0.1186	0.1196	0.1201	0.1203	0.1222
3	0.0852	0.0862	0.0864	0.0889	0.0871	0.0908
4	0.0574	0.0583	0.0586	0.0592	0.0593	0.0637
5	0.0360	0.0364	0.0371	0.0381	0.0378	0.0413
6	0.0209	0.0225	0.0218	0.0230	0.0224	0.0256
7	0.0112	0.0119	0.0119	0.0122	0.0124	0.0146
8	0.0056	0.0059	0.0060	0.0065	0.0064	0.0079
9	0.0025	0.0026	0.0029	0.0031	0.0031	0.0040
10	0.0011	0.0011	0.0013	0.0013	0.0014	0.0018
11	4.6e-4	4.6e-4	5.7e-4	5.3e-4	6.5e-4	6.7e-4
12	1.9e-4	1.2e-4	2.4e-4	2.2e-4	2.8e-4	2.4e-4
13	7.8e-5	4.3e-5	1.0e-4	2.7e-5	1.3e-4	1.3e-4
14	3.2e-5	0.0e+0	4.8e-5	1.0e-5	6.0e-5	1.6e-5

frequency collisions, the system capacity is enhanced, and no near-far problem exists.

- We also showed the analytical results of the classical DS CDMA systems where random codes are used. In such a case the mutual interference is the major bottle neck to the system performance. To make the system to be useful, the capacity has to be held at about $\frac{1}{10}$ of its hard-limit on capacity.

- We proposed the idea of using a single m-length sequence for all the users as codes. We have shown that, in the perfectly synchronous access environment such as in the down-link case, the capacity can asymptotically reach the hard limit which is equal to the period of code sequence. We also analyzed the quasi-synchronous access case, and we found that it is still superior to using the random codes. For similar mutual interference, we may accommodate 30 users in comparison with only 7 users for the case of random accessing.

- We also tested the voice activity cycle for this case. Due to the introduction of more than one sequence, we expect the gain in capacity to be far less than 3 times for similar BER. We also compared the performance with that when Gold codes are used. We found that their performance is about the same in the case of quasi-synchronous access.

- We analyzed the performance of orthogonal codes for both downlink and uplink case. For the case of downlink, orthogonal codes are optimum. In the case of uplink, all these three codes (Orthogonal, Gold and m-length codes) give nearly the same performance.

Chapter 5

Capacity Analysis Including Adjacent Cells

In chapter 4, we have described the models for analyzing the co-channel interference from users in the same cell. For CDMA PCS systems, co-channel interference from the adjacent cells will be an important factor to the system performance, because the same spectrum will be reused in the immediate adjacent cells. We will extend our system model to include the interference from the adjacent cells also.

5.1 Model of Path Loss

As it has been shown, CDMA is invariably interference limited; in the context of wireless microcellular communications, this means that the propagation characteristics of the channel play an intimately important role in determining the performance of the system. A lot of field measurements have shown that, the variation of loss with distance is reasonably described by a piecewise linear curve with a single break point. For the distance within the break point, the slope is about 2. Beyond that point, the slope is about 4.

A two ray model can reasonably explain the results of the field measurement. As

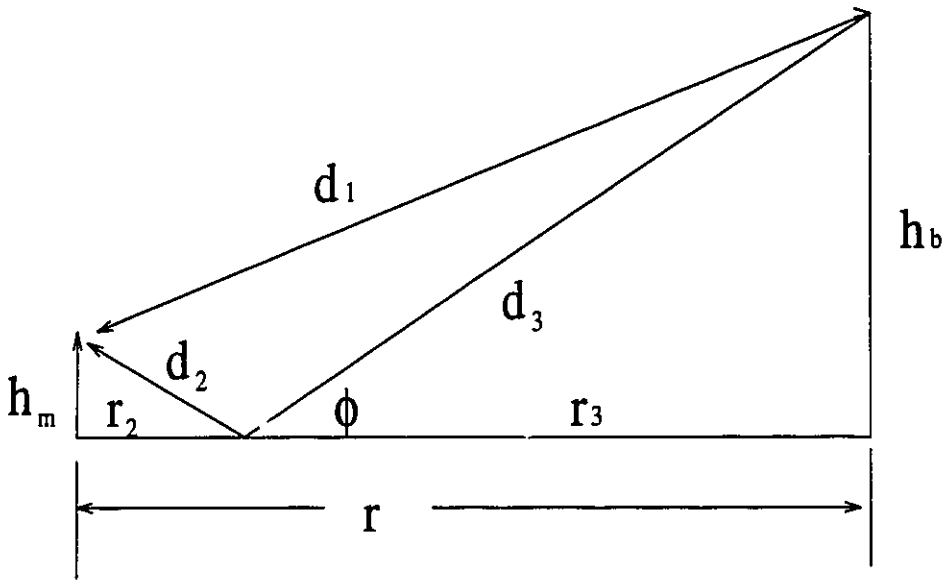

Figure 5.1: Two ray model of the propagation.

shown in Fig. 5.1, it consists of a direct path and a single ground bounce. The free space field intensity of the direct ray is:

$$E = \frac{\sqrt{30 g_a P}}{d_1} \tag{5.1}$$

where P is the power transmitted, g_a is the antenna gain. d_1 is the direct distance shown in Fig. 5.1. Received field intensity is the sum of the reflected and direct waves:

$$E_R = E(1 + \frac{d_1}{d_2 + d_3} R(\phi) e^{i\Delta}) \tag{5.2}$$

ϕ is the angle of incidence, Δ is the phase difference between the two waves, and d_2 and d_3 are shown in Fig. 5.1. $R(\phi)$ in the above equation is the reflection coefficient, for the case of vertical polarization[60],

$$R(\phi) = \frac{\epsilon \sin(\phi) - \sqrt{\epsilon - cos^2\phi}}{\epsilon \sin(\phi) + \sqrt{\epsilon - cos^2\phi}} \tag{5.3}$$

where ϵ is the dielectric constant, and it is readily shown that

$$\Delta = \frac{2\pi}{\lambda}[(1 + (\frac{h_b + h_m}{r})^2)^{\frac{1}{2}} - (1 + (\frac{h_b - h_m}{r})^2)^{\frac{1}{2}}] \tag{5.4}$$

The received power is:

$$\begin{aligned} P_r &= (\frac{|E_R|\lambda}{2\pi\sqrt{120}})^2 \\ &= P(\frac{\lambda}{4\pi d_1})^2|1+\frac{d_1}{d_2+d_3}R(\phi)e^{i\Delta}|^2 \end{aligned} \tag{5.5}$$

g is set to 1 for the omnidirectional antenna.

For far distances, $r \approx d_1 \approx d_2 + d_3$, and $R(\phi) = -1$. The received power is then

$$\begin{aligned} P_r &= P(\frac{\lambda}{4\pi r})^2|1-e^{i\Delta}|^2 \\ &= P(\frac{\lambda}{4\pi r})^2 \sin^2\frac{\Delta}{2} \end{aligned} \tag{5.6}$$

The largest distance for which a local maximum received power occurs is when (see figure 5.2)

$$\frac{\Delta}{2} = \frac{\pi}{2} \tag{5.7}$$

This distance is called the break point, denoted by R_b and is approximately given by

$$R_b \approx \frac{4h_b h_m}{\lambda} \tag{5.8}$$

In Fig. 5.2, we plotted the path loss versus distance for $\epsilon = 15$, according to the equation 5.6. The height of the base station antenna $h_b = 10$ meters, and the height of handset antenna $h_m = 1.5$ meter. The working frequency is assumed to be $f_c = 1.9$ GHz.

From the above plot, we can see that the envelope of the path-loss can be described by two segments. Within the break point at R_b, the envelope slope is nearly 20 dB/decade. Beyond that point, the envelope slope becomes much steeper, about 40 dB/decade. We show the two piece-wise linear segments fitting to the envelope by dotted line in figure 5.2.

$$\frac{P_r}{P} = \begin{cases} (\frac{\lambda}{2\pi r})^2 \sin^2\frac{R_b}{2r}\pi & r < R_b \\ \frac{\lambda^2 R_b^2}{16r^4} & r \gg R_b \end{cases} \tag{5.9}$$

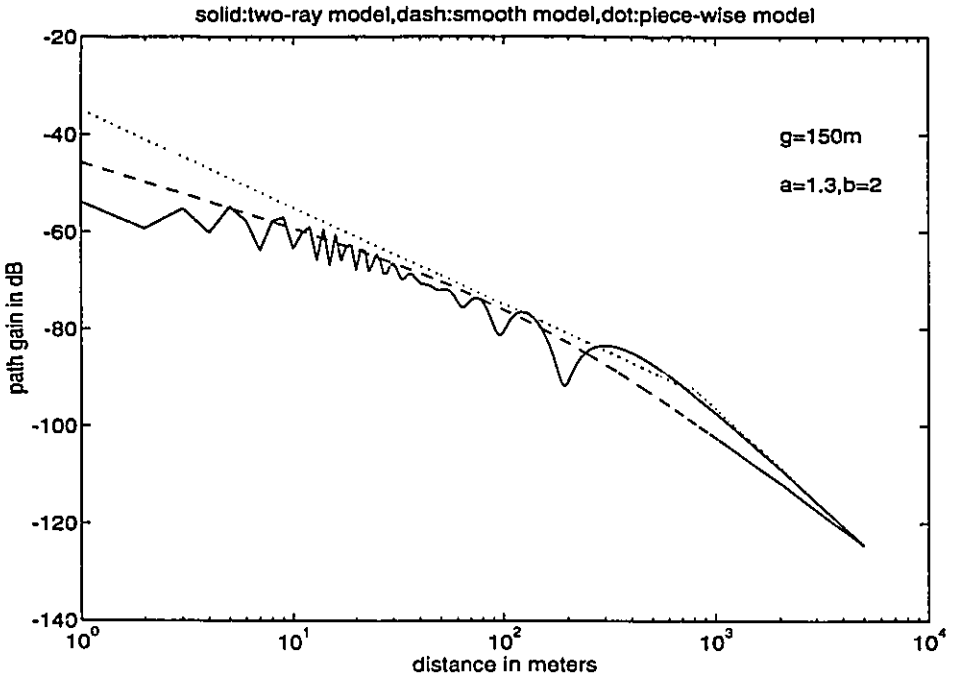

Figure 5.2: Computer simulated two ray mode, by solid line, together with the two piece-wise linear segments fitting model represented by dotted line, and the smooth model represented by dashed line.

It is clear to see that for distance less than R_b, the envelope of the power loss is proportional to $\frac{1}{r^2}$. We can use a linear curve whose slope is 20 dB/dec to fit this part. Beyond R_b, we can use another linear curve with slope 40 dB/dec to fit. The matching is good in both their intervals. However, it is not easy to choose the juncture, which cause the difficulty in the analysis of the interference.

A smooth model to fit the path-loss curve has been proposed by Harley[32] as

$$\frac{P_r}{P} = \frac{G}{r^a(1+\frac{r}{g})^b} \tag{5.10}$$

where g is the distance indicator of the break point. In the field tests and the computer simulations, the best value is $g = 150$ meters, for the $f = 1.9$ GHz band and the antenna height of base station is about 10 meters. The values of a and b vary very much depending on the propagation environment. a is anywhere between 1 to 4, and b is generally 2 or higher. In figure 5.2, the base station antenna height h_b is 10 meters, and the mobile antenna height h_m is 1.5 meters. The best fitting occurs at $a = 1.3$ and $b = 2$. In figure 5.3, in which the base station antenna height has been lowered to 5.3 meter, the best fitting is occurred at $a = 1.5, b = 2$. In figure 5.4, where $h_b = 3$ meters, the best fitting occurs at $a = 1.7, b = 2$.

In our system plan, we have assumed that in the home cell, all the other users use the same frequency hopping pattern as the desired user and have the same power at the receiver. Therefore the values of a and b will not affect the performance analysis. However, it is important for the performance analysis when the adjacent cells are considered, since their locations are independent of the user's locations in the home cell and generate different interference power. Equation (5.8) also tells us that we can adjust the antenna height of the base station to control the break point. A logical choice is to set the point near to the edge of the cell, such that within the cell, the power attenuates according to the inverse square law; outside the cell, the power decreases according to the inverse quadruple law. As seen in the figure 5.2–5.4, for the system in which base station antenna height is about 10 meters, the inverse quadruple law start from 400–500 meters away from the base station, which meets

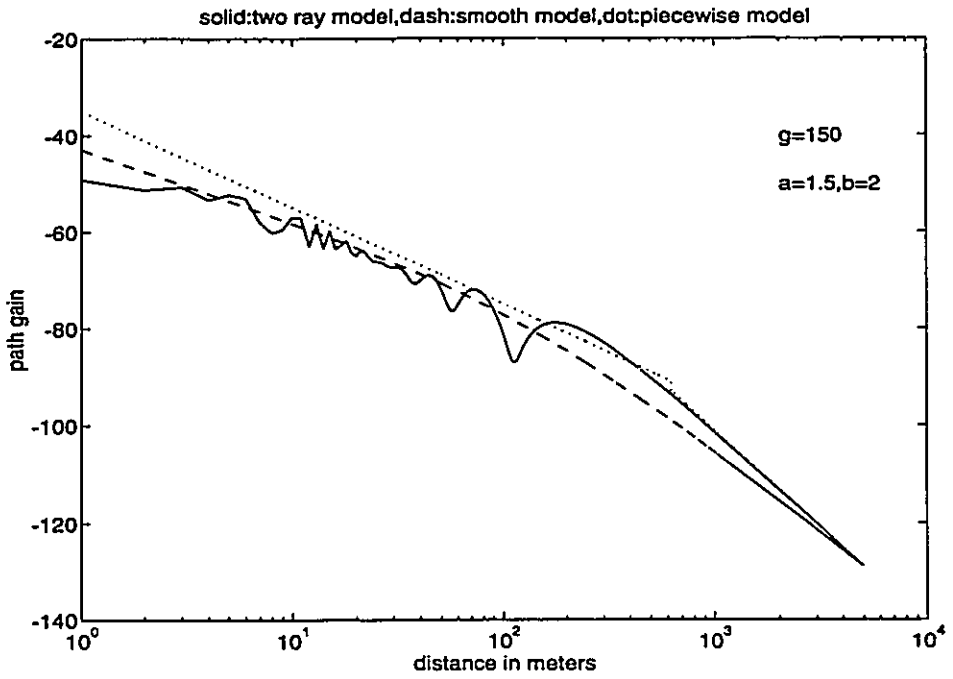

Figure 5.3: Computer simulated two ray mode, by solid line, together with the two pieces linear segment slope matching, represented by dotted line, and the smooth model, represented by dashed line.

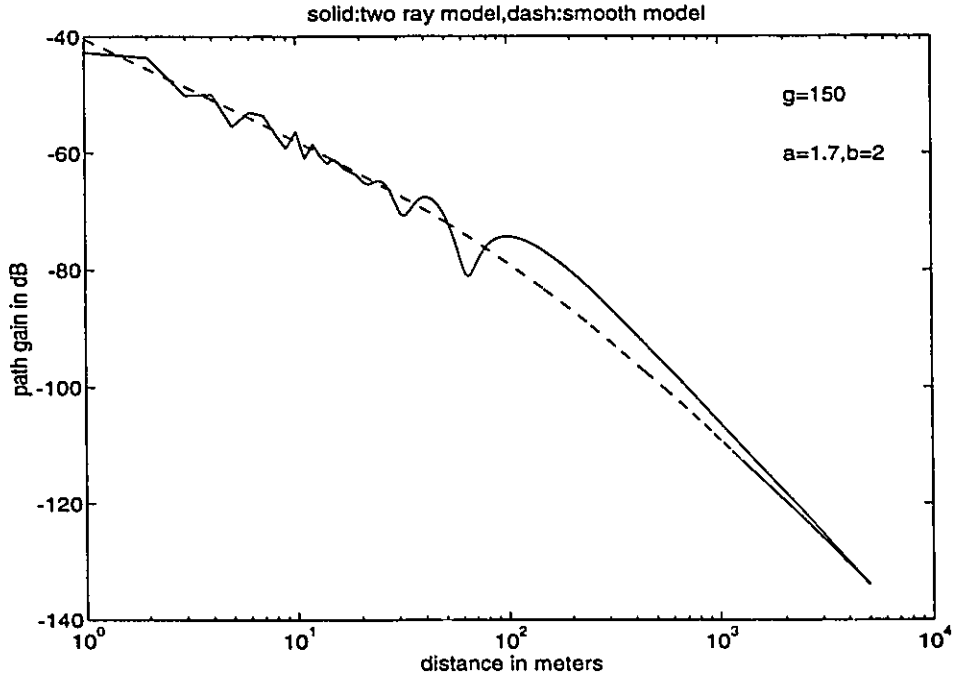

Figure 5.4: Computer simulated two ray mode, by solid line, together with the smooth model, represented by dashed line.

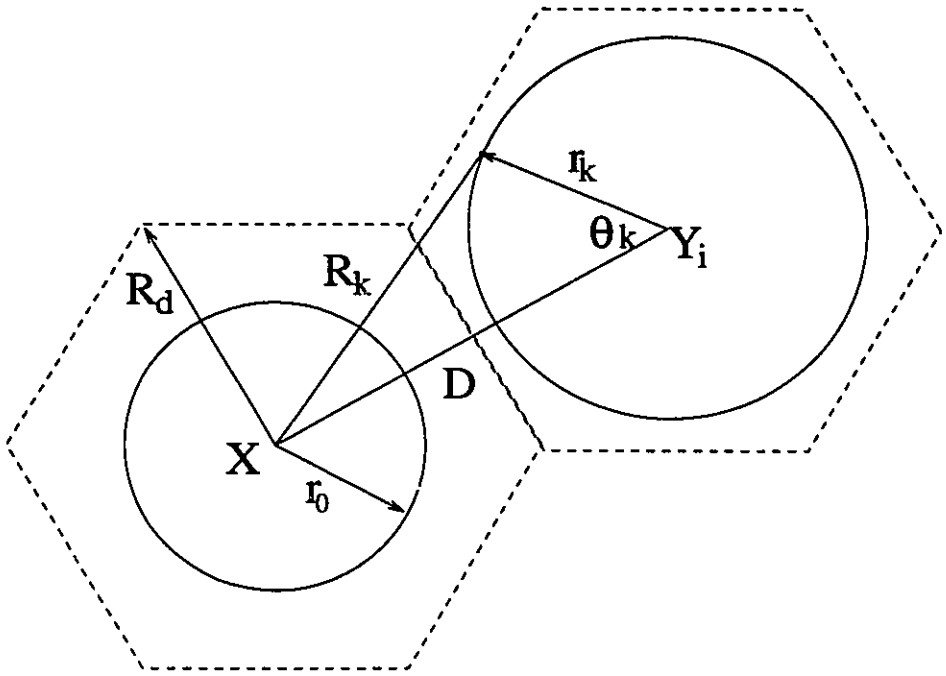

Figure 5.5: The interference from one of the adjacent cells Y_i, X denotes the home cell.

our requirement to the cell size. In the following sections, we will assume the power loss according to $\frac{1}{r^4}$ for the inferference from the adjacent cells. Within the cell, the power loss is calculated according to $\frac{G}{r^a(1+\frac{r}{g})^b}$.

5.2 Introduction to system model

In figure 5.5, we show the model for co-channel interference. As before, users having the same frequency hopping pattern are uniformly distributed in one circle in their home cell. Let cell X be the home cell we will analyse, and Y_i to be one of the six adjacent cells.

Since we are interested in the maximum capacity of the system which is defined as the maximum number of simultaneous users that can be accommodated in the system given a certain bit error rate, we assume that every cell has reached its maximum capacity which is the same for all the cells. Consequently in each cell there are K users

using the same frequency hopping pattern. The desired user is located on a circle with radius r_0 in X. The interferers in the cell Y_i are distributed on the circle with radius r_k, each one has an azimuth angle θ_k, as defined in figure 5.5. r_k is distributed within $[0, R_d]$, and θ_k is distributed within $[0, 2\pi)$. However, due to symmetry, we need only to consider users having $\theta_k \in [0, \pi]$, and the total interference is twice that of the half side.

The users on circle r_k in the i-th cell have the same power to Y_i:

$$P_r = \frac{G}{r_k^a(1+\frac{r_k}{g})^b}P \tag{5.11}$$

where P is the transmitted power. Their power to base station X is attenuated according to

$$P_r = \frac{Gg^b}{R_k^{a+b}}P \quad \text{since} \qquad R_k \gg g \tag{5.12}$$

where R_k is the distance of the kth user in the cell Y_i to the base station of cell X. R_k is determined by the two random variables r_k and θ_k, and a constant D which is the distance between to adjacent base stations, and

$$R_k = \sqrt{D^2 + r_k^2 - 2Dr_k\cos\theta_k} \tag{5.13}$$

The k-th interference signal from Y_i is

$$\begin{aligned} s_k(t) &= \sqrt{\frac{2PGg^b}{R_k^{a+b}}}b_k^{Y_i}(t)a_k^{Y_i}(t)\cos\{2\pi[f_c + f_k(t)]t + \phi_k\} \\ &= \frac{\sqrt{2PGg^b}}{[D^2 + r_k^2 - 2Dr_k\cos\theta_k]^{\frac{a+b}{4}}}b_k^{Y_i}(t)a_k^{Y_i}(t)\cos\{2\pi[f_c + f_k(t)]t + \phi_k\} \end{aligned} \tag{5.14}$$

here the $b_k^{Y_i}(t)$ and $a_k^{Y_i}(t)$ denote the data bit and the code chip for the kth user in the ith cell. ϕ_k denote the phase angle induced by the DPSK modulation.

The sum of the interference from cell Y_i is

$$r^{Y_i}(t) = \sum_{k=1}^{K} s_k(t - \tau_k)$$

$$= \sum_{k=1}^{K} \frac{\sqrt{2PGg^b}}{[D^2 + r_k^2 - 2Dr_k\cos\theta_k]^{\frac{a+b}{4}}} b_k^{Y_i}(t-\tau_k)a_k^{Y_i}(t-\tau_k)$$
$$\cdot\cos\{2\pi[f_c + f_k(t-\tau_k)](t-\tau_k) + \phi_k + \alpha(t-\tau_k)\} \qquad (5.15)$$

The phase angle $\alpha(t)$ is introduced by the frequency hopping, and assumed to be constant during one hopping interval, as required by DPSK demodulation. τ_k is the delay caused by the propagation and is a random variable depending on r_k and θ_k.

Assume the signal from the first user in the home cell X is the desired signal. At the receiver of base X, $r^{Y_i}(t)$ is correlated with $a_1(t)$, which is the code sequence of the desired signal, and the output is the interference to the final decision given by

$$\begin{aligned} J_c^{(i)} &= \int_0^T r^{Y_i}(t)a_1(t)\cos\{2\pi[f_c + f_k(t)]t - \beta(t)\}dt \\ &= \sum_{k=1}^{K} \frac{\frac{1}{2}\sqrt{2PGg^b}\cos\varphi_k}{[D^2 + r_k^2 - 2Dr_k\cos\theta_k]^{\frac{a+b}{4}}} \int_0^T b_k^{Y_i}(t-\tau_k)a_k^{Y_i}(t-\tau_k)a_1(t)dt \end{aligned} \qquad (5.16)$$

where $\beta(t)$ is the random phase caused by the local hopping pattern generator and $\varphi_k = \phi_k + \alpha_k - \beta(t)$ is the overall random phase uniformly distributed within $[0, 2\pi)$.

The total received signal intensity at the base station X, by considering the interference from the first layer adjacent cells, is

$$\begin{aligned} Z_c &= N_c + \sqrt{\frac{PG}{2r_0^a(1+\frac{r_0}{g})^b}} T b_0^{(1)}\cos\phi_1 + \sqrt{\frac{PG}{2r_0^a(1+\frac{r_0}{g})^b}} T \sum_{k=2}^{K} I_c^{(k,i)} \\ &+ \sum_{i=1}^{6}\sum_{k=1}^{K} \frac{\sqrt{PGg^b/2}\cos\varphi_k^i}{[D^2 + r_k^2 - 2Dr_k\cos\theta_k]^{\frac{a+b}{4}}} \int_0^T b_k^{Y_i}(t-\tau_k)a_k^{Y_i}(t-\tau_k)a_1(t)dt \end{aligned} \qquad (5.17)$$

The first term on the right hand side of the equal sign is the Gaussian noise with variance $N_0T/4$. The second term is the intensity of the desired signal. The third term is the total interference intensity from the home cell co-channel users, which we have analyzed in Chapter 4. The last term is the total interference intensity from the first tier adjacent cells, which includes 6 cells.

5.3 Interferers' delay distribution in the adjacent cells

As shown in Chapter 3 (equation (3.4 and 3.5)), the intergal in equation (5.17) can be written as

$$\int_0^T b_k^{Y_i}(t-\tau_k)a_k^{Y_i}(t-\tau_k)a_1(t)dt = b_{k,-1}R_{k,1}(\tau_k) + b_{k,0}\hat{R}_{k,1}(\tau_k) \tag{5.18}$$

here $b_{k,0}$ and $b_{k,-1}$ denote the current data bit and the last data bit of the kth user in the ith adjacent cell. Recall that (eqs. 3.6 and 3.7)

$$R_{k,1}(\tau_k) = C_{k,1}(l-N)T_c + [C_{k,1}(l+1-N) - C_{k,1}(l-N)](\tau_k - lT_c) \tag{5.19}$$

and

$$\hat{R}_{k,1}(\tau) = C_{k,1}(l)T_c + [C_{k,1}(l+1) - C_{k,1}(l)](\tau_k - lT_c) \tag{5.20}$$

We assume all the cells use the same time slots, or the clocks of all base stations have been synchronized. Then phase delays τ_k are caused by the propagation delay only. In such a case,

$$\begin{aligned}
\tau_k &= \frac{\sqrt{D^2 + r_k^2 - 2Dr_k\cos\theta_k}}{c} - \frac{T_c}{2} \\
&= \frac{D}{c}\sqrt{1 + \frac{r_k^2}{D^2} - 2\frac{r_k}{D}\cos\theta_k} - \frac{T_c}{2} \\
&= \sqrt{3}\frac{R_d}{c}\sqrt{1 + \frac{r_k^2}{D^2} - 2\frac{r_k}{D}\cos\theta_k} - \frac{T_c}{2} \\
&= \sqrt{3}T_c\sqrt{1 + \frac{r_k^2}{D^2} - 2\frac{r_k}{D}\cos\theta_k} - \frac{T_c}{2}
\end{aligned} \tag{5.21}$$

Here c denotes the speed of light, and we have used the assumption that the cell size and the chip duration have been chosen such that $\frac{R_d}{C} = T_c$. The term $\frac{T_c}{2}$ came from the fact that Base Stations deliberately make such a delay by assuming all the users are most likely located in the mid-way between the cell center and the boundary of the cells. It is easy to show that

$$0 \le \tau_k < \frac{5}{2}T_c \tag{5.22}$$

Recall that $l = \lfloor \tau_k \rfloor$ (section 3.1), so for $l = 0$, we require $\tau_k < T_c$, i.e

$$\sqrt{3}T_c\sqrt{1 + \frac{r_k^2}{D^2} - 2\frac{r_k}{D}\cos\theta_k} < \frac{3}{2}T_c \tag{5.23}$$

This imposes the lower bound for r_i in order to have $l = 0$:

$$r_k > \frac{1}{4 + 2\sqrt{3}}D = 0.1339D \tag{5.24}$$

and the condition for θ_k is

$$\theta_{min} = 0 \leq \theta_k \leq cos^{-1}\left[\frac{1}{8}\frac{D}{r_k} + \frac{1}{2}\frac{r_k}{D}\right] = \theta_{max} \tag{5.25}$$

Assuming K users uniformly distributed on the circle r_k, then the mean separation of two users is

$$\Delta\theta = \frac{2\pi}{K} \tag{5.26}$$

Thus on average, the number of users with $l = 0$ is

$$\begin{aligned} K_0 &= 2 \cdot \frac{K}{2\pi}[\theta_{max} - \theta_{min}] \\ &= \frac{K}{\pi}cos^{-1}\left[\frac{1}{8}\frac{D}{r_k} + \frac{1}{2}\frac{r_k}{D}\right] \end{aligned} \tag{5.27}$$

For $l = 1$, it requires

$$T_c \leq \tau_k < 2T_c \tag{5.28}$$

This is equivalent to

$$\frac{3}{2}T_c \leq \sqrt{3}T_c\sqrt{1 + \frac{r_k^2}{D^2} - 2\frac{r_k}{D}\cos\theta_k} < \frac{5}{2}T_c \tag{5.29}$$

It provides no restriction on r_k, and if $r_k < \frac{1}{4+2\sqrt{3}}D$, all of the users will have $l = 0$, as it is shown in figure 5.6:

For user with $l = 2$,

$$2T_c + \frac{T_c}{2} \leq \sqrt{3}T_c\sqrt{1 + \frac{r_k^2}{D^2} - 2\frac{r_k}{D}\cos\theta_k} < 3T_c + \frac{T_c}{2} \tag{5.30}$$

It requires

$$r_k \geq (\frac{5}{2\sqrt{3}} - 1).D = 0.4434D \tag{5.31}$$

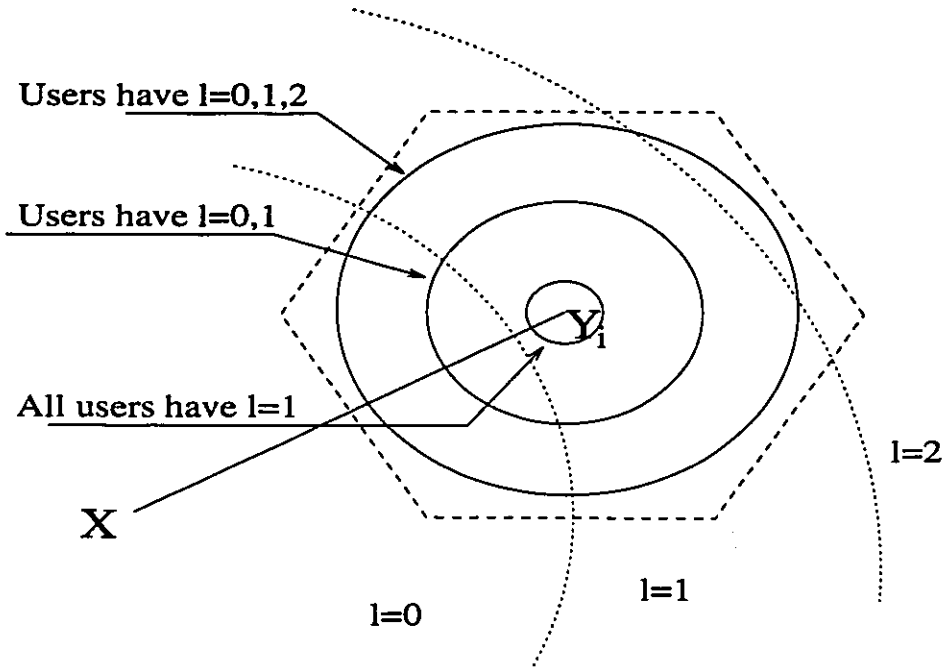

Figure 5.6: Delay distribution in different situation.

and the condition for θ_k is

$$\pi \geq \theta_k \geq \cos^{-1}[\frac{-13}{24}\frac{D}{r_k} + \frac{1}{2}\frac{r_k}{D}] \tag{5.32}$$

As a summary of the above derivation, we may classify the users with different l and different radius of the circle r_k:

1. If $0 < r_k < \frac{D}{4+2\sqrt{3}}$, all users have $l = 1$.

2. If $\frac{D}{4+2\sqrt{3}} \leq r_k < (\frac{5}{2\sqrt{3}} - 1)D$,

   - K_0 users have $l = 0$, $0 < \theta < \theta_0$. $K_0 = \frac{K}{\pi}\theta_0$
   - $K_1 = K - K_0$ users have $l = 1$, and $\theta_0 < \theta < \pi$.

   where $\theta_0 = \cos^{-1}[\frac{1}{8}\frac{D}{r_k} + \frac{1}{2}\frac{r_k}{D}]$

3. If $(\frac{5}{2\sqrt{3}} - 1)D \leq r_k < R_d$

   - K_0 users have $l = 0$, $0 < \theta < \theta_0$.

- K_1 users have $l = 1$, $\theta_0 < \theta < \theta_1$, $K_1 = \frac{K}{\pi}[\theta_1 - \theta_0]$
- K_2 user have $l = 2$, and $K_2 = K - K_0 - K_1$.

where $\theta_1 = \cos^{-1}[-\frac{13}{24}\frac{D}{r_k} + \frac{1}{2}\frac{r_k}{D}]$

5.4 Evaluation of the interference from the adjacent cells

We may now evaluate the total interference power. The interference is modeled as Gaussian random process, so its power equals the variance. First, we take the square of Z_c

$$\begin{aligned} Z_c^2 &= N_c^2 + \frac{PG}{2r_0^a(1+\frac{r_0}{g})^b}T^2\cos^2\phi_1 \\ &+ \frac{PG}{2r_0^a(1+\frac{r_0}{g})^b}T^2(\sum_{k=2}^{K} I_c^{(k,1)})^2 + (\sum_{i=1}^{6} J_i)^2 \\ &+ 2N_c\sqrt{\frac{PG}{2r_0^a(1+\frac{r_0}{g})^b}Tb_0^{(1)}}\cos^2\phi_1 + 2N_c\sqrt{\frac{PG}{2r_0^a(1+\frac{r_0}{g})^b}T}\sum_{k=2}^{K} I_c^{(k,1)} \\ &+ 2N_c\sum_{i=1}^{6} J_i + 2\cdot\frac{PG}{2r_0^a(1+\frac{r_0}{g})^b}T^2\cos\phi_1\sum_{k=2}^{K} I_c^{(k,1)} \\ &+ 2\sqrt{\frac{PG}{2r_0^a(1+\frac{r_0}{g})^b}Tb_0^{(1)}}\cos\phi_1\sum_{i=1}^{6} J_i \\ &+ 2\sqrt{\frac{PG}{2r_0^a(1+\frac{r_0}{g})^b}T}\sum_{k=2}^{K} I_c^{(k,1)}\sum_{i=1}^{6} J_i \end{aligned} \tag{5.33}$$

$\mathrm{E}[\cos\phi] = 0$ for uniformly distributed ϕ, and all the other random variables also have zero mean, then by assuming also they are independent, we have

$$\begin{aligned} \mathrm{E}\{Z_c^2\} &= \frac{1}{4}N_0T + \frac{PG}{4r_0^a(1+\frac{r_0}{g})^b}T^2 \\ &+ \frac{PG}{2r_0^a(1+\frac{r_0}{g})^b}T^2\mathrm{E}\{\sum_{k=2}^{K}(I_c^{(k,1)})^2\} + \mathrm{E}\{\sum_{i=1}^{6} J_i^2\} \end{aligned} \tag{5.34}$$

The terms on the right hand side of equation 5.34 have clear physical meaning to us now. The first term is due to the thermal noise in the channel, which is assumed to be gaussian with variance N_0. The second term is the average received power of the desired signal. The third term is the variance of the interference from the home cell co-channel users. In chapter 4 we have modeled these as the gaussian processes with the same variance. The last term is the variances of the interference from the adjacent cells located on the first tier.

The evaluation of the last term can be conducted as follows by assuming that all the random variables are independent.

$$
\begin{aligned}
\mathrm{E}\{J_i^2\} &= \sum_{k=1}^{K} \mathrm{E}\left\{ \left[\frac{\sqrt{PGg^b/2}\cos\varphi_k^i}{[D^2+r_k^2-2Dr_k\cos\theta_k]^{\frac{a+b}{4}}} \int_0^T b_k^{Y_i}(t-\tau_k) a_k^{Y_i}(t-\tau_k) a_1(t) dt \right]^2 \right\} \\
&= \sum_{k=1}^{K} \mathrm{E}\left\{ \frac{\frac{1}{4}PGg^b}{[D^2+r_k^2-2Dr_k\cos\theta_k]^{\frac{a+b}{2}}} \left[b_{k,-1} R_{k,1}(\tau_k) + b_{k,0}\hat{R}_{k,1}(\tau_k) \right]^2 \right\} \\
&= \sum_{k=1}^{K} \mathrm{E}\left\{ \frac{\frac{1}{4}PGg^b}{[D^2+r_k^2-2Dr_k\cos\theta_k]^{\frac{a+b}{2}}} R_{k,1}^2(\tau_k) \right\} \\
&+ \sum_{k=1}^{K} \mathrm{E}\left\{ \frac{\frac{1}{4}PGg^b}{[D^2+r_k^2-2Dr_k\cos\theta_k]^{\frac{a+b}{2}}} \hat{R}_{k,1}^2(\tau_k) \right\} \\
&= \frac{1}{4}PGg^b \sum_{k=1}^{K} \mathrm{E}\left\{ \frac{R_{k,1}^2(\tau_k)}{[D^2+r_k^2-2Dr_k\cos\theta_k]^{\frac{a+b}{2}}} \right\} \\
&+ \frac{1}{4}PGg^b \sum_{k=1}^{K} \mathrm{E}\left\{ \frac{\hat{R}_{k,1}^2(\tau_k)}{[D^2+r_k^2-2Dr_k\cos\theta_k]^{\frac{a+b}{2}}} \right\} \\
&= \frac{1}{4}PGg^b \sum_{k=1}^{K_0} \mathrm{E}\left\{ \left(\frac{C_{k,1}(-N)(1-\alpha_k)T_c + C_{k,1}(1-N)\alpha_k T_c}{[D^2+r_k^2-2Dr_k\cos\theta_k]^{\frac{a+b}{4}}} \right)^2 \right\} \qquad \text{(I)} \\
&+ \frac{1}{4}PGg^b \sum_{k=1}^{K_0} \mathrm{E}\left\{ \left(\frac{C_{k,1}(0)(1-\alpha_k)T_c + C_{k,1}(1)\alpha_k T_c}{[D^2+r_k^2-2Dr_k\cos\theta_k]^{\frac{a+b}{4}}} \right)^2 \right\} \qquad \text{(II)} \\
&+ \frac{1}{4}PGg^b \sum_{k=1}^{K_1} \mathrm{E}\left\{ \left(\frac{C_{k,1}(1-N)(1-\alpha_k)T_c + C_{k,1}(2-N)\alpha_k T_c}{[D^2+r_k^2-2Dr_k\cos\theta_k]^{\frac{a+b}{4}}} \right)^2 \right\} \qquad \text{(III)} \\
&+ \frac{1}{4}PGg^b \sum_{k=1}^{K_1} \mathrm{E}\left\{ \left(\frac{C_{k,1}(1)(1-\alpha_k)T_c + C_{k,1}(2)\alpha_k T_c}{[D^2+r_k^2-2Dr_k\cos\theta_k]^{\frac{a+b}{4}}} \right)^2 \right\} \qquad \text{(IV)}
\end{aligned}
$$

$$+ \quad \frac{1}{4}PGg^b \sum_{k=1}^{K_2} \mathrm{E}\left\{\left(\frac{C_{k,1}(2-N)(1-\alpha_k)T_c + C_{k,1}(3-N)\alpha_k T_c}{[D^2+r_k^2-2Dr_k\cos\theta_k]^{\frac{a+b}{4}}}\right)^2\right\} \qquad \text{(V)}$$

$$+ \quad \frac{1}{4}PGg^b \sum_{k=1}^{K_2} \mathrm{E}\left\{\left(\frac{C_{k,1}(2)(1-\alpha_k)T_c + C_{k,1}(3)\alpha_k T_c}{[D^2+r_k^2-2Dr_k\cos\theta_k]^{\frac{a+b}{4}}}\right)^2\right\} \qquad \text{(VI)} \tag{5.35}$$

All the functions $C_{k,1}$ above are partial correlation functions and are defined in chapter 3 (eq. (3.10)). The first two terms (I and II) correspond to the interference signals with $l = 0$. The third and the fourth term (III and IV) correspond to the that of $l = 1$, and the last two terms (V and VI) correspond to that of $l = 2$. α_k in eq. (5.35) above is the continuous fraction of the delay and takes on the following values:

$$\begin{aligned}\alpha_k &= \frac{\tau_k}{T_c} - l = \sqrt{3}\sqrt{1+\frac{r_k^2}{D^2}-2\frac{r_k}{D}\cos\theta_k} - l \\ &= \begin{cases} \sqrt{3}\sqrt{1+\frac{r_k^2}{D^2}-2\frac{r_k}{D}\cos\theta_k} & l=0 \\ \sqrt{3}\sqrt{1+\frac{r_k^2}{D^2}-2\frac{r_k}{D}\cos\theta_k}-1 & l=1 \\ \sqrt{3}\sqrt{1+\frac{r_k^2}{D^2}-2\frac{r_k}{D}\cos\theta_k}-2 & l=2 \end{cases}\end{aligned} \tag{5.36}$$

Now we are in the position to evaluate (I)-(VI) in equation (5.35) term by term. For convenience, we define the following integrals:

$$I_1(l=0) = \int_0^{\theta_0} \frac{d\theta}{[1+\frac{r_k^2}{D^2}-2\frac{r_k}{D}\cos\theta_k]^{\frac{a+b}{2}-1}} \tag{5.37}$$

$$I_{\frac{3}{2}}(l=0) = \int_0^{\theta_0} \frac{d\theta}{[1+\frac{r_k^2}{D^2}-2\frac{r_k}{D}\cos\theta_k]^{\frac{a+b}{2}-\frac{1}{2}}} \tag{5.38}$$

$$I_2(l=0) = \int_0^{\theta_0} \frac{d\theta}{[1+\frac{r_k^2}{D^2}-2\frac{r_k}{D}\cos\theta_k]^{\frac{a+b}{2}}} \tag{5.39}$$

$$I_1(l=1) = \int_{\theta_0}^{\theta_1} \frac{d\theta}{[1+\frac{r_k^2}{D^2}-2\frac{r_k}{D}\cos\theta_k]^{\frac{a+b}{2}-1}} \tag{5.40}$$

$$I_{\frac{3}{2}}(l=1) = \int_{\theta_0}^{\theta_1} \frac{d\theta}{[1+\frac{r_k^2}{D^2}-2\frac{r_k}{D}\cos\theta_k]^{\frac{a+b}{2}-\frac{1}{2}}} \tag{5.41}$$

$$I_2(l=1)=\int_{\theta_0}^{\theta_1}\frac{d\theta}{[1+\frac{r_k^2}{D^2}-2\frac{r_k}{D}\cos\theta_k]^{\frac{a+b}{2}}} \tag{5.42}$$

$$I_1(l=2)=\int_{\theta_1}^{\pi}\frac{d\theta}{[1+\frac{r_k^2}{D^2}-2\frac{r_k}{D}\cos\theta_k]^{\frac{a+b}{2}-1}} \tag{5.43}$$

$$I_{\frac{3}{2}}(l=2)=\int_{\theta_1}^{\pi}\frac{d\theta}{[1+\frac{r_k^2}{D^2}-2\frac{r_k}{D}\cos\theta_k]^{\frac{a+b}{2}-\frac{1}{2}}} \tag{5.44}$$

$$I_2(l=2)=\int_{\theta_1}^{\pi}\frac{d\theta}{[1+\frac{r_k^2}{D^2}-2\frac{r_k}{D}\cos\theta_k]^{\frac{a+b}{2}}} \tag{5.45}$$

We first take θ_k as the random variable and carry out the expection over it, while taking r_k as fixed value. This is because r_k is assoicated with the hopping patterns and for a given hopping pattern, r_k has a deterministic value. For the first term in equation (5.35), since $C_{k,1}(-N)=0$, we have

$$\begin{aligned}
I &= \frac{1}{4}PGg^b\sum_{k=1}^{K_0}\mathrm{E}\left\{\left(\frac{C_{k,1}(1-N)\alpha_k T_c}{[D^2+r_k^2-2Dr_k\cos\theta_k]^{\frac{a+b}{4}}}\right)^2\right\}\\
&= \frac{3PGg^bT_c^2}{4D^{a+b}}\sum_{k=1}^{K_0}C_{k,1}^2(1-N)\mathrm{E}\left\{\frac{1+\frac{r_k^2}{D^2}-2\frac{r_k}{D}\cos\theta_k}{[1+\frac{r_k^2}{D^2}-2\frac{r_k}{D}\cos\theta_k]^{\frac{a+b}{2}}}\right\}\\
&= \frac{3PGg^bT_c^2}{4D^{a+b}}\sum_{k=1}^{K_0}C_{k,1}^2(1-N)\frac{1}{\theta_0}\int_0^{\theta_0}\frac{d\theta_k}{[1+\frac{r_k^2}{D^2}-2\frac{r_k}{D}\cos\theta_k]^{\frac{a+b}{2}-1}}\\
&= \frac{3PGg^bT_c^2}{4D^{a+b}}\sum_{k=1}^{K_0}C_{k,1}^2(1-N)\frac{1}{\theta_0}I_1(l=0)\\
&= \frac{3PGg^bT_c^2}{4\pi D^{a+b}}K_0\overline{C_{k,1}^2(1-N)}\frac{1}{\theta_0}I_1(l=0)\\
&= \frac{3PGg^bT_c^2}{4\pi D^{a+b}}K\overline{C_{k,1}^2(1-N)}I_1(l=0)
\end{aligned} \tag{5.46}$$

Here $\overline{C_{k,1}^2(1-N)}$ denotes the average value of $C_{k,1}^2(l)$ among all the possible l. In the last step we have used the relation given by equation (5.27)

Similarly, we may evaluate the second term

$$II = \frac{1}{4}PGg^b\sum_{k=1}^{K_0}\mathrm{E}\left\{\left(\frac{C_{k,1}(0)T_c+[C_{k,1}(1)-C_{k,1}(0)]\alpha_k T_c}{[D^2+r_k^2-2Dr_k\cos\theta_k]^{\frac{a+b}{4}}}\right)^2\right\}$$

$$
\begin{aligned}
&= \frac{PGg^bT_c^2}{4D^{a+b}}\sum_{k=1}^{K_0}\mathrm{E}\left\{\frac{C_{k,1}^2(0)+2\sqrt{3}C_{k,1}^2(0)[C_{k,1}^2(1)-C_{k,1}^2(0)]\sqrt{1+\frac{r_k^2}{D^2}-2\frac{r_k}{D}\cos\theta_k}}{[1+\frac{r_k^2}{D^2}-2\frac{r_k}{D}\cos\theta_k]^{\frac{a+b}{2}}}\right.\\
&+ \left.\frac{3[C_{k,1}^2(1)-C_{k,1}^2(0)]^2(1+\frac{r_k^2}{D^2}-2\frac{r_k}{D}\cos\theta_k)}{[1+\frac{r_k^2}{D^2}-2\frac{r_k}{D}\cos\theta_k]^{\frac{a+b}{2}}}\right\}\\
&= \frac{PGg^bT_c^2}{4D^{a+b}}\sum_{k=1}^{K_0}C_{k,1}^2(0)\frac{1}{\theta_0}\int_0^{\theta_0}\frac{d\theta}{[1+\frac{r_k^2}{D^2}-2\frac{r_k}{D}\cos\theta_k]^{\frac{a+b}{2}}}\\
&+ \frac{2\sqrt{3}PGg^bT_c^2}{4D^{a+b}}\sum_{k=1}^{K_0}C_{k,1}^2(0)[C_{k,1}^2(1)-C_{k,1}^2(0)]\frac{1}{\theta_0}\int_0^{\theta_0}\frac{d\theta}{[1+\frac{r_k^2}{D^2}-2\frac{r_k}{D}\cos\theta_k]^{\frac{a+b}{2}-\frac{1}{2}}}\\
&+ \frac{3PGg^bT_c^2}{4D^{a+b}}\sum_{k=1}^{K_0}[C_{k,1}^2(1)-C_{k,1}^2(0)]^2\frac{1}{\theta_0}\int_0^{\theta_0}\frac{d\theta}{[1+\frac{r_k^2}{D^2}-2\frac{r_k}{D}\cos\theta_k]^{\frac{a+b}{2}-1}}\\
&= \frac{PGg^bT_c^2}{4D^{a+b}}\frac{K}{\pi}\overline{C_{k,1}^2(0)}I_2(l=0)\\
&+ \frac{\sqrt{3}PGg^bT_c^2}{2D^{a+b}}\frac{K}{\pi}\overline{C_{k,1}^2(0)[C_{k,1}^2(1)-C_{k,1}^2(0)]}I_{\frac{3}{2}}(l=0)\\
&+ \frac{3PGg^bT_c^2}{4D^{a+b}}\frac{K}{\pi}\overline{[C_{k,1}^2(1)-C_{k,1}^2(0)]^2}I_1(l=0) \qquad (5.47)
\end{aligned}
$$

The other terms are given as follows:

$$
\begin{aligned}
III &= \frac{PGg^bT_c^2}{4D^{a+b}}\sum_{k=1}^{K_1}\mathrm{E}\left\{\left(\frac{\sqrt{3}[C_{k,1}(2-N)-C_{k,1}(1-N)]\sqrt{1+\frac{r_k^2}{D^2}-2\frac{r_k}{D}\cos\theta_k}}{[1+\frac{r_k^2}{D^2}-2\frac{r_k}{D}\cos\theta_k]^{\frac{a+b}{4}}}\right.\right.\\
&+ \left.\left.\frac{C_{k,1}(1-N)+[C_{k,1}^2(1-N)-C_{k,1}^2(2-N)]}{[1+\frac{r_k^2}{D^2}-2\frac{r_k}{D}\cos\theta_k]^{\frac{a+b}{4}}}\right)^2\right\}\\
&= \frac{PGg^bT_c^2}{4D^{a+b}}\sum_{k=1}^{K_1}\mathrm{E}\left\{\frac{[C_{k,1}(1-N)-C_{k,1}(2-N)]^2}{[1+\frac{r_k^2}{D^2}-2\frac{r_k}{D}\cos\theta_k]^{\frac{a+b}{2}}}\right\}\\
&+ \frac{2\sqrt{3}PGg^bT_c^2}{4D^{a+b}}\sum_{k=1}^{K_1}\mathrm{E}\left\{\frac{3C_{k,1}(2-N)C_{k,1}(1-N)-2C_{k,1}^2(1-N)-C_{k,1}^2(2-N)}{[1+\frac{r_k^2}{D^2}-2\frac{r_k}{D}\cos\theta_k]^{\frac{a+b}{2}-\frac{1}{2}}}\right\}\\
&+ \frac{3PGg^bT_c^2}{4D^{a+b}}\sum_{k=1}^{K_1}\mathrm{E}\left\{\frac{[C_{k,1}(2-N)-C_{k,1}(1-N)]^2}{[1+\frac{r_k^2}{D^2}-2\frac{r_k}{D}\cos\theta_k]^{\frac{a+b}{2}-1}}\right\}\\
&= \frac{PGg^bT_c^2}{4D^{a+b}}\frac{K}{\pi}\overline{[2C_{k,1}(1-N)-C_{k,1}(2-N)]^2}I_2(l=1)\\
&+ \frac{\sqrt{3}PGg^bT_c^2}{2D^{a+b}}\frac{K}{\pi}\overline{[3C_{k,1}(2-N)C_{k,1}(1-N)-2C_{k,1}^2(1-N)-C_{k,1}^2(2-N)]}
\end{aligned}
$$

$$\cdot I_{\frac{3}{2}}(l=1)$$

$$+ \quad \frac{3PGg^bT_c^2}{4D^{a+b}}\frac{K}{\pi}\overline{[C_{k,1}(2-N)-C_{k,1}(1-N)]^2}I_1(l=1) \tag{5.48}$$

$$\begin{aligned} IV &= \frac{PGg^bT_c^2}{4D^{a+b}}\sum_{k=1}^{K_1}\mathrm{E}\left\{\left(\frac{\sqrt{3}[C_{k,1}(2)-C_{k,1}(1)]\sqrt{1+\frac{r_k^2}{D^2}-2\frac{r_k}{D}\cos\theta_k}}{[1+\frac{r_k^2}{D^2}-2\frac{r_k}{D}\cos\theta_k]^{\frac{a+b}{4}}}\right.\right. \\ &+ \left.\left.\frac{C_{k,1}(1)+[C_{k,1}(1)-C_{k,1}(2)]}{[1+\frac{r_k^2}{D^2}-2\frac{r_k}{D}\cos\theta_k]^{\frac{a+b}{4}}}\right)^2\right\} \\ &= \frac{PGg^bT_c^2}{4D^{a+b}}\frac{K}{\pi}\overline{[2C_{k,1}(1)-C_{k,1}(2)]^2}I_2(l=1) \\ &+ \frac{\sqrt{3}PGg^bT_c^2}{2D^{a+b}}\frac{K}{\pi}\overline{[3C_{k,1}(2)C_{k,1}(1)-2C_{k,1}^2(1)-C_{k,1}^2(2)]}I_{\frac{3}{2}}(l=1) \\ &+ \frac{3PGg^bT_c^2}{4D^{a+b}}\frac{K}{\pi}\overline{[C_{k,1}(2)-C_{k,1}(1)]^2}I_1(l=1) \end{aligned} \tag{5.49}$$

$$\begin{aligned} V &= \frac{PGg^bT_c^2}{4D^{a+b}}\sum_{k=1}^{K_2}\mathrm{E}\left\{\left(\frac{\sqrt{3}[C_{k,1}(3-N)-C_{k,1}(2-N)]\sqrt{1+\frac{r_k^2}{D^2}-2\frac{r_k}{D}\cos\theta_k}}{[1+\frac{r_k^2}{D^2}-2\frac{r_k}{D}\cos\theta_k]^{\frac{a+b}{4}}}\right.\right. \\ &+ \left.\left.\frac{3C_{k,1}(2-N)-2C_{k,1}(3-N)}{[1+\frac{r_k^2}{D^2}-2\frac{r_k}{D}\cos\theta_k]^{\frac{a+b}{4}}}\right)^2\right\} \\ &= \frac{PGg^bT_c^2}{4D^{a+b}}\frac{K}{\pi}\overline{[3C_{k,1}(2-N)-2C_{k,1}(3-N)]^2}I_2(l=2) \\ &+ \frac{\sqrt{3}PGg^bT_c^2}{2D^{a+b}}\frac{K}{\pi}\overline{[5C_{k,1}(2-N)C_{k,1}(3-N)-3C_{k,1}^2(2-N)-2C_{k,1}^2(3-N)]} \\ &\cdot I_{\frac{3}{2}}(l=2) \\ &+ \frac{3PGg^bT_c^2}{4D^{a+b}}\frac{K}{\pi}\overline{[C_{k,1}(3-N)-C_{k,1}(2-N)]^2}I_1(l=2) \end{aligned} \tag{5.50}$$

$$VI = \frac{PGg^bT_c^2}{4D^{a+b}}\sum_{k=1}^{K_2}\mathrm{E}\left\{\left(\frac{3C_{k,1}(2)-2C_{k,1}(3)}{[1+\frac{r_k^2}{D^2}-2\frac{r_k}{D}\cos\theta_k]^{\frac{a+b}{4}}}\right.\right.$$

$$+\frac{\sqrt{3}[C_{k,1}(3)-C_{k,1}(2)]\sqrt{1+\frac{r_k^2}{D^2}-2\frac{r_k}{D}\cos\theta_k}}{[1+\frac{r_k^2}{D^2}-2\frac{r_k}{D}\cos\theta_k]^{\frac{a+b}{4}}}\Bigg)^2\Bigg\}$$

$$= \frac{PGg^bT_c^2}{4D^{a+b}}\frac{K}{\pi}\overline{[3C_{k,1}(2)-2C_{k,1}(3)]^2}I_2(l=2)$$
$$+\frac{\sqrt{3}PGg^bT_c^2}{2D^{a+b}}\frac{K}{\pi}\overline{[5C_{k,1}(2)C_{k,1}(3)-3C_{k,1}^2(2)-2C_{k,1}^2(3)]}I_{\frac{3}{2}}(l=2)$$
$$+\frac{3PGg^bT_c^2}{4D^{a+b}}\frac{K}{\pi}\overline{[C_{k,1}(3)-C_{k,1}(2)]^2}I_1(l=2) \qquad (5.51)$$

So far we have evaluated $\mathrm{E}\{J_i^2\}$ by treating θ_k as a random variable. The interference depends on the power profile determined by parameters D, G, g, P, the total number of users K, the code property given by functions $C_{k,1}$, and the integrals $I_1, I_2, I_{\frac{3}{2}}$. Those integrals are function of r_k. I_1 and I_2 can be calculated in close forms, as given by appedix A. However, $I_{\frac{3}{2}}$ can only be evaluated in numerical methods.

5.5 Averaged Interference over the adjacent cells

The interference power evaluated in the previous section is for a given cell with fixed r_k. However, since we have six cells in total, r_k will randomly take on values anywhere between $[0, R_d]$. Therefore we want to obtain an average interference power over the r_k.

To do the average over r_k, we need to know the PDF of r_k. We have made the hypothesis that θ_k is uniformly distributed within $[0, 2\pi)$. We also assume that users are uniformly distributed in the cell, so for each element of area $rdrd\theta$, we will find the same number of users. Under those requirements, the PDF of r_k is

$$f(r) = \frac{2r}{R_d^2} \qquad (5.52)$$

The average of $\mathrm{E}\{J_i^2(r_k)\}$ can be carried out as following:

$$\overline{J_i^2(r_k)} = \int_0^{R_d} \mathrm{E}\{J_i^2(r_k)\}\frac{2r_k}{R_d^2}dr_k$$

$$
\begin{aligned}
&= \int_0^{\frac{D}{4+2\sqrt{3}}} \mathrm{E}\{J_i^2(r_k)\}\frac{2r_k}{R_d^2}dr_k + \int_{\frac{D}{4+2\sqrt{3}}}^{\frac{5-2\sqrt{3}}{2\sqrt{3}}D} \mathrm{E}\{J_i^2(r_k)\}\frac{2r_k}{R_d^2}dr_k \\
&\quad + \int_{\frac{5-2\sqrt{3}}{2\sqrt{3}}D}^{\frac{D}{\sqrt{3}}} \mathrm{E}\{J_i^2(r_k)\}\frac{2r_k}{R_d^2}dr_k \\
&= 6\int_0^{\frac{D}{4+2\sqrt{3}}} \mathrm{E}\{J_i^2(r_k)\}\frac{r_k}{D}d\frac{r_k}{D} + 6\int_{\frac{D}{4+2\sqrt{3}}}^{\frac{5-2\sqrt{3}}{2\sqrt{3}}D} \mathrm{E}\{J_i^2(r_k)\}\frac{r_k}{D}d\frac{r_k}{D} \\
&+ 6\int_{\frac{5-2\sqrt{3}}{2\sqrt{3}}D}^{\frac{D}{\sqrt{3}}} \mathrm{E}\{J_i^2(r_k)\}\frac{r_k}{D}d\frac{r_k}{D} \\
&= \frac{3PGg^bT_c^2}{4D^{a+b}}\frac{K}{\pi}\overline{C_{k,1}^2(1-N)}6\int_{\frac{D}{4+2\sqrt{3}}}^{\frac{D}{\sqrt{3}}} I_1(l=0)\frac{r_k}{D}d\frac{r_k}{D} \\
&+ \frac{PGg^bT_c^2}{4D^{a+b}}\frac{K}{\pi}\overline{C_{k,1}^2(0)}6\int_{\frac{D}{4+2\sqrt{3}}}^{\frac{D}{\sqrt{3}}} I_2(l=0)\frac{r_k}{D}d\frac{r_k}{D} \\
&+ \frac{\sqrt{3}PGg^bT_c^2}{2D^{a+b}}\frac{K}{\pi}\overline{C_{k,1}(0)[C_{k,1}(1)-C_{k,1}(0)]}6\int_{\frac{D}{4+2\sqrt{3}}}^{\frac{D}{\sqrt{3}}} I_{\frac{3}{2}}(l=0)\frac{r_k}{D}d\frac{r_k}{D} \\
&+ \frac{PGg^bT_c^2}{4D^{a+b}}\frac{K}{\pi}\overline{[C_{k,1}(1)-C_{k,1}(0)]^2}6\int_{\frac{D}{4+2\sqrt{3}}}^{\frac{D}{\sqrt{3}}} I_1(l=0)\frac{r_k}{D}d\frac{r_k}{D} \\
&+ \frac{PGg^bT_c^2}{4D^{a+b}}\frac{K}{\pi}\Big\{\overline{[2C_{k,1}(1-N)-C_{k,1}(2-N)]^2} \\
&+ \overline{[2C_{k,1}(1)-C_{k,1}(2)]^2}\Big\}6\int_0^{\frac{D}{\sqrt{3}}} I_2(l=1)\frac{r_k}{D}d\frac{r_k}{D} \\
&+ \frac{\sqrt{3}PGg^bT_c^2}{4D^{a+b}}\frac{K}{\pi}\Big\{3\overline{C_{k,1}(2-N)C_{k,1}(1-N)} + 3\overline{C_{k,1}(2)C_{k,1}(1)} \\
&\quad - 2\overline{C_{k,1}^2(1-N)} - \overline{C_{k,1}^2(2-N)} - 2\overline{C_{k,1}^2(1)} - \overline{C_{k,1}^2(2)}\Big\} \\
&\quad \cdot 6\int_0^{\frac{D}{\sqrt{3}}} I_{\frac{3}{2}}(l=1)\frac{r_k}{D}d\frac{r_k}{D} \\
&+ \frac{3PGg^bT_c^2}{4D^{a+b}}\frac{K}{\pi}\Big\{\overline{[C_{k,1}(2-N)-C_{k,1}(1-N)]^2} \\
&+ \overline{[C_{k,1}(2)-C_{k,1}(1)]^2}\Big\}6\int_0^{\frac{D}{\sqrt{3}}} I_1(l=1)\frac{r_k}{D}d\frac{r_k}{D} \\
&+ \frac{PGg^bT_c^2}{4D^{a+b}}\frac{K}{\pi}\Big\{\overline{[3C_{k,1}(2-N)-2C_{k,1}(3-N)]^2} \\
&+ \overline{[3C_{k,1}(2)-2C_{k,1}(3)]^2}\Big\}6\int_{\frac{5-2\sqrt{3}}{2\sqrt{3}}D}^{\frac{D}{\sqrt{3}}} I_2(l=2)\frac{r_k}{D}d\frac{r_k}{D} \\
&+ \frac{\sqrt{3}PGg^bT_c^2}{2D^{a+b}}\frac{K}{\pi}\Big\{5\overline{C_{k,1}(2-N)C_{k,1}(3-N)} - 2\overline{C_{k,1}^2(2-N)} \\
&\quad - 2\overline{C_{k,1}^2(3-N)} + 5\overline{C_{k,1}(2)C_{k,1}(3)} - 2\overline{C_{k,1}^2(2)} - \overline{C_{k,1}^2(3)}\Big\}
\end{aligned}
$$

$$\cdot 6\int_{\frac{5-2\sqrt{3}}{2\sqrt{3}}D}^{\frac{D}{\sqrt{3}}} I_{\frac{3}{2}}(l=2)\frac{r_k}{D}d\frac{r_k}{D}$$

$$+ \quad \frac{3PGg^bT_c^2}{4D^{a+b}}\frac{K}{\pi}\left\{\overline{[C_{k,1}(3-N)-C_{k,1}(2-N)]^2}\right.$$

$$\left.+\,\overline{[C_{k,1}(3)-C_{k,1}(2)]^2}\right\}6\int_{\frac{5-2\sqrt{3}}{2\sqrt{3}}D}^{\frac{D}{\sqrt{3}}} I_2(l=2)\frac{r_k}{D}d\frac{r_k}{D} \tag{5.53}$$

Generally we cannot evaluate those integrals in the above equations in close forms. For the case of $a = b = 2$, numerical results can be obtained as following:

$$6\int_{\frac{D}{4+2\sqrt{3}}}^{\frac{D}{\sqrt{3}}} I_1(l=0)\frac{r_k}{D}d\frac{r_k}{D} = 2.1281 \tag{5.54}$$

$$6\int_{\frac{D}{4+2\sqrt{3}}}^{\frac{D}{\sqrt{3}}} I_{\frac{3}{2}}(l=0)\frac{r_k}{D}d\frac{r_k}{D} = 3.401 \tag{5.55}$$

$$6\int_{\frac{D}{4+2\sqrt{3}}}^{\frac{D}{\sqrt{3}}} I_1(l=2)\frac{r_k}{D}d\frac{r_k}{D} = 5.6388 \tag{5.56}$$

$$6\int_{0}^{\frac{D}{\sqrt{3}}} I_1(l=1)\frac{r_k}{D}d\frac{r_k}{D} = 1.5819 \tag{5.57}$$

$$6\int_{0}^{\frac{D}{\sqrt{3}}} I_{\frac{3}{2}}(l=1)\frac{r_k}{D}d\frac{r_k}{D} = 1.4633 \tag{5.58}$$

$$6\int_{0}^{\frac{D}{\sqrt{3}}} I_2(l=1)\frac{r_k}{D}d\frac{r_k}{D} = 1.1568 \tag{5.59}$$

$$6\int_{\frac{5-2\sqrt{3}}{4+2\sqrt{3}}D}^{\frac{D}{\sqrt{3}}} I_1(l=2)\frac{r_k}{D}d\frac{r_k}{D} = 0.1113 \tag{5.60}$$

$$6\int_{\frac{5-2\sqrt{3}}{4+2\sqrt{3}}D}^{\frac{D}{\sqrt{3}}} I_{\frac{3}{2}}(l=2)\frac{r_k}{D}d\frac{r_k}{D} = 0.0744 \tag{5.61}$$

$$6\int_{\frac{5-2\sqrt{3}}{4+2\sqrt{3}}D}^{\frac{D}{\sqrt{3}}} I_2(l=2)\frac{r_k}{D}d\frac{r_k}{D} = 0.0498 \tag{5.62}$$

In such a case, the $J_i(r_k)$ can be written as

$$\begin{aligned}
\overline{J_i^2(r_k)} &= 0.5080\frac{PGg^bT_c^2}{D^{a+b}}\left\{\overline{C_{k,1}^2(1-N)}+\overline{[C_{k,1}(1)-C_{k,1}(0)]^2}\right\} \\
&+ 0.9375\frac{PGg^bT_c^2}{D^{a+b}}\overline{C_{k,1}(0)[C_{k,1}(1)-C_{k,1}(0)]} \\
&+ 0.4487\frac{PGg^bT_c^2}{D^{a+b}}\overline{C_{k,1}^2(0)} \\
&+ 0.3777\frac{PGg^bT_c^2}{D^{a+b}}\left\{\overline{[C_{k,1}(1-N)-C_{k,1}(2-N)]^2}\right. \\
&\quad \left.+\overline{[C_{k,1}(1)-C_{k,1}(2)]^2}\right\} \\
&+ 0.4033\frac{PGg^bT_c^2}{D^{a+b}}\{3\overline{C_{k,1}(2-N)C_{k,1}(1-N)}+3\overline{C_{k,1}(2)C_{k,1}(1)} \\
&- 2\overline{C_{k,1}^2(1-N)}-\overline{C_{k,1}^2(2-N)}-2\overline{C_{k,1}^2(1)}-\overline{C_{k,1}^2(2)}\} \\
&+ 0.0921\frac{PGg^bT_c^2}{D^{a+b}}\left\{\overline{[2C_{k,1}(1-N)-C_{k,1}(2-N)]^2}\right. \\
&\quad \left.+\overline{[2C_{k,1}(1)-C_{k,1}(2)]^2}\right\} \\
&+ 0.0266\frac{PGg^bT_c^2}{D^{a+b}}\left\{\overline{[C_{k,1}(3-N)-C_{k,1}(2-N)]^2}\right. \\
&\quad \left.+\overline{[C_{k,1}(3)-C_{k,1}(2)]^2}\right\} \\
&+ 0.0205\frac{PGg^bT_c^2}{D^{a+b}}\left\{5\overline{C_{k,1}(2-N)C_{k,1}(3-N)}-2\overline{C_{k,1}^2(2-N)}\right. \\
&- \left.2\overline{C_{k,1}^2(3-N)}+5\overline{C_{k,1}(2)C_{k,1}(3)}-2\overline{C_{k,1}^2(2)}-\overline{C_{k,1}^2(3)}\right\} \\
&+ 0.0040\frac{PGg^bT_c^2}{D^{a+b}}\left\{\overline{[3C_{k,1}(2-N)-2C_{k,1}(3-N)]^2}\right. \\
&+ \left.\overline{[3C_{k,1}(2)-2C_{k,1}(3)]^2}\right\}
\end{aligned} \tag{5.63}$$

Up to now, the only unknown terms in the interference power from adjacent cells are those code related functions. This analysis shows that the most significant contribution to the interference from the adjacent cells are the users distributed in the zones with $l = 0$ and $l = 1$. Their power profiles are about one magnitude higher than that of the zone with $l = 2$. The users in the zone of $l = 0$ are the closest to the home cell, and the users in the zone of $l = 1$ have the most population. Users with $l = 2$ make relatively insignificant contributions, as a result of its small area

(and therefore small population) as well as the fast power attenuation by way of the inverse fourth power law. To further quantitatively analysis equation (5.63), we need to evaluate those code related terms.

5.6 Code modelling by random sequences

It is convenient to model the code sequences as random i.i.d sequences for general purpose. We have seen that such modelling works well for m-length code and orthogonal codes. Recall those statistical properties of random codes given in equation (3.15)-(3.17),

$$\overline{C_{k,1}^2(N-|l|)} = |l| \tag{5.64}$$

$$\mathrm{E}\{C_{k,1}(l)C_{k,1}(m)\} = 0 \tag{5.65}$$

$$\overline{\theta_{k,1}^2(l)} = \overline{C_{k,1}^2(l)} + \overline{C_{k,1}^2(l-N)} \tag{5.66}$$

and

$$\overline{\theta_{k,1}^2(l)} = N \tag{5.67}$$

Then we have

$$\begin{aligned}
\frac{\overline{J_i^2}}{\frac{PG_g{}^bT_c^2K}{D^4}} &= 0.5080\{\theta_{k,1}(0)+\theta_{k,1}(1)\} - 0.9375\theta_{k,1}(0) + 0.4487\theta_{k,1}(0) \\
&\quad +0.3777\{\theta_{k,1}(1)+\theta_{k,1}(2)\} + 0.4033\{-2\theta_{k,1}(1)-\theta_{k,1}(2)\} \\
&\quad +0.1098\{4\theta_{k,1}(1)+\theta_{k,1}(2)\} + 0.0266\{\theta_{k,1}(3)+\theta_{k,1}(2)\} \\
&\quad +0.0205\{-3\theta_{k,1}(2)-2\theta_{k,1}(3)\} + 0.004\{9\theta_{k,1}(2)+4\theta_{k,1}(3)\} \\
&= 0.5080\{N+N\} - 0.9375N + 0.4487N \\
&\quad +0.3777\{N+N\} + 0.4033\{-2N-N\} + 0.1098\{4N+N\} \\
&\quad +0.0266\{N+N\} + 0.0205\{-3N-2N\} + 0.004\{9N+4N\} \\
&= 0.6244N
\end{aligned} \tag{5.68}$$

Equation (5.68) gives the mean interference level from an adjacent cell. In that final result, $0.5272N$ or 84% is contributed from the zone of $l = 0$. $0.0945N$ or 15%

is contributed from the zone of $l = 1$. The rest or less than 1% is contributed from the zone of $l = 2$. As we mentioned before, the population of users in zone of $l = 1$ is even larger than that of zone of $l = 0$; however, the interference is smaller. That is the result of rapid attenuation of transmission power. We therefore conclude that power path loss plays a crucial role in the performance of CDMA-PCS systems, and the contributions to the interference from cells outside the first tier are negligible.

Define the received signal bit energy as

$$E_b = \frac{PGg^b}{r_0^a(g + r_0)^b} T^3 \tag{5.69}$$

The signal to noise ratio can be expressed as

$$\frac{D_c^2 + D_s^2}{2\mathrm{Var}\{Z_c\}} = \frac{1}{\left[\frac{E_b}{N_0}\right]^{-1} + 2(K-1)\mathrm{E}\{I_c^{(k,1)}\} + 24\frac{r_0^2(g+r_0)^2}{D^4}\frac{K \cdot 0.6244N}{N^2}} \tag{5.70}$$

In the above expression, the first term in the denominator of right hand side is due to random noise. The second term is caused by the interference of the users in home cell, which we have analyzed in chapter 4. The last term is the result of interference from all the six adjacent cells in the first tier. We can see that it is the function of total number of users K, and the location of the desired user, r_0. The other parameters g, D, and N are related to the system configuration. From equation (5.70), we can calculate the BER for a user in terms of how many other users accessing the system simultaneously using equation (4.4).

5.7 Average of Desired Signal Power

We may wish to know BER for users with averaged signal power over r_0 ($\overline{P(r)}$), such at the average performance of the system can be known and capacity can be estimated. As it is shown in equation (5.33), the power of the desired signal is:

$$D_c^2 = \frac{PGg^b}{2r_0^a(g + r_0)^b} T^2 \cos^2 \phi_1 \tag{5.71}$$

Here r_0 is the distance of the desired user to the base station in home cell. To get the average signal power, we need to take the expectation over r_0 since the desired user may appear anywhere in the home cell. More specifically, we need to evaluate

$$\int_0^{R_d} \frac{1}{r_0^a(g+r_0)^b}\frac{2r_0}{R_d^2}dr_0 \tag{5.72}$$

For the case $a = b = 2$, this becomes

$$\frac{2}{R_d^2}\int_0^{R_d} \frac{1}{r_0(g+r_0)^2}dr_0 \tag{5.73}$$

however, this integral has the pole at $r_0 = 0$. To avoid this difficulty, and also to be more realistic, the received power is set to a constant if the desired user is very close to the base station. Let δ denote the distance within which the received power is constant. Then the integral above can be evaluated as

$$\frac{2}{R_d^2}\int_0^{R_d} \frac{1}{r_0(g+r_0)^2}dr_0 = \frac{2}{R_d^4}(\frac{R_d}{g})^2\left\{\ln\frac{R_d}{\delta} - \ln(1+\frac{R_d}{g}) - \frac{\frac{R_d}{g}}{1+\frac{R_d}{g}}\right\} \tag{5.74}$$

The final result is not sensitive to the choice of δ due to the logarithmic function, so long as it is greater than 1. In our systme simulation, we choose $\delta = 25$ meters.

To get the BER for users with average signal power, we need to replace $r_0^2(g+r_0)^2$ in equation (5.70) by the inverse of right hand side of equation (5.74). The third term (III) in the denominator of equation (5.70) becomes

$$III = 24\cdot\frac{1}{2}(\frac{R_d}{D})^4(\frac{g}{R_d})^2\left\{\frac{1}{\ln\frac{R_d}{\delta} - \ln(1+\frac{R_d}{g}) - \frac{\frac{R_d}{g}}{1+\frac{R_d}{g}}}\right\}\frac{K\cdot 0.6244N}{N^2} \tag{5.75}$$

Therefore we can see the average result depends only on those geometric paramters. By setting $R_d = 500$ meters, $D/R_d = \sqrt{3}$, $g = 150$ meters and $\delta = 25$ meters, we have

$$\begin{aligned} III &\approx 0.1579\cdot\frac{K\cdot 0.6244N}{N^2} \\ &= 0.0983\cdot\frac{K}{N} \end{aligned} \tag{5.76}$$

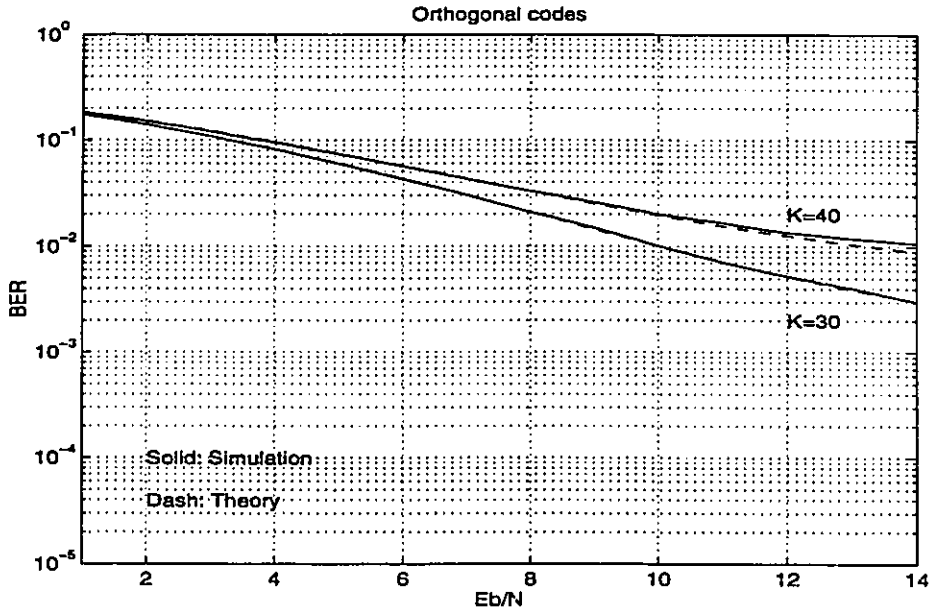

Figure 5.7: Performance of orthogonal codes

Thus the BER of a user with mean signal power ($\overline{P(r)}$) can be expressed as:

$$P_e = \frac{1}{2}\exp\left\{-\frac{1}{\left[\frac{E_b}{N_0}\right]^{-1} + 2(K-1)\mathrm{E}\{I_c^{(k,1)}\} + 0.0983 \cdot \frac{K}{N}}\right\} \tag{5.77}$$

Equation (5.77) gives the expectation of the performance for users in the cell.

5.8 Performance of orthogonal codes

By combining the results we have in this chapter and the results in chapter 4, we can get the performance of this system using orthogonal codes:

$$P_e = \frac{1}{2}\exp\left\{-\frac{1}{\left[\frac{E_b}{N_0}\right]^{-1} + \frac{(K-1)(N+2)}{N^2}\alpha^2 + 24\frac{r_0^2(g+r_0)^2}{D^4}\frac{K\cdot 0.6244N}{N^2}}\right\} \tag{5.78}$$

for a given radius r_0. In figure 5.7 and table 5.1, we show the result for $r_0 = 250$ meters.

Table 5.1: BER performance for desired user located 250 meters away from base station, using orthogonal code

$\frac{E_b}{N_0}$	K=30		K=40	
dB	theory	simulation	theory	simulation
1	0.1741	0.1736	0.1838	0.1840
2	0.1397	0.1398	0.1512	0.1506
3	0.1085	0.1086	0.1213	0.1201
4	0.0816	0.0821	0.0953	0.0947
5	0.0595	0.0595	0.0734	0.0739
6	0.0422	0.0425	0.0559	0.0562
7	0.0294	0.0301	0.0422	0.0427
8	0.0203	0.0207	0.0319	0.0328
9	0.0139	0.0149	0.0244	0.0259
10	0.0097	0.0102	0.0188	0.0200
11	0.0068	0.0071	0.0149	0.0166
12	0.0050	0.0052	0.0120	0.0134
13	0.0037	0.0040	0.0110	0.0118
14	0.0028	0.0030	0.0084	0.0106

$\frac{E_b}{N_0}$	K=50	
dB	theory	simulation
1	0.1931	0.1893
2	0.1620	0.1575
3	0.1336	0.1284
4	0.1086	0.1024
5	0.0873	0.0820
6	0.0698	0.0633
7	0.0559	0.0498
8	0.0450	0.0397
9	0.0366	0.0316
10	0.0303	0.0256
11	0.0255	0.0201
12	0.0219	0.0171
13	0.0192	0.0146
14	0.0171	0.0128

In table (5.1) and figure (5.7), the theoretical values are given by equation (5.78), and the simulated results are given by the Monte-Carlo simulations. In each simulation, we made 50 runs and for each run we have randomly generated r_k for all the six adjacent cells. The final simulated BER is the average of that of 50 runs, similar to the simulations in chapter 4. We can see the good agreements between the theoretical and the simulated results which support the validity of our model.

By comparing with the performance for orthogonal codes in the uplink as given in chapter 4, we can see the substantial degradation due to the inclusion of interference from adjacent cells. For $K = 50$ users, a BER of 10^{-3} can be reached at the $E_b/N =$ 10dB approximately, as shown in figure (4.15). However, when we include adjacent cell interference, we can see that even for $K = 40$ users, it is not possible to reach the same BER, no matter how we increase E_b/N. In figure 5.7 we observe that the BER curve is tapering off to a fixed limiting value as the E_b/N_0 increases. This apparent lower bound given by

$$P_e = \frac{1}{2}\exp\left\{-\frac{1}{\frac{(K-1)(N+2)}{N^2}\alpha^2 + 24\frac{r_0^2(g+r_0)^2}{D^4}\frac{K\cdot 0.6244N}{N^2}}\right\} \tag{5.79}$$

is caused by mutual interference from the home cell as well as the adjacent cells. When the lower bound appears, it means the system capacity is limited by the mutual interference. Increasing users' signal power won't help, since the interference power will be increased simultaneously, and the signal-to-interference ratio will remain the same. When the bandwidth and path-loss are fixed, the only way to reduce interference level is to reduce the number of simultaneous users. Again we see the capacity of a CDMA system is bounded by the mutual interference generated by its users, even though orthogonal codes are used.

The mean BER in a cell can be estimated by equation (5.68). In figure (5.8) we show the BER curves for different number of users. In table (5.2), we show the calculated results and the simulated results.

The results show that, to have BER below 10^{-3} within 14 dB, we can only put 20 users in each cell for every hopping patterns, or with the inclusion of adjacent cell

Table 5.2: Mean BER using orthogonal code

$\frac{E_b}{N_0}$	K=20		K=30	
dB	theory	simulation	theory	simulation
1	0.1649	0.1713	0.1759	0.1792
2	0.1290	0.1344	0.1419	0.1434
3	0.0966	0.1022	0.1109	0.1149
4	0.0691	0.0729	0.0841	0.0925
5	0.0471	0.0493	0.0620	0.0653
6	0.0307	0.0328	0.0447	0.0455
7	0.0192	0.0205	0.0317	0.0320
8	0.0116	0.0121	0.0222	0.0228
9	0.0069	0.0074	0.0156	0.0147
10	0.0040	0.0042	0.0111	0.0107
11	0.0024	0.0022	0.0081	0.0079
12	0.0014	0.0015	0.0060	0.0063
13	8.7e-4	7.9e-4	0.0046	0.0051
14	5.6e-4	6.5e-4	0.0036	0.0040
$\frac{E_b}{N_0}$	K=40		K=50	
dB	theory	simulation	theory	simulation
1	0.1863	0.1912	0.1961	0.2005
2	0.1541	0.1608	0.1657	0.1703
3	0.1247	0.1298	0.1377	0.1403
4	0.0988	0.1014	0.1130	0.1158
5	0.0771	0.0803	0.0919	0.0978
6	0.0595	0.0605	0.0745	0.0774
7	0.0457	0.0499	0.0606	0.0613
8	0.0352	0.0363	0.0496	0.0502
9	0.0274	0.0285	0.0411	0.0419
10	0.0216	0.0222	0.0345	0.0350
11	0.0174	0.0177	0.0296	0.0301
12	0.0143	0.0147	0.0258	0.0262
13	0.0121	0.0125	0.0229	0.0231
14	0.0104	0.0107	0.0207	0.0210

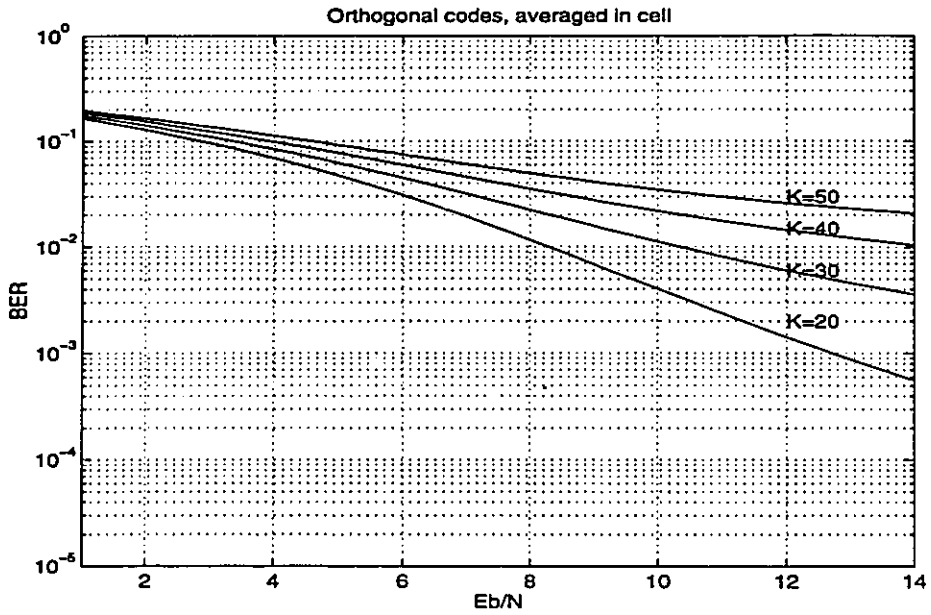

Figure 5.8: Averaged performance of orthogonal codes in a cell

interference, the system capacity can only reach about 30% of its hard limit.

5.9 Performance of Gold codes

For Gold codes, we carried out simulations to get the mean BER when the adjacent cell interference is included. The result is shown in figure (5.9) and table (5.3). We can see a slightly degradation in performance for Gold codes, in comparison with that of orthogonal codes. For BER to reach 10^{-3}, the number of users on each hopping pattern must be below 20, for $E_b/N_0 \simeq 14$ dB.

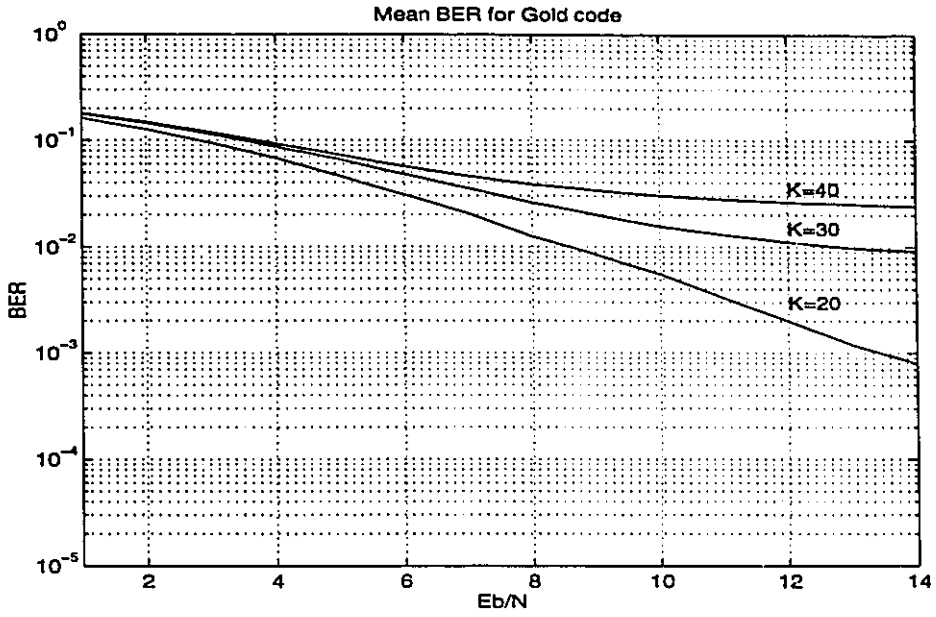

Figure 5.9: Performance of Gold codes

Table 5.3: Mean BER using Gold codes

$\frac{E_b}{N_0}$	K=20	K=30	K=40
1	0.1634	0.1780	0.1816
2	0.1266	0.1449	0.1486
3	0.0946	0.1143	0.1192
4	0.0681	0.0871	0.0929
5	0.0462	0.0662	0.0729
6	0.0306	0.0477	0.0567
7	0.0207	0.0354	0.0459
8	0.0125	0.0259	0.0383
9	0.0085	0.0199	0.0338
10	0.0055	0.0155	0.0300
11	0.0033	0.0130	0.0278
12	0.0020	0.0111	0.0262
13	0.0012	0.0098	0.0251
14	8.0e-4	0.0091	0.0241

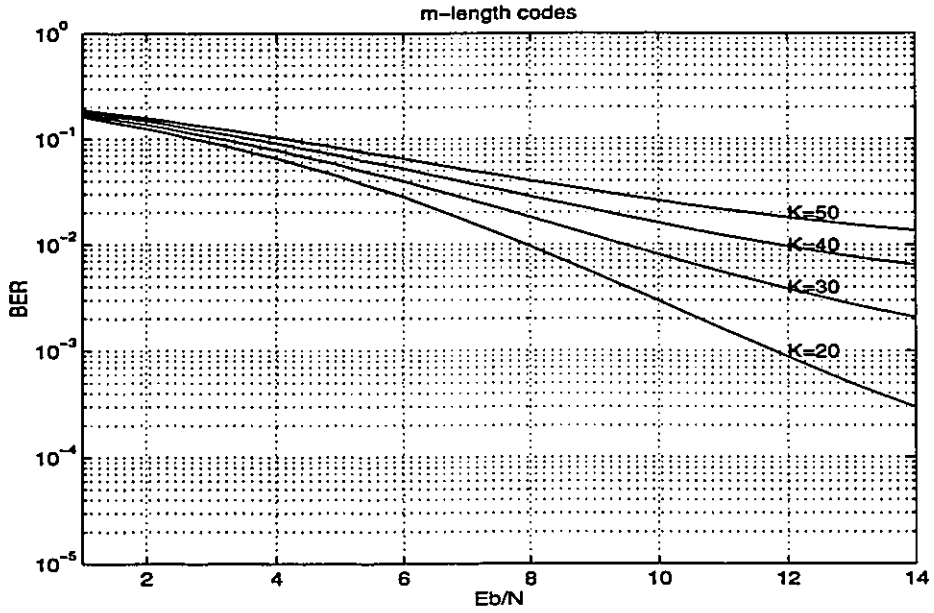

Figure 5.10: Performance of m-length codes

5.10 Performance of m-length codes

Again, by combining the results we have in this chapter and the results in chapter 4, we can get the performance for m-length codes:

$$P_e = \frac{1}{2}\exp\left\{-\frac{1}{\left[\frac{E_b}{N_0}\right]^{-1} + 2(K-1)\sigma_{k,i}^2 + 24\frac{r_0^2(g+r_0)^2}{D^4}\frac{K\cdot 0.6244N}{N^2}}\right\} \tag{5.80}$$

for a given radius r_0. $\sigma_{k,i}^2$ is given by equation (4.68). In figure 5.10 and table 5.4, we show the results for $r_0 = 250$ meters. When using a single m-length sequence as the code, we get the best performance. The performance of orthogonal codes is close to this. Both of them are the optimum codes.

Table 5.4: BER of users located 250 meters away, using a single m-length sequence as codes

$\frac{E_b}{N_0}$	K=20		K=30	
dB	theory	simulation	theory	simulation
1	0.1623	0.1619	0.1719	0.1723
2	0.1260	0.1219	0.1371	0.1413
3	0.0933	0.0945	0.1056	0.1011
4	0.0657	0.0603	0.0785	0.0802
5	0.0438	0.0428	0.0564	0.0603
6	0.0277	0.0282	0.0393	0.0401
7	0.0167	0.0170	0.0268	0.0272
8	0.0096	0.0098	0.0179	0.0182
9	0.0053	0.0058	0.0120	0.0118
10	0.0029	0.0032	0.0081	0.0083
11	0.0016	0.0018	0.0055	0.0056
12	8.8e-4	9.7e-4	0.0038	0.0040
13	5.0e-4	6.2e-4	0.0027	0.0030
14	2.9e-4	4.2e-4	0.0021	0.0023
$\frac{E_b}{N_0}$	K=40		K=50	
dB	theory	simulation	theory	simulation
1	0.1810	0.1790	0.1897	0.1911
2	0.1478	0.1455	0.1580	0.1601
3	0.1176	0.1147	0.1291	0.1304
4	0.0912	0.0892	0.1036	0.1044
5	0.0693	0.0667	0.0821	0.0872
6	0.0518	0.0491	0.0646	0.0650
7	0.0383	0.0366	0.0507	0.0511
8	0.0283	0.0270	0.0400	0.0395
9	0.0210	0.0201	0.0319	0.0323
10	0.0158	0.0150	0.0258	0.0260
11	0.0122	0.0120	0.0213	0.0222
12	0.0096	0.0097	0.0179	0.0181
13	0.0077	0.0080	0.0154	0.0160
14	0.0064	0.0068	0.0135	0.0141

5.11 Performance by considering of voice activity cycle

One of the important factors for CDMA systems to increase the capacity is the voice activity cycle. In voice communications, users usually take 35% of the total time in speaking, while in the rest of time they are listening and thinking. If each user has a dedicate channel for himself, about 2/3 capacity is wasted. In TDMA systems, it is possible to use very sophisticated algorithm to detect the "quiet" time slots and assign the new user to these slots. But it requires a complex system since the detection process will take considerable overhead of the empty slot. However, a CDMA system can almost automatically take advantage of the empty time without increasing the complexity. If a user stops speaking, he does not transmit signal. Conceptually users transmit ternary codes of $\{+1, 0, -1\}$, instead of binary codes of $\{+1, -1\}$. Here the code 0 corresponds to the quiet period. During this period all the other users will get no interference from this user and the average effect is the reduced interference level. In real implementation, certain measurement must be taken to quench the user's signal during the non-speaking periods.

As we have shown in Chapter 4, it will not triple the capacity due to the using of non-optimum codes(e.g., using of two m-length sequences to provide codes). However, from the previous results, we knew that such a CDMA system can perform reasonably well (at BER of 10^{-3}) at very low capacity (about a third of the hard limit). It is possible to increase the capacity by a fold of 3 after take advantage of the voice activity cycle, since it is just around the hard limit and the optimum codes can be used.

The simulation results are shown in figure (5.11) and table(5.5). We found that to reach BER of 10^{-3}, we can put about 60 users on each hopping pattern.

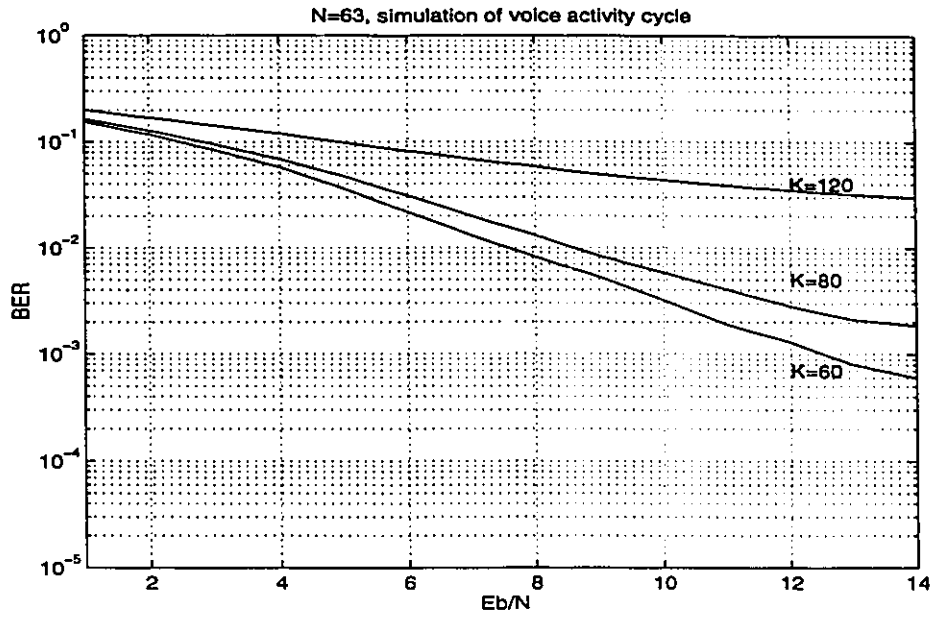

Figure 5.11: Voice activity cycle simulations for m-length codes

Table 5.5: Mean BER of m-length codes, voice activity cycle tests

$\frac{E_b}{N_0}$	K=60	K=80	K=120
1	0.1547	0.1647	0.1996
2	0.1188	0.1286	0.1703
3	0.0846	0.0959	0.1435
4	0.0576	0.0686	0.1197
5	0.0365	0.0475	0.0986
6	0.0218	0.0310	0.0817
7	0.0121	0.0199	0.0682
8	0.0081	0.0130	0.0580
9	0.0053	0.0084	0.0491
10	0.0032	0.0058	0.0433
11	0.0019	0.0040	0.0386
12	0.0013	0.0028	0.0349
13	0.0008	0.0021	0.0320
14	0.0006	0.0018	0.0299

5.12 Discussion

The effects of interference from adjacent cells are the major concerns in this chapter. From section 5.1 to section 5.7, we developed the models to estimate such interference power. For a special path-loss law ($a = b = 2$) we deduced the formula of bit-error-rate based on the assumptions that codes are random-like within their periods. We must point out that equation (5.70) is not valid for other kinds of path-loss besides $a = b = 2$. Those intergals defined in eqs. (5.54)–(5.62) must be recalculated for such different parameters. For more precise estimation, one should use the mean value of the partial correlation functions $C_{k,i}$ given in chapter 3 instead of using random code model.

We have calculated the BER for different codes and compared them with the simulation results. Good agreements are observed. Generally speaking, the adjacent cells contributed considerable interference and it makes the BER a constant as transmission power increases. Using a single m-length sequence as code gives the best performance. However, it can yield satisfactory BER only at very low capacity ($\frac{1}{3}N$) which makes its capacity the same as that of TDMA (frequency reuse pattern of 3 assumed). Fortunately voice activity cycle effect can greatly compensate the loss of capacity in such a case. A three-fold increase in capacity can be achieved by using this effect.

The total capacity in each cell of this system can now be ready to estimate. It is simply the number of users in each hopping pattern multiply by the number of hopping patterns, i.e:

$$\text{Capacity} = K \times N_f \tag{5.81}$$

where N_f is the number of hopping patterns. We have shown that we can put 60 users in each hopping pattern, after considering the voice activity cycle, and the number of hopping patterns in our system is 40, so the total number of simultaneous users we can put is around 2400.

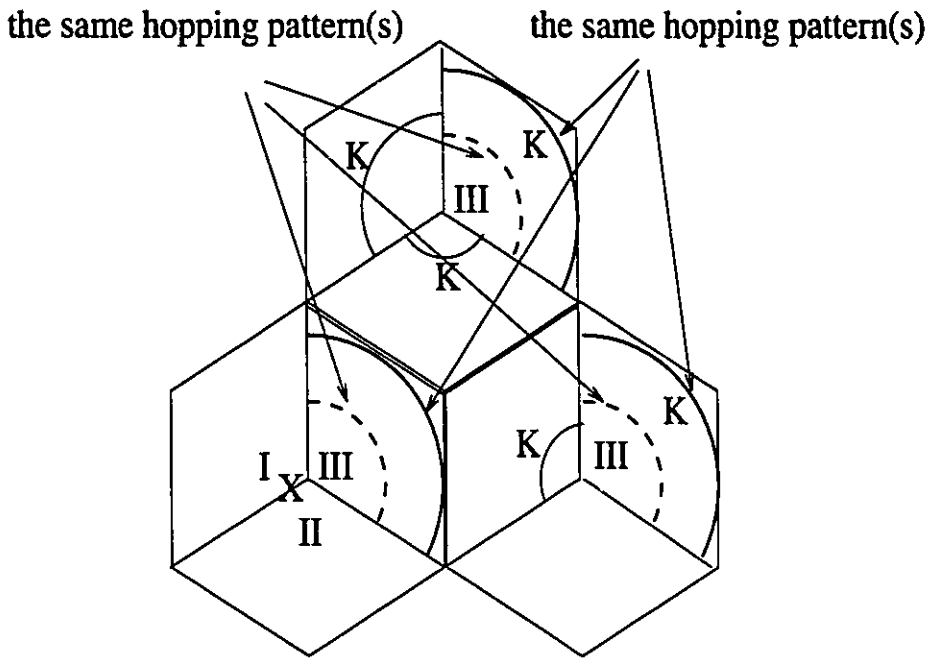

Figure 5.12: Split cell by 3 sections

Another way to increase the capacity is to split the cell, as shown in figure 5.12. This can be realized by using directional antennas which have the beam width of 120°. Ideally each sector has interference from two adjacent cells only. However, if we reuse the same hopping pattern in all the three sectors, the total number of users in these two adjacent cells will be tripled, as shown in the figure 5.12. In the case that the distances of these three groups are randomly distributed, the averaged performance can be also found by equation (5.70). However, the parameter K becomes the number of users in each sector, and we can have totally $3K$ users in one cell using the same hopping pattern that generate the same amount of interference as that of the K users on each hopping pattern without doing the cell sectorization. For real implementation, however, we will expect the gain in capacity to be less than 3 fold due to the sidelobe interference between the antennas.

We should point out that the BER estimated in equation (5.70) depends on r_0, the distance of the desired user to the home base station. Users with different r_0 will experience different performance, and the BER of users located close to the boundary

will be much greater than those near the base station. One way to relieve this problem is to taking the advantage of a split cell. We may divide the total number of hopping patterns into three sets (as the I, II and III shown in the figure) of the same size, and the sectors having the same orientation use the same set. Within each set the hopping patterns are assigned in the fixed order according to r_0. In figure 5.12 we show this idea. The distance between those users located on the dark solid arcs and the distance between those located on the dash arcs are relatively the same, such that the ratios of user's signal power to the interference power are relatively the same, so are the BERs. In this way we can reduce the variance of BER within the cell and let all the users have the same access to the system. In such a scheme the sectorization of cell does not directly triple the capacity. However, we can remove these possible "capacity vacua" at the boundaries of the cell where the BER may become unacceptable, and improve the overall performance.

Chapter 6

Summary and Conclusions

6.1 Summary of the work

The main objective of this thesis is to design a PCS system with high capacity. We found that the hybrid DS/FH CDMA method is a promising technology to achieve this goal. Designing such a system and analyzing its capacity are the major contributions of this thesis.

Using CDMA techniques for high capacity PCS systems is originated by observing the evolution path of cellular systems, where the DS-CDMA technology has been claimed to offer the highest capacity. However, there are serious problems in implementation of DS-CDMA to PCS. Due to the wider bandwidth for PCS, DS-CDMA requires codes with longer period. This will cause the long acquisition problem. The second problem for DS-CDMA system is the "near-far" problem. Both these two problems reduce the system performance, and require complicated hardware solutions to combat them.

The idea of applying hybrid DS/FH CDMA technique to PCS system is initiated for trying to solve the long acquisition problem. We also found that by taking advantage of FH, we can solve the "near-far" problem without increasing the system complexity. These have been discussed thoroughly in chapter 2.

Unlike FDMA or TDMA, the capacity of CDMA systems is limited by the mutual interference of users, and the interference level is determined by two major factors: one is the synchronization level, another is the code property. The most important property of the codes is the cross-correlation. The lower is the cross correlation among the codes, the less is the interference level, and the higher the capacity will be. In chapter 3, we discussed the properties of different codes. We have shown that the bound of mean square value of cross correlation for random sequences is approximately equal to the period of the code, N. By using the preferred pairs of m-length codes, or other deliberately designed codes such as Gold codes, that bound can be improved. Finally we showed that the optimum codes in the sense of minimum cross correlation is the orthogonal codes and we also showed the ways to construct the orthogonal codes.

Another detriment to the system performance is the imperfection of synchronization. One reason is the random access of the users to the network. In chapter 4 we have shown that asynchronous DS-CDMA systems are very inefficient and the capacity can be only 10% of that of TDMA or FDMA system. Hybrid CDMA systems with random frequency hopping perform even worse. We proposed to implement time slots and deterministic coordinated hopping patterns. Such a measure not only helps to save the acquisition and power control parts as discussed in chapter 2, but also increases the capacity dramatically, in the way of establishing synchronous access and avoiding frequency collisions. Another reason of imperfect synchronization is caused by propagation delays. There is no way to eliminate these delays, although we have managed to restrain the maximum delay to less than half of the chip duration(T_c). Therefore at best we can only have quasi-synchronous access for uplink. For the downlink, however, we can have completely synchronous access.

Synchronous access does not guarantee a better performance for CDMA systems. In fact, if random sequences are employed, it is even worse than asynchronous access, as discussed in chapter 4. However, for the well designed codes, we will have a great

capacity gain. The optimum codes we proposed to use are: the codes started from a unique phase of a single m-length sequence, the Gold codes and the orthogonal codes. We did theoretical analysis as well as simulations for their performance. It is shown that for downlink, orthogonal codes offer the best performance which can reduce the mutual interference to 0. For the uplink, their performance are relatively the same, and depends on the offset of synchronization. Voice activity test in chapter 4 tells us that for low level mutual interference environment, we should not expect much gain in capacity. One important issue from these results is that the overall capacity of the system is bounded by uplink.

A major concern in applying CDMA to PCS is the additional interference from adjacent cells, since it has a frequency reuse pattern of 1, in contrast with 3 or 4 for TDMA and 7 for FDMA. In chapter 5, We have developed the mathematical models for calculating the mean interference power from the adjacent cells located on the first tier. The results revealed significant impairment of capacity due to this interference. The models developed in chapter 5 are valid for a wide class of path-lossing law, although we just gave the numerical analysis for a special case $a = b = 2$. System capacity is affected by these power indices, which are related to the antenna height of BS as well as the propagation environment. This is significant for the design of the real cells.

Voice activity cycle also plays an important role to system capacity. It can triple the capacity in one cell to approach the hard limit N. Without it, the capacity can only be about $\frac{N}{3}$, for an acceptable BER (10^{-3}) and reasonable E_b/N_0. Nevertheless the capacity of this hybrid system can have the potential of much higher than that of TDMA system.

Users located near the boundary of the cell will suffer extensive interference from adjacent cells. This is more serious for CDMA systems than the other multiple access systems since frequency reuse pattern is 1. A remedy we pointed out is to sectorize the cell such that different interfering groups are separated relatively equally and have

similar signal-to-interference ratio.

Conclusions of this th sis can be made as follows:

1. Hybrid DS/FH CDMA technology can effectively solve the long acquisition and near-far problems.

2. By implementing time slots and coordinated frequency hopping, Synchronous access can be achieved in downlink and quasi-synchronous access in uplink. With the employment of optimum codes, this will greatly improve the capacity of this CDMA system, and make it comparable to that of TDMA or FDMA systems if interference of adjacent cells and voice activity cycle are ignored.

3. Voice activity cycle has important impact to CDMA systems and potentially triple the capacity without adding any complexity when mutual interference is the only dominanted bottleneck. If the mutual interference has already been suppressed by using optimum codes, we do not expect much more gain.

4. Finally, for this PCS system, our analytical model and numerical simulation show that in each cell, the capacity can approach its hard limit for a reasonable BER of 10^{-3} and ratio of bit energy to noise power spectral density E_b/N_0 about 10 dB. Therefore this CDMA system potentially offers capacity 1.5 times larger than that of TDMA system.

6.2 Future work

What are beyond the scope of this thesis but are still important to the system capacity are the fading channel analysis and error correct coding(ECC) techniques.

Radio channels inevitably suffer the power fading, from multipath propagations, users rambling around, external interference, etc. Generally fading channels will degrade the system performance regardless of their multiple access methods. CDMA systems offer better immunity to fading. It is worth pointing out that RAKE receivers

are specially versatile for multi-path environment. It combines the energy of the same signal pulse but arrives at different time and offer time diversity. Already investigations on this can be found in the literature (e.g. [44]).

As we have seen, to keep a high capacity, the BER can only be as low as 10^{-3}. This is satisfactory to voice communications. For other applications like data communications, we expect a BER of 10^{-8} or less. We cannot count on voice activity cycle or increasing signal power in such cases. Reducing the number of users is neither an efficient nor an economical way. Error correct coding will be the most promising method to achieve this goal.

Finally this thesis focuses on system capacity analysis. It raises both theoretical and practical interests in traffic analysis. For voice communications, it means how many subscribers are allowed for a given block probability. For data communications, interests are on the throughput analysis. Both are important topics for future research.

Appendix A

Evaluation of integrals I_1 and I_2

The integrals I_1 and I_2 can be evaluated in close forms:

$$\begin{aligned} I_1 &= \int_{\theta_{min}}^{\theta_{max}} \frac{1}{1+\frac{r^2}{D^2}-2\frac{r}{D}\cos\theta} d\theta \\ &= \frac{2}{1-\frac{r^2}{D^2}} \arctan\left(\frac{D+r}{D-r}\tan\frac{\theta_{max}}{2}\right) \\ &\quad -\frac{2}{1-\frac{r^2}{D^2}} \arctan\left(\frac{D+r}{D-r}\tan\frac{\theta_{min}}{2}\right) \end{aligned} \tag{A.1}$$

$$\begin{aligned} I_2 &= \int_{\theta_{min}}^{\theta_{max}} \frac{1}{\left(1+\frac{r^2}{D^2}-2\frac{r}{D}\cos\theta\right)^2} d\theta \\ &= \frac{4\frac{r}{D}\tan\frac{\theta_{max}}{2}}{(1-\frac{r^2}{D^2})^2\left[(1-\frac{r}{D})^2+(1+\frac{r}{D})^2\tan^2\frac{\theta_{max}}{2}\right]} \\ &\quad +\frac{1-\frac{r^2}{D^2}}{(1-\frac{r^2}{D^2})^3} \arctan\left(\frac{D+r}{D-r}\tan\frac{\theta_{max}}{2}\right) \\ &\quad -\frac{4\frac{r}{D}\tan\frac{\theta_{min}}{2}}{(1-\frac{r^2}{D^2})^2\left[(1-\frac{r}{D})^2+(1+\frac{r}{D})^2\tan^2\frac{\theta_{min}}{2}\right]} \\ &\quad +\frac{1-\frac{r^2}{D^2}}{(1-\frac{r^2}{D^2})^3} \arctan\left(\frac{D+r}{D-r}\tan\frac{\theta_{min}}{2}\right) \end{aligned} \tag{A.2}$$

Bibliography

[1] R. Agusti, "On the Performance Analysis of Asynchronous FH-SSMA Communications" *IEEE Trans. Comm.*, Vol. Com-37, No. 5, May, pp488, 1989

[2] D. R. Anderson, and P. A. Wintz, "Analysis of a spread spectrum multiple access system with a hard limiter", *IEEE Trans. Comm.*, Vol. Com-17, No. 2, April, pp285,1969

[3] P. Balaban,, and J. Salz, "Dual diversity combining and equalization in digital cellular mobile radio", *IEEE Trans. Vehicular Tech.* Vol. 40, No. 2, May, pp342, 1991

[4] D. Borth, and M. B. Pursley, "Analysis of Direct-Sequence Spread Spectrum Multiple Access Communication Over Rician Fading Channels" *IEEE Trans. Comm.*, Vol. Com-27, No. 10, Oct., pp1566, 1979

[5] R. J. C. Bultitude, S. A. Mahmoud, and W. A. Sullivan, "A Comparison of Indoor Radio Propagation Characteristics at 910 MHz and 1.75 GHz", *IEEE J. on Sel. Areas in Comm.* Vol. 7, No. 1, Jan., pp20, 1977

[6] G. R. Cooper, and R. W. Nettleton, "A Spread Spectrum Technique for High-Capacity Mobile Communications", *IEEE Trans. Vehicular Tech.*, Vol. 27, No. 4, Nov., pp264, 1978

[7] D. C. Cox, "Personal Communications-A Viewpoint", *IEEE Comm. Magazine*, Nov., pp8, 1990

[8] D. C. Cox, "Universal Digital Portable Radio Communications", *Proc. IEEE* Vol. 75, No. 4, April., pp436, 1987

[9] J. L. Dornstetter, and D. Verhulst, "Cellular Efficiency with Slow Frequency Hopping: Analysis of the Digital SFH900 Mobile System", *IEEE J. Sel. Areas in Comm.* Vol. 5, No. 5, June., pp835, 1987

[10] V. Dasilva, and E. S. Sousa, "Performance of orthogonal CDMA codes for quasi-synchronous communication systems", *Proc. ICUPC'93*, pp995, 1993

[11] R. H. Dou, and L. B. Milstein, "Error Probability Bounds and Approximations for DS Spread Spectrum Communication Systems with Multiple Tone or Multiple Access Interference" *IEEE Trans. Comm.* Vol. 32, No. 5, May, pp493, 1984

[12] B. Eklundh, "Channel Utilization and Blocking Probability in a Cellular Mobile Telephone System with Directed Retry", *IEEE Trans. Comm.*, Vol. 34, No. 4, April, pp329, 1986.

[13] A. K. Elhakeem, M. A. Rahman, P. Balasubramanian, and T. Le-Ngoc, "Modified SUGAR/DS: a new CDMA scheme", *IEEE J. Sel. Areas in Comm.*, Vol. 10, No. 4, May, pp690, 1992.

[14] K. Feher, "MODEMS for Emerging Digital Cellular-Mobile Radio System", *IEEE Trans. Vehicular Tech.*, Vol. 40, No. 2, May, pp355, 1991.

[15] "Wireless personal communications", edited by M. J. Feuerstein and T. S. Rappaport, Kluwer Academic, 1993.

[16] C. D. Frank, and M. B. Pursley, "On the Statistical Dependence of Hits in Frequency Hop Multiple Access", *IEEE Trans. Comm.*, Vol. Com-38, No. 9, Sept., pp1438, 1990.

[17] E. Geraniotis, "Direct-Sequence Spread Spectrum Multiple Access Communications Over Nonselective and Frequency-Selective Rician Fading Channels" *IEEE Trans. Comm.*, Vol. Com-34, No. 8, Aug. pp756, 1986.

[18] E. Geraniotis, "Noncoherent Hybrid DS-SFH Spread-Spectrum Multiple-Access Communications" *IEEE Trans. Comm.*, Vol. Com-34, No. 9, Sept. pp862, 1986.

[19] E. Geraniotis, "Coherent Hybrid DS-SFH Spread-Spectrum Multiple-Access Communications" *IEEE J. Sel. Areas in Comm.* Vol. SAC-3, No. 5, Sept. pp695, 1985.

[20] E. Geraniotis, "Performance of Noncoherent Direct-Sequence Spread-Spectrum Multiple-Access Communications" *IEEE J. Sel. Areas in Comm.* Vol. SAC-3, No. 5, Sept. pp687, 1985.

[21] E. Geraniotis, and M. B. Pursley, "Error Probabilities for Slow Frequency Hopped Spread Spectrum Multiple Access Communications Over Fading Channels" *IEEE Trans. Comm.* Vol. Com-30, No. 5, May, pp996, 1982.

[22] E. Geraniotis, and M. B. Pursley, "Error Probabilities for Direct Sequence Spread Spectrum Multiple Access Communications–Part II: Approximations" *IEEE Trans. Comm.* Vol. Com-30, No. 5, May, pp985, 1982.

[23] E. Geraniotis, and M. B. Pursley, "Peformance of Noncoherent Direct Sequence Spread Spectrum Communications Over Specular Multipath Fading Channels" *IEEE Trans. Comm.* Vol. Com-34, No. 3, March, pp219, 1982.

[24] K. S. Gilhousen, I. M. Jacobs, R. Padovani, A. J. Viterbi, L. A. Weaver, and C. E. Wheatley III, "On the Capacity of a Cellular CDMA System", *IEEE Trans. Vehicular Tech.*, Vol. 40, No. 2, May, pp303, 1991.

[25] K. S. Gilhousen, I. M. Jacobs, R. Padovani, A. J. Viterbi, and L. A. Weaver, "Increased Capacity Using CDMA for Mobile Satellite Communication", *IEEE J. Sel. Areas in Comm.*, Vol. 8, No. 4, May, pp503, 1990.

[26] J. W. Gluck, and E. Geraniotis, "Throughput and Packet Error Probability of Cellular Frequency Hopped Spread Spectrum Radio Networks", *IEEE J. Sel. Areas in Comm.*, Vol. 7, No. 1, Jan, pp148, 1989.

[27] R. Gold, "Optimal Binary Sequences for Spread Spectrum Multiplexing", *IEEE Trans. Infor. Theory* Vol. IT-13, Oct. pp619, 1967.

[28] R. Gold, "maximal Recursive Sequences with 3-valued Recursive Cross-Correlation Functions" *IEEE Trans. Infor. Theory* Vol. IT-14, Jan. pp154, 1968.

[29] S. W. Golomb, *Shift Register Sequences.* San Francisco, CA: Holden-Day, 1967.

[30] D. J. Goodman, "Second Generation Wireless Information Networks", *IEEE Trans. Vehicular Tech.*, Vol. 40, No. 2, May, pp366, 1991

[31] U. Grob, A. L. Welti, E. Zollinger, R. Kung and H. Kaufmann, "Microcellular direct sequence spread spectrum radio system using N-path RAKE receiver", *IEEE J. Sel. Areas in Comm.* , Vol. 8, No. 5, June, pp772, 1990

[32] P. Harley, "Short Distance Attenuation Measurements at 900 MHz and 1.8 GHz Using Low Antenna Heights for Microcells", *IEEE J. on Sel. Areas in Comm.* Vol. 7, No. 1, Jan. pp5, 1989.

[33] M. v. Hegde, and W. E. Stark, "Capacity of frequency hop spread spectrum multiple access communication systems", *IEEE Trans. Comm.* Vol. 38, No. 7, July. pp1050, 1990.

[34] J. K. Holmes, "Acquisition Time Performance of PN Spread-Spectrum Systems", *IEEE Trans. Comm.* Vol. 25, No. 8, Aug., pp778, 1977.

[35] J. M. Holtzman, "A simple, accurate method to calculate spread spectrum multiple access error probabilities", *IEEE Trans. Comm.* Vol. 40, No. 3, March, pp461, 1992.

[36] G. K. Huth, "Optimization of coded spread spectrum system performance", *IEEE Trans. Comm.* Vol. 25, No. 8, Aug., pp763, 1977.

[37] *IEEE communications magazine, special issue on PCS*, Vol. 30, No. 12, Dec., 1992.

[38] *IEEE journal on selected areas in communications, spread-spectrum communications I*, May, 1990.

[39] *IEEE journal on selected areas in communications, spread-spectrum communications II*, June, 1990.

[40] *IEEE transactions on communications, special issue on spread-spectrum communications* , Aug., 1977.

[41] *IEEE transactions on communications, special issue on spread-spectrum communications, Part I* , May, 1982.

[42] *IEEE transactions on communications, special issue on spread-spectrum communications, Part II* , May, 1982.

[43] M. Kavehrad, and B. Ramamurthi, "Direct-Sequence Spread Spectrum with DPSK Modulation and Diversity for Indoor Wireless Communications", *IEEE Trans. Comm.*, Vol. Com-35, No. 2, Feb., pp224, 1987.

[44] C. Kchao, "Direct sequence spread spectrum cellular radio", Ph. D. Dissertation, School of Electrical Engineering, Georgia Institute of Tech., 1991.

[45] B. Z. Kobb, "Personal Wireless", *IEEE Spectrum*, June, pp20, 1993.

[46] R. Kohno, H. Imai, M. Hatori, and S. Pasupathy, "Combination of an adaptive array antenna and a canceller of interference for direct sequence spread spectrum multiple access system", *IEEE J. Sel. Areas in Comm.*, Vol. 8, No. 4, May, pp675, 1990.

[47] J. F. Kuehls, and E. Geraniotis, "Presence detection of binary phase shift keyed and direct sequence spread spectrum signals using a prefilter delay and multiply device", *IEEE J. Sel. Areas in Comm.*, Vol. 8, No. 5, June, pp915, 1990.

[48] W.H. Lam, and R. Steele, "Performanc of direct-sequence spread spectrum multiple access systems in mobile radio", *IEE Proc.*, Vol. 138,, No. 1, Feb., pp1, 1991.

[49] W. C. Y. Lee, "Smaller Cells for Greater Performance", *IEEE Comm. Magazine*, Nov., pp19, 1991.

[50] W. C. Y. Lee, "Overview of Cellular CDMA", *IEEE Trans. Vehicular Tech.*, Vol. 40, No. 2, May, pp291, 1991.

[51] W. C. Y. Lee, "Spectrum Efficiency in Cellular", *IEEE Trans. Vehicular Tech.*, Vol. 38, No. 2, May, pp69, 1989.

[52] W. C. Y. Lee, "Mobile cellular telecommunications systems", McGraw-Hill, 1989.

[53] W. C. Y. Lee, "Mobile communications engineering", McGraw-Hill, 1982.

[54] J. S. Lehnert, and M. B. Pursley, "Error Probabilities for Binary Direct Sequence Spread Spectrum Communications with Random Signature Sequences", *IEEE Trans. Comm.*, Vol. 35, No. 1, Jan., pp87, 1987.

[55] J. S. Lehnert, and M. B. Pursley, "Multipath diversity reception of spread spectrum multiple access communications", *IEEE Trans. Comm.*, Vol. 35, No. 11, Nov., pp1189, 1987.

[56] Y. H. Lee, and S. Tantaratana, "Sequential Acquistion of PN Sequences for DS/SS Communications: Design and Performance", *IEEE J. Sel. Areas in Comm.*, Vol. 10, No. 4, May, pp750, 1992.

[57] F. J. MacWilliams, and J. A. Sloane, "Pseudo-Random Sequences and Arrays", *Proc. IEEE* , Vol. 64, No. 12, Dec., pp1715, 1976.

[58] M. I. Mandell, " A comparision of CDMA and frequency hopping in a cellular environment", Ph.D. dissertation, California Institute of Technology, 1993.

[59] L. B. Milstein, T. S. Rappaport, and R. Barghouti, "Performance Evaluation for Cellular CDMA", *IEEE J. Sel. Areas. in Comm.* , Vol. 10, No. 4, May, pp680, 1992

[60] L. B. Milstein, D. L. Schilling, R. L. Pickholtz, V. Erceg, M. Kullback, e. G. Kanterakis, D. S. Fishman, W. H. Biederman, and D. C. Salerno, "On the Feasibility of a CDMA Overlay for Personal Communications Networks", *IEEE J. Sel. Areas. in Comm.* , Vol. 10, No. 4, May, pp655, 1992.

[61] R. K. Morrow, and J. S. Lehnert, "Bit-to-bit error dependence in slotted DS/SSMA packet systems with random signature sequences", *IEEE Trans. Comm.* , Vol. 37, No. 10, Oct., pp1052, 1989.

[62] S. M. Pan, D. E. Dodds, and S. Kumar, "Acquisition time distribution for spread spectrum receivers", *IEEE J. Sel. Areas. in Comm.* , Vol. 8, No. 5, June, pp800, 1990.

[63] M. Pandit, "Mean Acquisition Time of Active and Passive-Correlation Acquisiton Systems for Spread Spectrum Communication Systems", *IEE Proc.*, Vol. 128, No. 4, Aug., pp211, 1981.

[64] R. L. Pickholtz, L. B. Milstein, D. L. Schilling, "Spread Spectrum for Mobile Communications", *IEEE Trans. Vehicular Tech.*, Vol. 40, No. 2, May, pp313, 1991.

[65] R. L. Pickholtz, D. L. Schilling, and L. B. Milstein, "Theory of Spread-Spectrum Communications–A Tutorial", *IEEE Trans. Comm.*, Vol. 30, No. 5, May, pp855, 1982

[66] A. Polydoros, and C. L. Weber, "A unified approach to serial search spread spectrum code acquistion-Part I: General Theory", *IEEE Trans. Comm.*, Vol. 32, No. 5, May, pp542, 1984

[67] R. Prasad, and A. Kegel, "Effects of Rician Faded and Log-Normal Shadowed Signals on Spectrum Efficiency in Microcellular Radio", *IEEE Trans. Vehicular Tech.*, Vol. 42, No. 3, Aug., pp274, 1993

[68] M. B. Pursley, "The Role of Spread Spectrum in Packet Radio Networks", *Proc. IEEE*, Vol. 75, No. 1, Jan., pp116, 1987

[69] M. B. Pursley, D. V. Sarwate, and W. E. Stark, "Error probability for direct sequence spread multiple access communications-part I: Upper and Lower Bounds", *IEEE Trans. Comm.*, Vol. 30, No. 5, May., pp975, 1982

[70] M. B. Pursley, "Performance Evaluation for Phase-Coded Spread-Spectrum Multiple Access Communication-Part I: System Analysis", *IEEE Trans. Comm.*, Vol. Com-25, No. 8, Aug., pp795, 1977

[71] M. B. Pursley, and D. Sarwate, "Performance Evaluation for Phase-Coded Spread-Spectrum Multiple Access Communication-Part II: Code Sequence Analysis", *IEEE Trans. Comm.*, Vol. Com-25, No. 8, Aug., pp800, 1977

[72] M. B. Pursley, and H. F. A. Roefs, "Numerical Evaluation of Correlation Parameters for Optimal Phases of Binary Shift-Register Sequences" *IEEE Trans. Comm.*, Vol. Com-27, No. 10, Oct., pp1597, 1979

[73] M. B. Pursley, and D. V. Sarwate, "Evaluation of correlation parameters for periodic sequences", *IEEE Trans. Info. Theory*, Vol. , July, pp508, 1977

[74] K. Raith, "Capacity of Digital Cellular TDMA Systems", *IEEE Trans. Vehicular Tech.*, Vol. 40, No. 2, May, pp323, 1991.

[75] T. S. Rappaport, "The Wireless Revolution", *IEEE Comm. Magazine*, Nov., pp60, 1991.

[76] D. Raychaudhuri, "Performance Analysis of Random Access Packet-Switched Code Division Multiple Access Systems", *IEEE Trans. Comm.*, June, pp895, 1981.

[77] H. F. A. Roefs, "Binary sequences for spread spectrum multiple access communication", Ph.D. dissertation, Dept. Elec. Eng., Univ. Illinois at Urbana-Champaign, 1977.

[78] D. V. Sarwate, and M. B. Pursley, "Crosscorrelation Properties of Pseudorandom and Related Sequences", *Proc. IEEE*, Vol. 68, No. 5, May, pp593, 1980.

[79] D. V. Sarwate, "Bounds on crosscorrelation and autocorrelation of sequences", *IEEE TRans. Inform. Theory*, Vol. 25, pp720, 1979.

[80] R. Sampaio-Neto, and R. a. Scholtz, "Precorrelation filter design for spread spectrum code tracking in interference", *IEEE J. Sel. Areas in Comm.*, Vol. 3, No. 5, Sept, pp662, 1985.

[81] D. L. Schilling, L. B. Milstein, R. L. Pickholtz, F. Bruno, E. Kanterakis, M. Kullback, V. Erceg, W. Biederman, D. Fishman, and D. Salerno, "Broadband

CDMA for Personal Communications Systems", *IEEE Comm. Magazine*, Nov., pp60, 1991

[82] D. L. Schilling, L. B. Milstein, R. L. Pickholtz, M. Kullback, and F. Miller, "Spread spectrum for commerical communicaitons", *IEEE Comm. Magazine*, April, pp66, 1991

[83] R. A. Scholtz, "The origins of spread spectrum communications", *IEEE Trans. Comm.*, Vol. Com-30, No. 5, May, pp822, 1982

[84] R. A. Scholtz, "The Spread Spectrum Concept" *IEEE Trans. Comm.*, Vol. Com-25, No. 8, Aug., pp748, 1977.

[85] M. Schwartz, W. R. Bennett, and S. Stein, "Communication systems and techniques", McGraw-Hill, 1966.

[86] K. S. Shanmugam, "Digital and Analog Communication Systems", John Wiley & Sons, 1985.

[87] M. K. Simon, D. Divsalar, "On the implementation and performance of single and double differential detection schemes", *IEEE Trans. Comm.*, Vol. 40, No. 2, Feb., pp278, 1992.

[88] M. K. Simon, J. K. Omura, R. A. Scholtz, and B. K. Levitt, "Spread spectrum communications I-III", Computer Science Press, 1985.

[89] E. S. Sousa, "The effect of clock and carrier frequency offsets on the performance of a direct sequence spread spectrum multiple access system", *IEEE J. Sel. Areas in Comm.*, Vol. 8, No. 4, May, pp580, 1990.

[90] E. S. Sousa, "Interference modeling in a direct sequence spread spectrum packet radio network", *IEEE Trans. Comm.*, Vol. 38, No. 9, Sept., pp1475, 1990.

[91] G. L. Stuber, and C. Kchao, "Analysis of a multiple cell direct sequence CDMA cellular mobile radio system", *IEEE J. Sel. Areas in Comm.*, Vol. 10, No. 4, May, pp559, 1992.

[92] S. C. Swales, D. J. Purle, T. Busby, and M. A. Beach, "The application of frequency hopping CDMA for future universal personal communications systems", *Proc. ICUPC'93*, pp960, 1993.

[93] G. L. Turin, "The effects of multipath and fading on the performance of direct sequence CDMA systems", *IEEE Trans. Vehicular Tech.*, Vol. 33, No. 3, Aug., pp213, 1984.

[94] G. L. Turin, "Introduction to spread spectrum antimultipath techniques and their application to urban digital radio", *Proc. IEEE* , Vol. 68, No. 3, Marc, pp328, 1980.

[95] M. K. Varanasi, and B. Aazhang, "Multistage detection in asynchronous code division multiple access communications", *IEEE Trans. Comm.*, Vol. 38, No. 4, April. pp509, 1990.

[96] D. Verhulst, M. Mouly, and J. Szpirglas, "Slow frequency hopping multiple access for digital cellular radiotelephone", *IEEE J. Sel. Areas in Comm.*, Vol. 2, No. 4, July. pp563, 1984.

[97] A. J. Viterbi, "When Not to Spread Spectrum-a Sequel" *IEEE Comm. Magazine*, April. pp12, 1985.

[98] A. J. Viterbi, "Spread Spectrum Communications-Myths and Realities", *IEEE Comm. Magazine*, May, pp11, 1979.

[99] J. Wang, and M. Moeneclaey, "Hybrid DS/SFH Spread-Spectrum Multiple Access with Predetection Diversity and Coding for Indoor Radio", *IEEE J. Sel. Areas in Comm.*, Vol. 10, No. 4, May, pp705, 1992.

[100] C. L. Weber, G. K. Huth, and B. H. Batson, "Performance Considerations of Code Division Multiple Access Systems", *IEEE Trans. Vehicular Tech.*, Vol. 30, No. 1, Feb., pp3, 1981.

[101] A. L. Welti, B. Z. Bobrovsky, "Mean time to lose lock for a coherent second order PN-code tracking loop-the singular pertrubation approach", *IEEE J. Sel. Areas in Comm.*, Vol. 8, No. 5, June, pp809, 1990.

[102] H. H. Xia, H. L. Bertoni, L. R. Maciel, A. L. Stewart, and R. Rowe, "Radio Propagation Characteristics for Line-of-Sight Microcellular and Personal Communications", *IEEE Trans. on Ant. Prop.*, Vol. 41, No. 10, Oct., pp1439, 1993.

[103] Z. Xie, R. T. Short,, and C. K. Rushforth, "A family of suboptimum dietecors for coherent multiuser communications", *IEEE J. Sele. Areas in Comm.*, Vol. 8, No. 4, May., pp683, 1990.

[104] M. D. Yacoub, "Foundations of Mobile Radio Engineering", CRC press, 1993.

[105] K. Yang, and G. L. Stuber, "Throughput analysis of a slotted frequency hop multiple access network", *IEEE J. Sel. Areas in Comm.*, Vol. 8, No. 4, May, pp588, 1990 .

[106] R. E. Ziemer, and R. L. Peterson, "Digital Communications and spread sectrum systems", MacMillian, 1985.